プラズマ中のダスト粒子挙動のシミュレーション

21 July, 2011

Y. Tanaka (Kanazawa Univ.),
A.Yu.Pigarov, R.D.Smirnov, S.I.Krasheninnikov (UCSD),
N.Asakura, H.Takenaga (JAEA),
N.Ohno (Nagoya Univ.), Y. Uesugi (Kanazawa Univ.)

Background-1

- Dust in fusion devices is one of the most critical issues, mainly related to the safety hazard.
  - Enhancement of the tritium inventory
  - Risk of explosion at an accidental air or coolant leakage
- Dust may be an important contributor of impurities in the main and SOL plasmas in some devices (← The impurities may increase radiation loss)

⇨ Numerical simulation is a powerful tool nowadays for basic understanding of dust particle formation and its transport in edge plasma condition of fusion devices.

-Ion drag force & dust potential, etc
-Electron emission
-Improved to treat various materials

DUSTT code has been developed by Dr.A.Pigarov, UCSD cooperating UEDGE code (Dr.T.Rognlien, LLNL)

-Present work

Calculation of behaviors of C dust particles in a plasma in JT-60U configuration with DUSTT code

-Behavior of individual dust launched from different wall positions with different initial radii and different initial velocities.

1-100 micron

-Statistical analysis of dust particles with different initial velocities.

-Calculation of trajectories, temporal evolution in temperature, mass, electronic charge, velocity etc of dust particles in a plasma in JT-60U.

Behavior of ablating particles in plasmas

Other examples:

-Spallation particle flight from polymer bulk irradiated by plasmas

-Evaporation simulation of polymer particle

Underlying physics equations of dust particles in a plasma-1

-Equation of motion of dust particle:

$$\frac{4}{3}\pi r_{\mathrm{d}}^{3}\rho_{\mathrm{d}}\frac{d\boldsymbol{v}_{\mathrm{d}}}{dt}=\underline{\zeta}\left(\boldsymbol{F}_{\mathrm{c}}+\boldsymbol{F}_{\mathrm{o}}\right)+\boldsymbol{F}_{\mathrm{a}}-eZ_{\mathrm{d}}\boldsymbol{E}+M_{\mathrm{d}}\boldsymbol{g}$$

Spinning effect is neglected

-Ion friction forces

-Neutral particle friction forces

-Shape factor(=1.0 for sphere)

-Gravity

-Electric field force due to charging of the dust

-Equation of mass of dust particle:

$$\frac{d}{dt}\left(\rho_{\mathrm{d}}\frac{4}{3}\pi r_{\mathrm{d}}^{3}\right)=-4\pi r_{\mathrm{d}}^{2}m_{\mathrm{s}}\Gamma_{\mathrm{s}}$$

-Mass flux due to physical & chemical sputtering, RES, thermal evaporation/sublimation

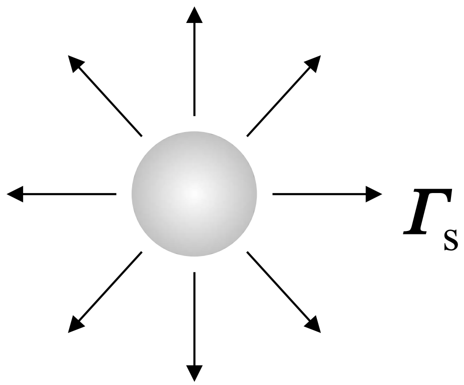

Uniform mass loss in radial direction
→ Dust shape is always sphere.

Underlying physics equations of dust particles in a plasma-2

-Equation of energy (uniform temperature profile assumption inside a dust particle):

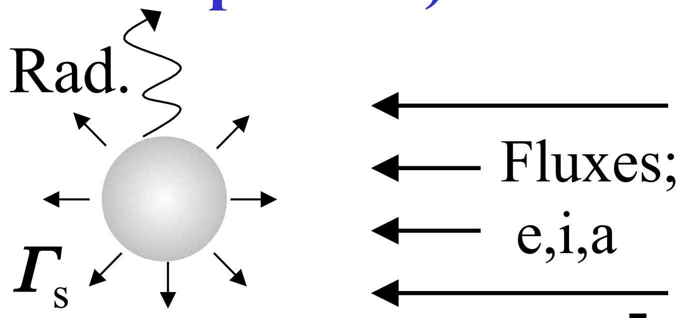

$$\left.\begin{array}{l}\dfrac{d}{dt}\left(\rho_{\mathrm{d}}\dfrac{4}{3}\pi r_{\mathrm{d}}^{3}\displaystyle\int_{0}^{T_{\mathrm{d}}} c_{\mathrm{pd}}\,dT\right) \\ \quad (T_{\mathrm{d}} < T_{\mathrm{m}},\quad T_{\mathrm{m}} < T_{\mathrm{d}}) \\ \\ \dfrac{d}{dt}\left(\rho_{\mathrm{d}}\dfrac{4}{3}\pi r_{\mathrm{d}}^{3} H_{\mathrm{m}}\eta_{\ell}\right) \\ \quad (T_{\mathrm{d}} = T_{\mathrm{m}})\end{array}\right\} = 4\pi r_{\mathrm{d}}^{2}\left[\begin{array}{l}\underline{(P_{\mathrm{kin,i}} + P_{\mathrm{kin,a}} + P_{\mathrm{kin,e}} + P_{\mathrm{pot}})} \\ -(\underline{P_{\mathrm{rad}} + P_{\mathrm{ps}} + P_{\mathrm{cs}} + P_{\mathrm{res}}} \\ \underline{+P_{\mathrm{evap}} + P_{\mathrm{e-emit}}})\end{array}\right]$$

-Liquid fraction

For melting process

-Latent heat for melting

-Heating power transfer from ions, electrons & neutrals in a plasma

-Cooling power due to thermal radiaiton, physical & chemical sputtering, RES, thermal evaporation, electron emission

Calculation of floating potential of dust from quasi-equilibrium (1)

-Quasi-equilibrium condition for dust:

$$\Gamma_e = \Gamma_i + \Gamma_e^{TE} + \Gamma_e^{SEE}$$

$$\phi_d[V] = -\frac{T_i[eV]}{e}\chi = \frac{Z_d e^2}{r_d}$$

(Floating potential of dust)

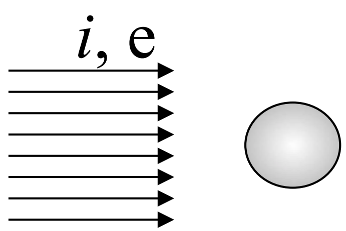

For negative floating potential of dust

-Electron flux from thermoionic emission (Richardson-Dushman's equation):

$$\Gamma_e^{TE} = \sigma_{sb}\left(\frac{4\pi m_e (kT_d)^2}{h^3}\right)\exp\left(-\frac{W_d}{kT_d}\right)$$

-Electron flux from plasma:

$$\Gamma_e = \frac{1}{4} n_e \left(\frac{8T_e}{\pi m_e}\right)^{\frac{1}{2}} \exp\left[-\left(\frac{T_i}{T_e}\right)\chi\right]$$

-Ion flux from plasma:

$$\Gamma_i = n_e \left(\frac{2T_i}{m_i}\right)^{\frac{1}{2}} \frac{u}{4}\left\{\left(1 + \frac{1}{2u^2} + \frac{\chi}{u^2}\right)\mathrm{erf}(u) + \frac{e^{-u^2}}{u\sqrt{\pi}}\right\}$$

Relative drift velocity:

$$u = \frac{|v_i - v_d|}{v_n} = \frac{|v_i - v_d|}{\left(\frac{2T_i}{m_i}\right)^{1/2}}$$

If Γ_e^{TE} or Γ_e^{SEE} is high, the floating potential of dust can be positive.

Calculation of floating potential of dust from quasi-equilibrium (2)

-Quasi-equilibrium condition for dust:

$$\Gamma_e = \Gamma_i + \Gamma_e^{TE} + \Gamma_e^{SEE}$$

$$\phi_d[\mathrm{V}] = -\frac{T_i[\mathrm{eV}]}{e}\chi = \frac{Z_d e^2}{r_d}$$

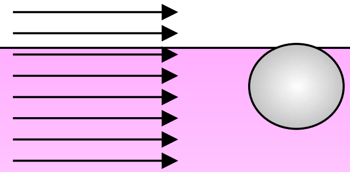

For positive floating potential of dust

-Electron flux from thermoionic emission (Richardson-Dushman's equation):

$$\Gamma_e^{TE} = \sigma_{sb}\left(\frac{4\pi m_e (kT_d)^2}{h^3}\right)\exp\left(-\frac{W_d}{kT_d}\right)$$

-Electron flux from plasma:

$$\Gamma_e = \frac{1}{4} n_e \left(\frac{8T_e}{\pi m_e}\right)^{\frac{1}{2}}\left[1-\left(\frac{T_i}{T_e}\right)\chi\right]$$

-Ion flux from plasma:

$$\Gamma_i = n_e\left(\frac{2T_i}{m_i}\right)^{\frac{1}{2}}\frac{u}{8}\left\{\left(1+\frac{1}{2u^2}+\frac{\chi}{u^2}\right)\left[\mathrm{erf}(u+\sqrt{-\chi})+\mathrm{erf}(u+\sqrt{-\chi})\right] + \frac{1}{u^2\sqrt{\pi}}\left[(u+\sqrt{-\chi})\exp[-(u-\sqrt{-\chi})^2]+(u-\sqrt{-\chi})\exp[-(u+\sqrt{-\chi})^2]\right]\right\}$$

Relative drift velocity:

$$u = \frac{|\boldsymbol{v}_i - \boldsymbol{v}_d|}{v_n} = \frac{|\boldsymbol{v}_i - \boldsymbol{v}_d|}{\left(\frac{2T_i}{m_i}\right)^{1/2}}$$

Parameters of background plasma calculated with UEDGE code

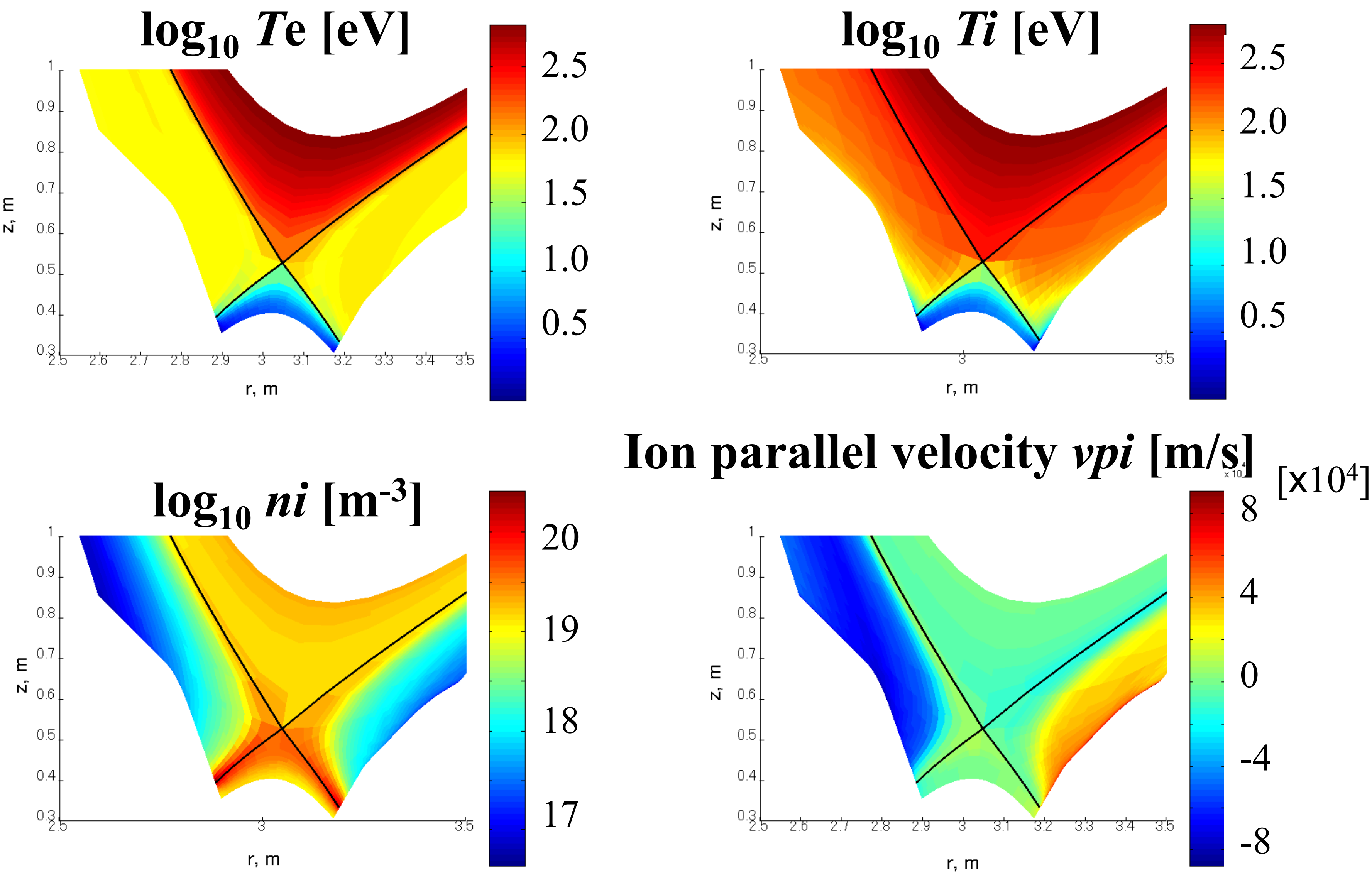

Calculated by Dr. Pigarov, UCSD

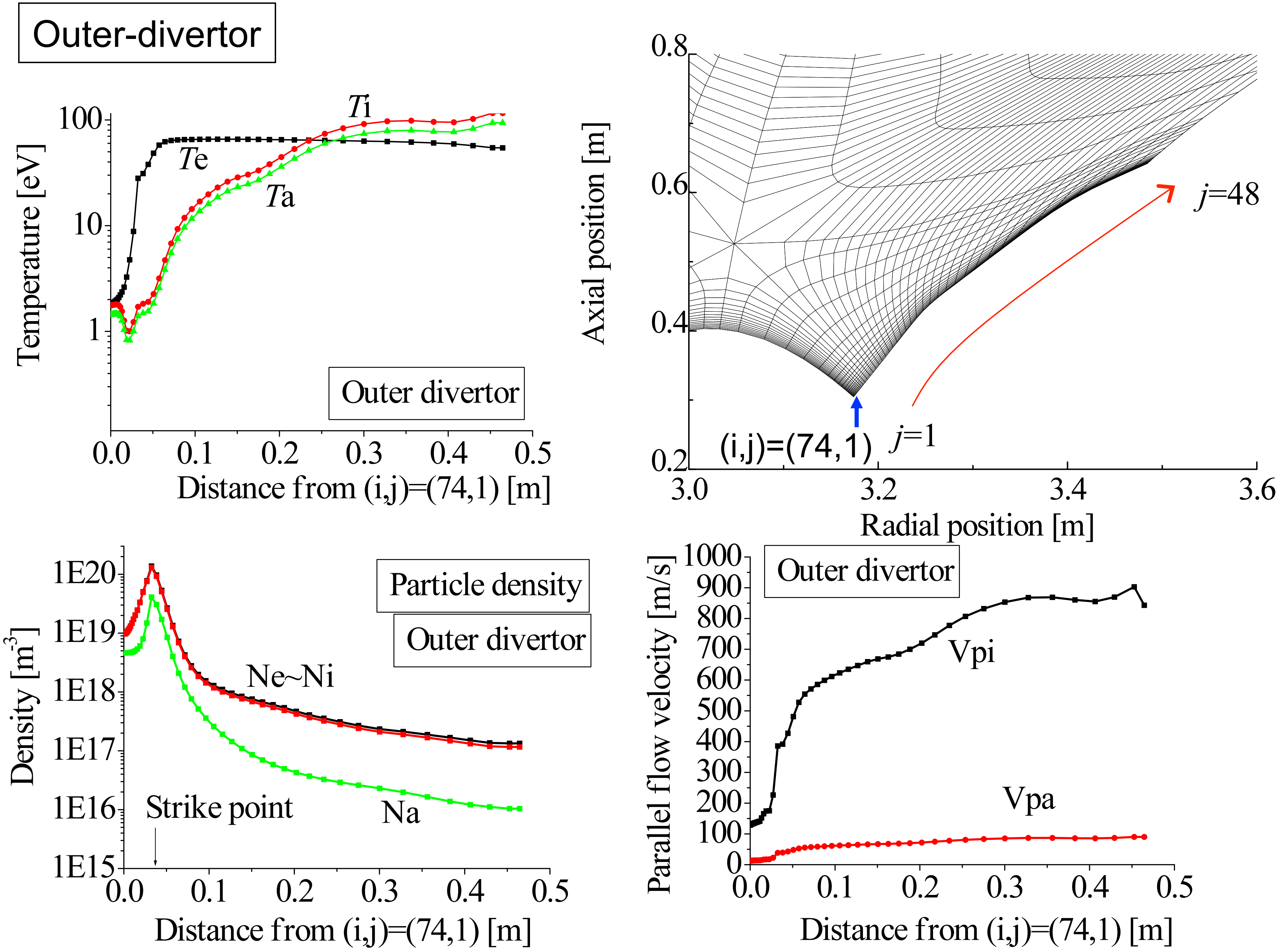

Outer-divertor
Ti
Te
Ta
Temperature [eV]
100
10
1
Outer divertor
0.0 0.1 0.2 0.3 0.4 0.5
Distance from (i,j)=(74,1) [m]
Axial position [m]
0.8
0.6
0.4
0.2
j=48
(i,j)=(74,1)
j=1
3.0 3.2 3.4 3.6
Radial position [m]
Density [m-3]
1E20
1E19
1E18
1E17
1E16
1E15
Particle density
Outer divertor
Ne~Ni
Strike point
Na
0.0 0.1 0.2 0.3 0.4 0.5
Distance from (i,j)=(74,1) [m]
Parallel flow velocity [m/s]
1000 900 800 700 600 500 400 300 200 100 0
Outer divertor
Vpi
Vpa
0.0 0.1 0.2 0.3 0.4 0.5
Distance from (i,j)=(74,1) [m]

Trajectories of the dust from outer region for different initial dust velocities -#O1

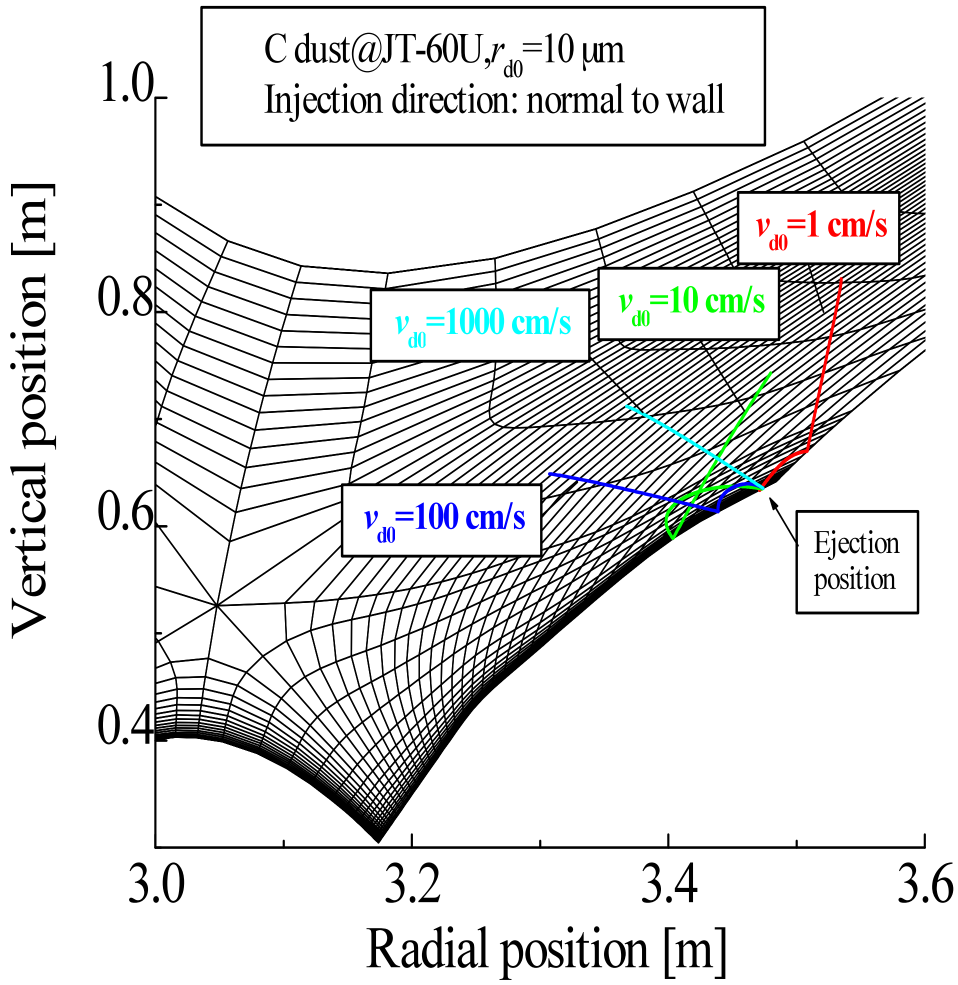

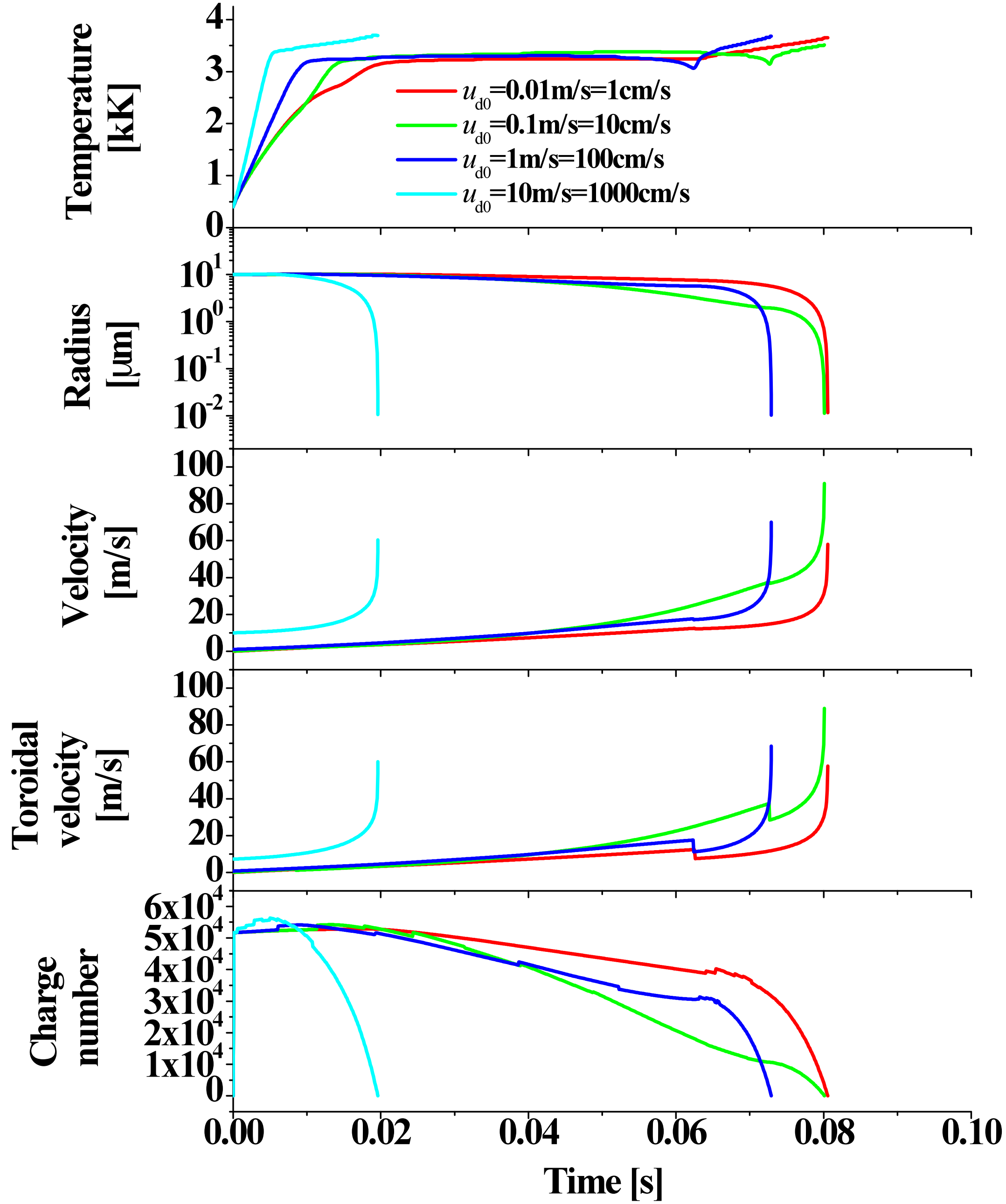

Trajectories of the dust from outer region for different initial dust radii -#O3

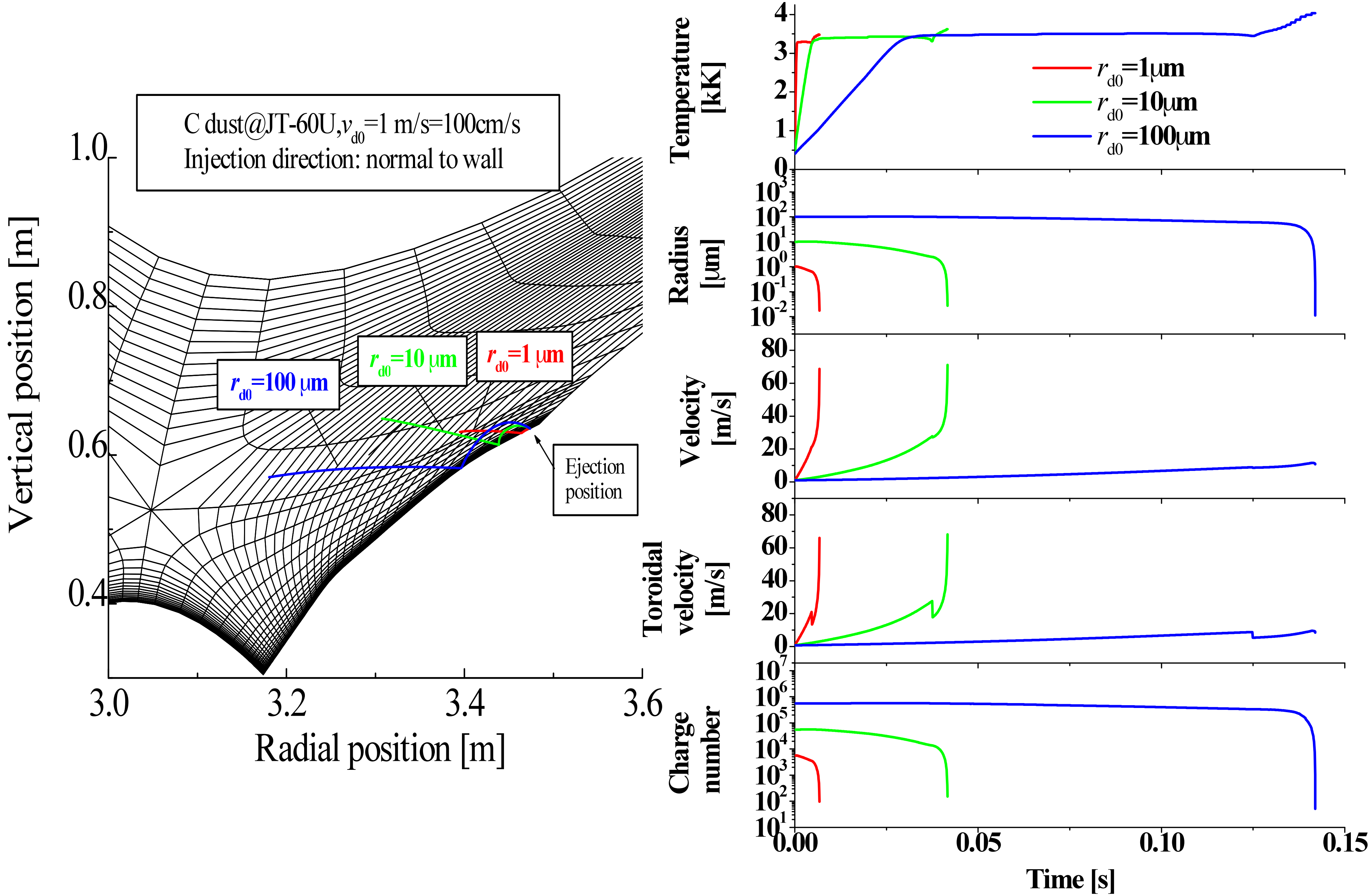

Applied forces onto the dust

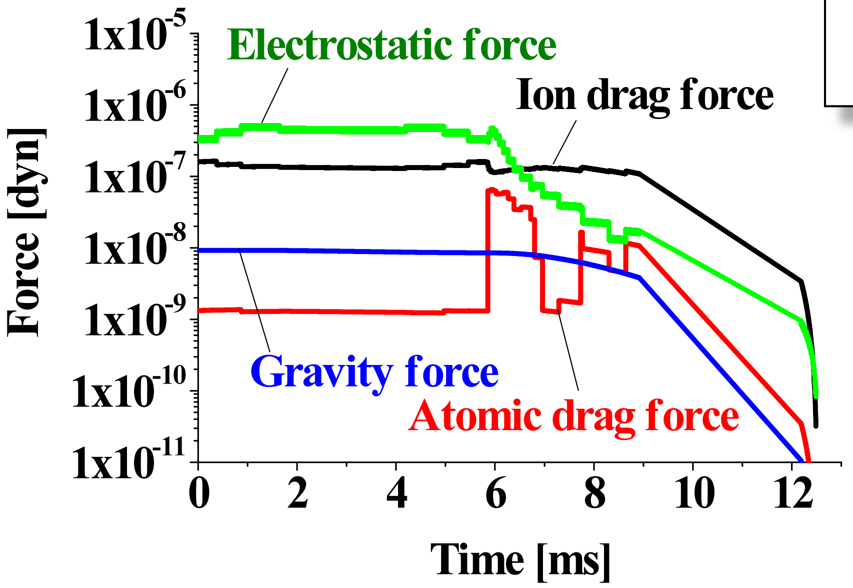

-Initially, electrostatic force is dominant, and then is ion drag force

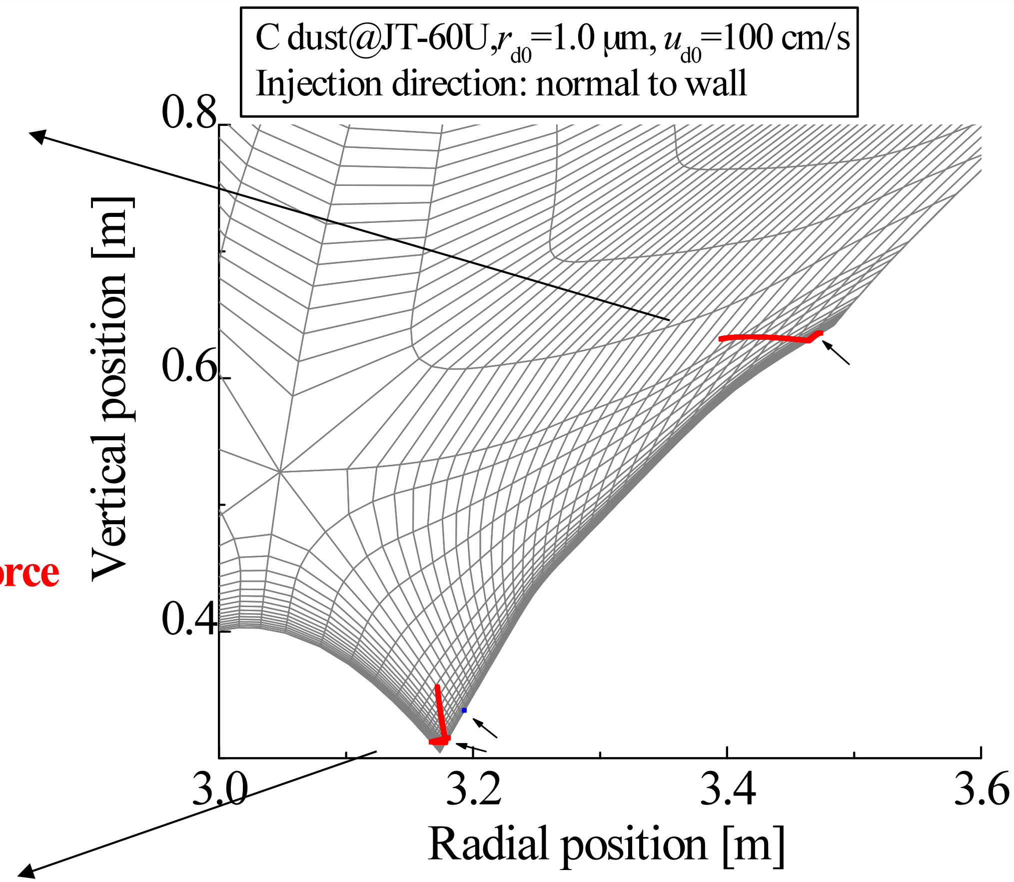

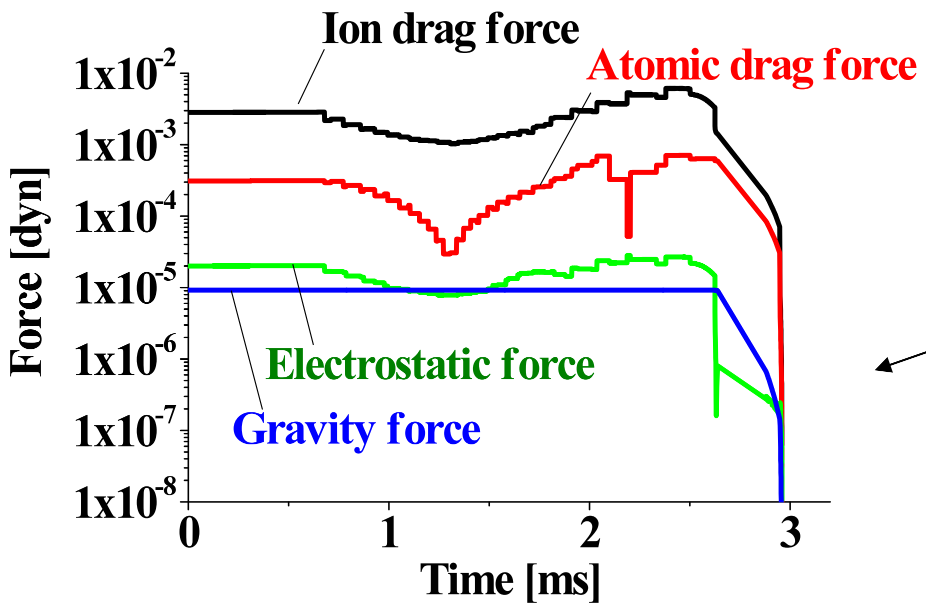

-Dominant force is ion drag force, and atomic drag force.

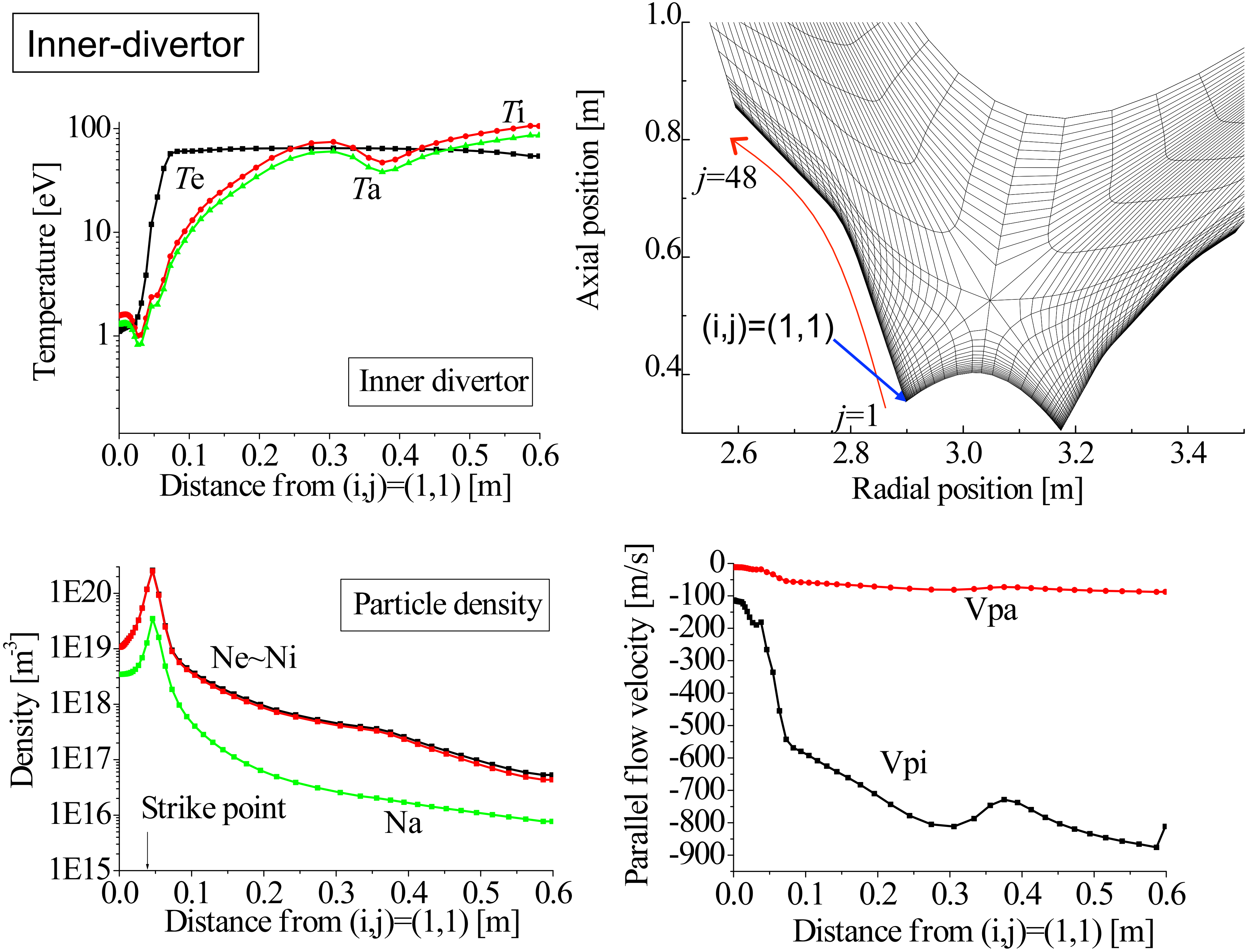
Inner-divertor
Temperature [eV]
100
10
1
Ti
Te
Ta
Inner divertor
0.0 0.1 0.2 0.3 0.4 0.5 0.6
Distance from (i,j)=(1,1) [m]
Axial position [m]
1.0
0.8
0.6
0.4
j=48
(i,j)=(1,1)
j=1
2.6 2.8 3.0 3.2 3.4
Radial position [m]
Density [m^-3]
1E20
1E19
1E18
1E17
1E16
1E15
Particle density
Ne~Ni
Strike point
Na
0.0 0.1 0.2 0.3 0.4 0.5 0.6
Distance from (i,j)=(1,1) [m]
Parallel flow velocity [m/s]
0
-100
-200
-300
-400
-500
-600
-700
-800
-900
Vpa
Vpi
0.0 0.1 0.2 0.3 0.4 0.5 0.6
Distance from (i,j)=(1,1) [m]

Trajectories of the dust from inner region for different initial dust radii -#I3

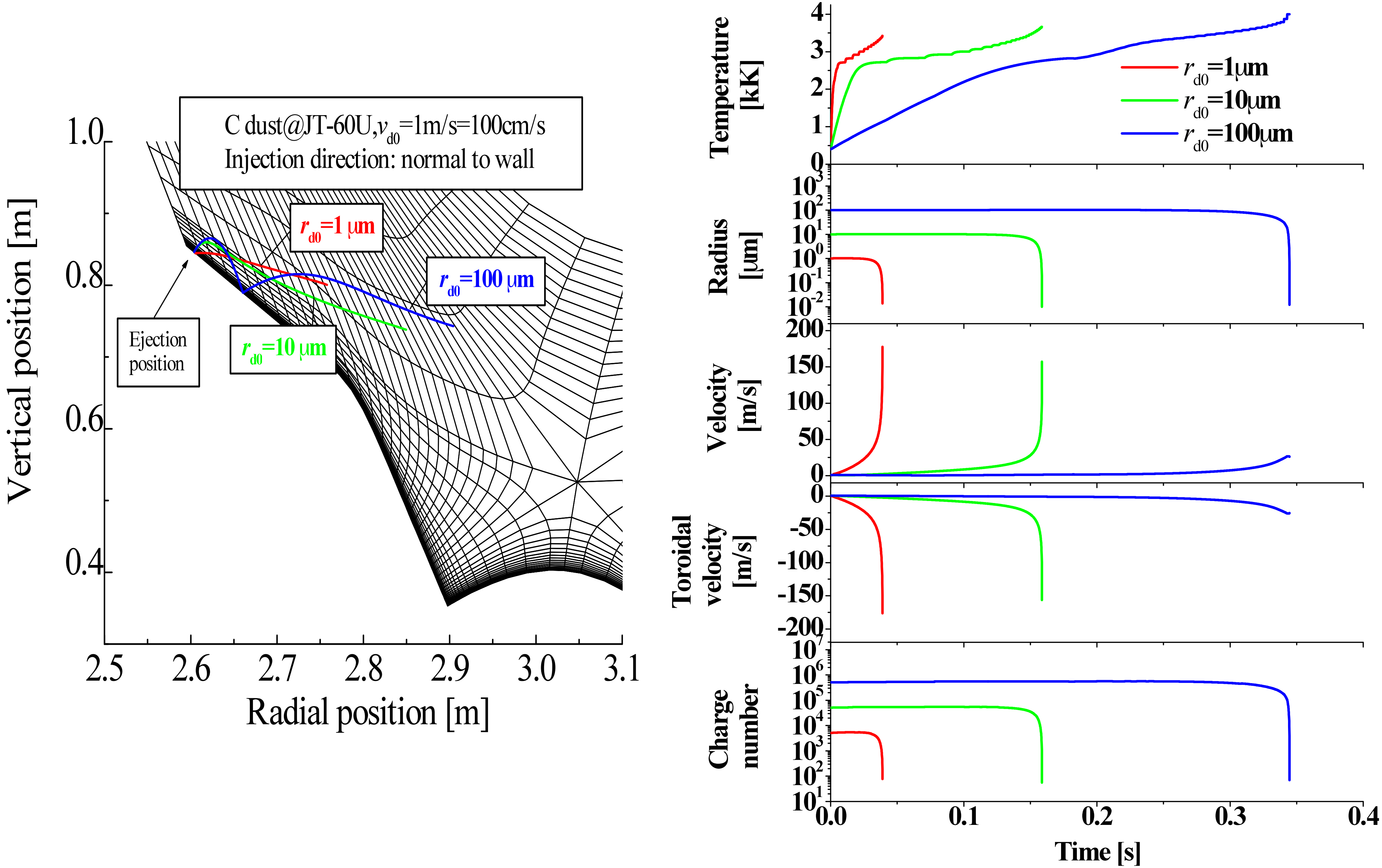

Applied forces onto the dust

-Initially, electrostatic force is dominant, and then is ion drag force

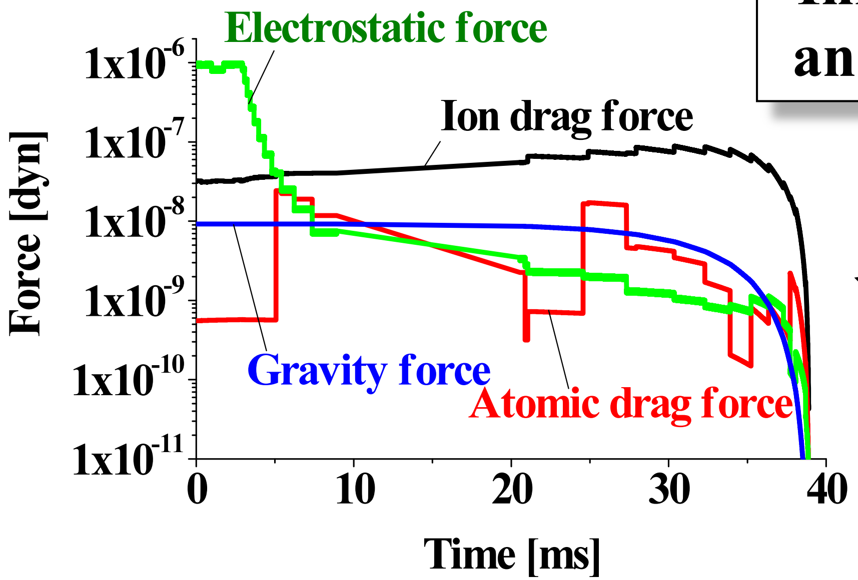

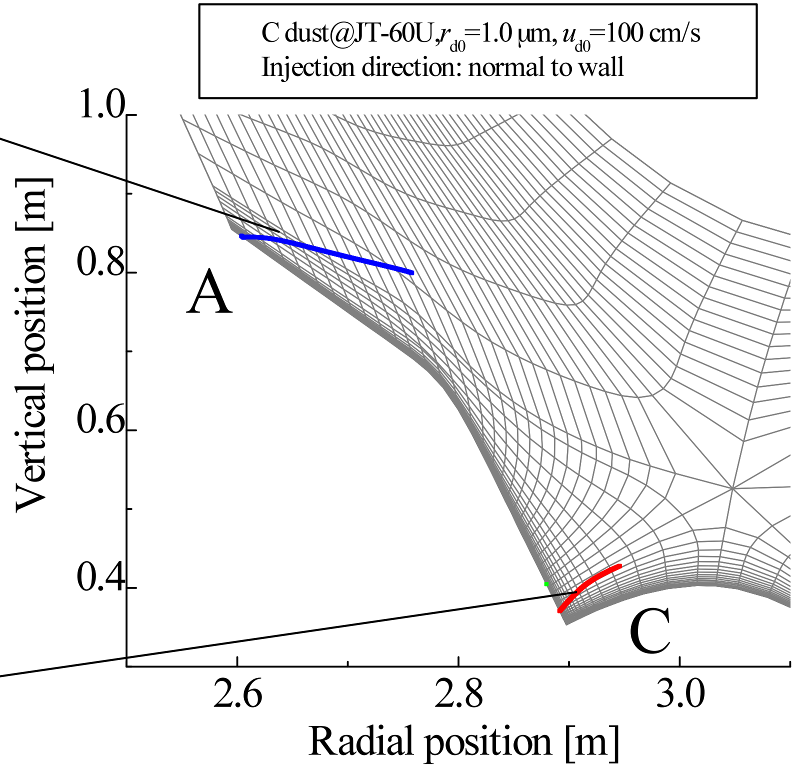

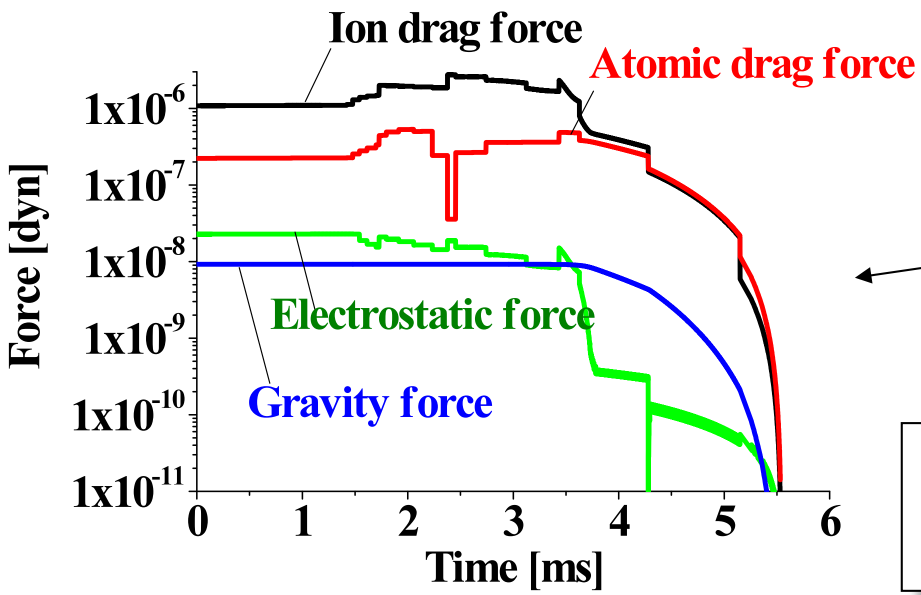

-Dominant force is ion drag force, and atomic drag force.

Dome

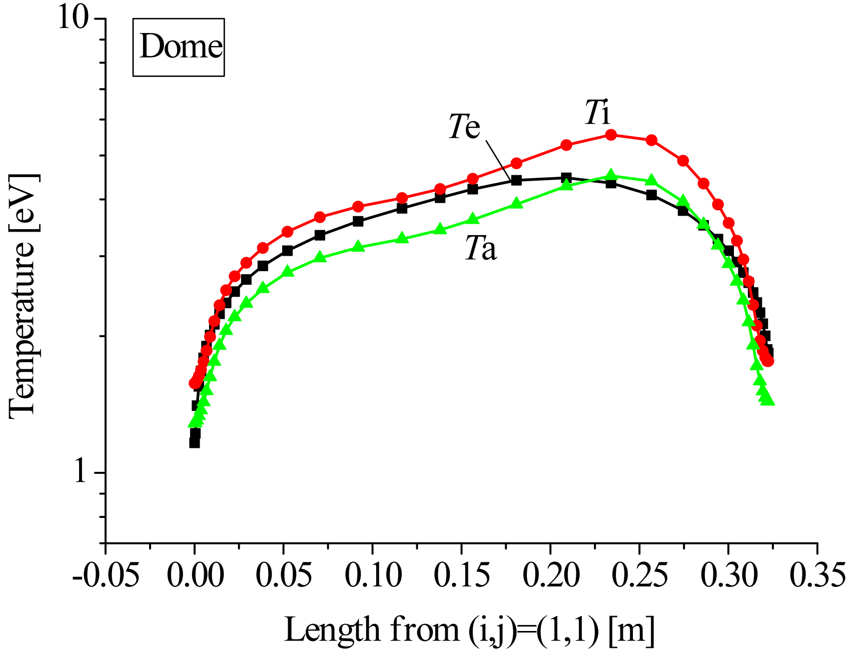
Dome
Te
Ti
Ta
Temperature [eV]
10
1
-0.05 0.00 0.05 0.10 0.15 0.20 0.25 0.30 0.35
Length from (i,j)=(1,1) [m]

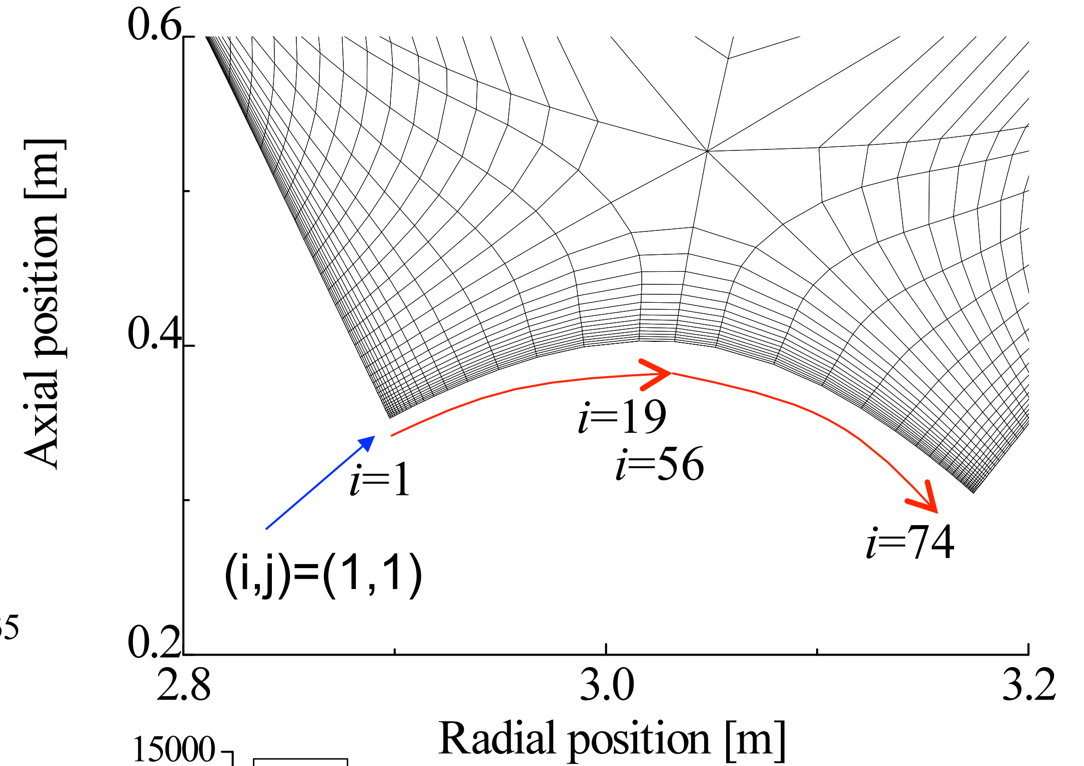
0.6
0.4
0.2
Axial position [m]
i=19
i=56
i=1
i=74
(i,j)=(1,1)
2.8
3.0
3.2
Radial position [m]

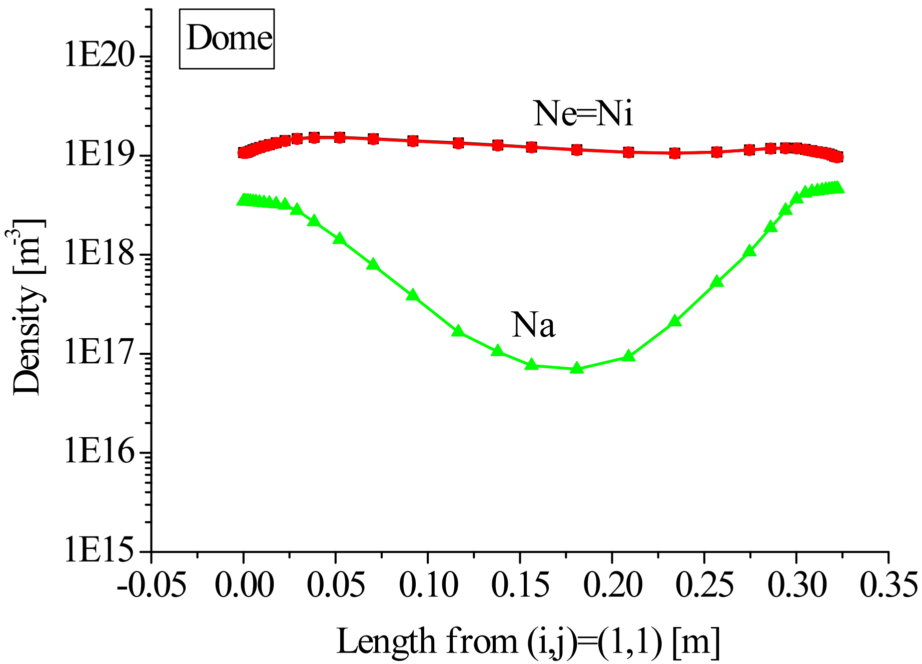
Dome
Ne=Ni
Na
Density [m^-3]
1E20
1E19
1E18
1E17
1E16
1E15
-0.05 0.00 0.05 0.10 0.15 0.20 0.25 0.30 0.35
Length from (i,j)=(1,1) [m]

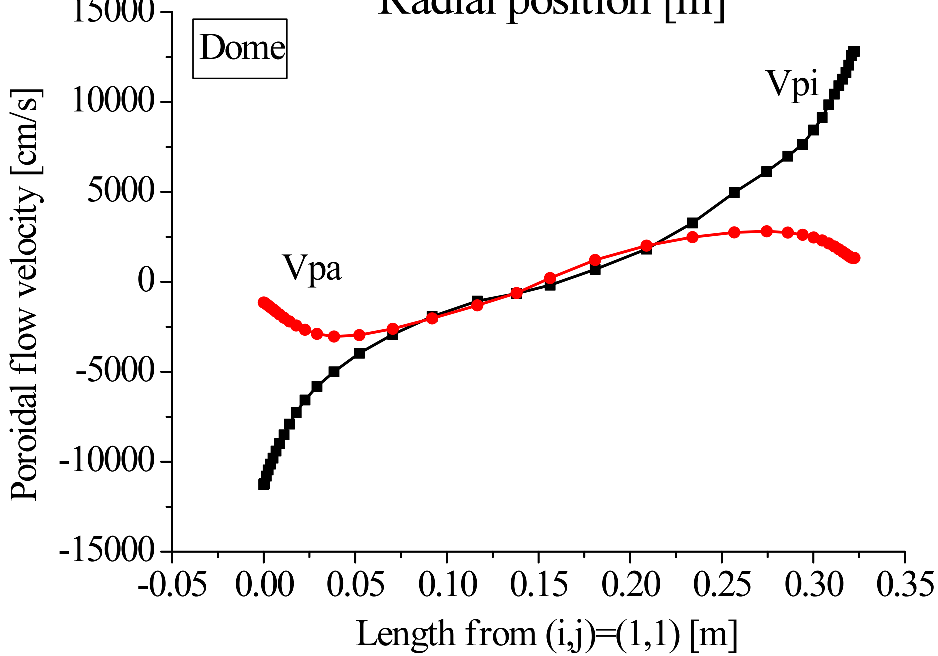
Dome
Vpi
Vpa
Poroidal flow velocity [cm/s]
15000
10000
5000
0
-5000
-10000
-15000
-0.05 0.00 0.05 0.10 0.15 0.20 0.25 0.30 0.35
Length from (i,j)=(1,1) [m]

Trajectories of the dust from private region for different initial dust velocities -#P1

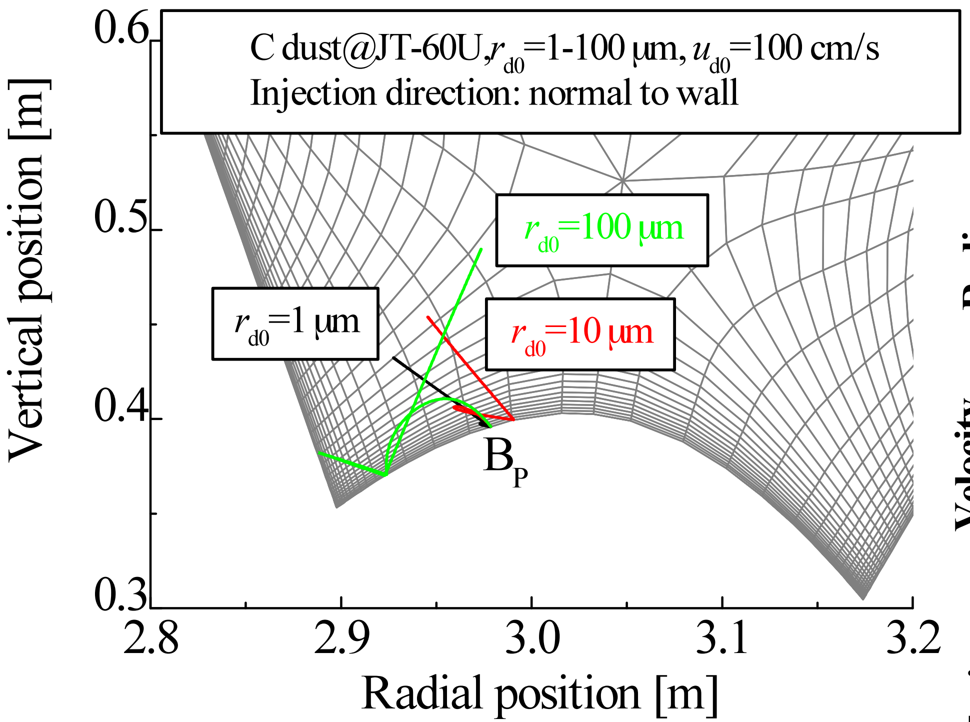

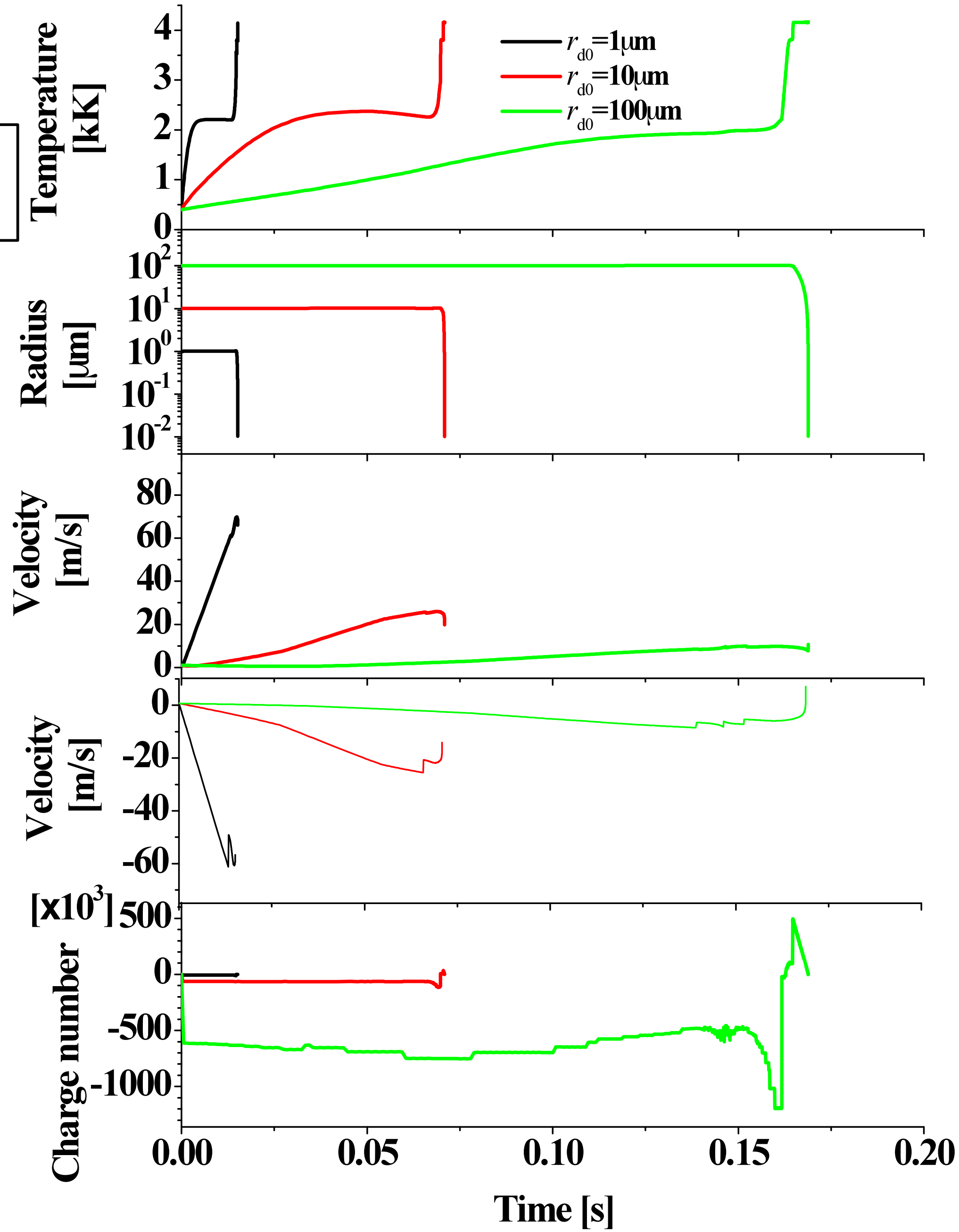

Statistical analysis of dust behavior-1
-Different position & initial velocity

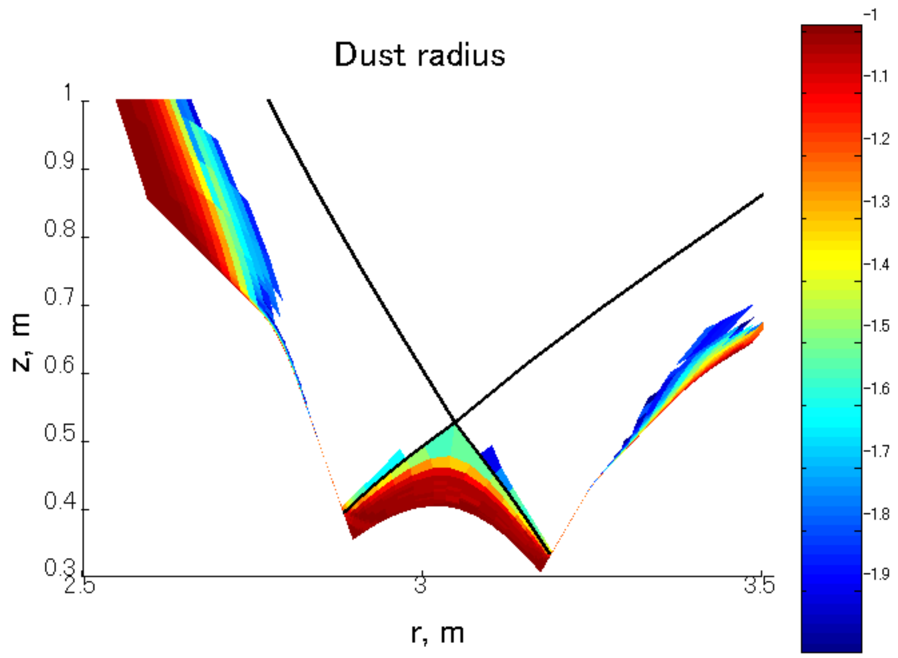

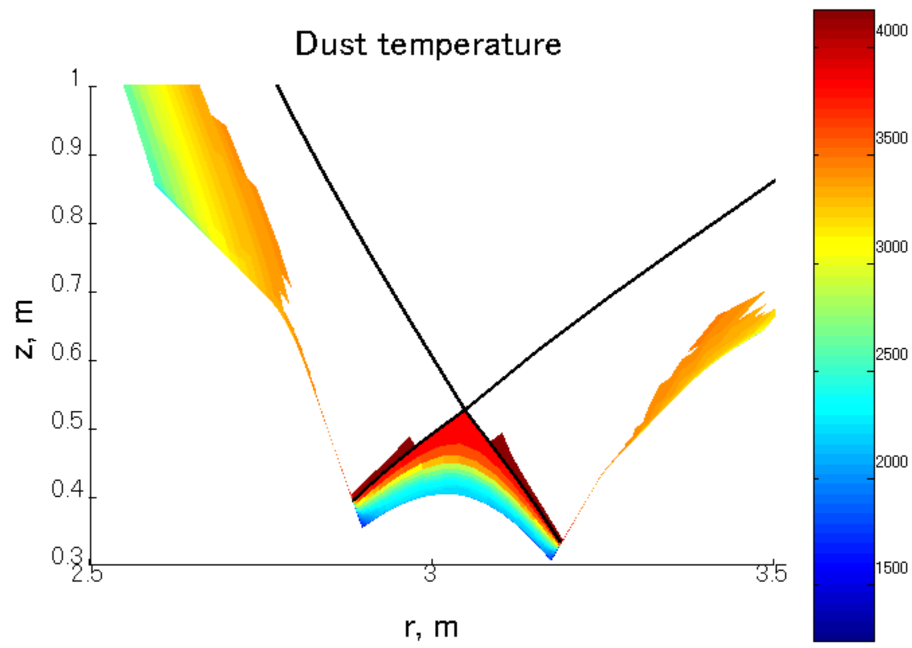

-Near the strike point, a dust particle is rapidly heated and sublimated, which causes short penetration length.
-A dust particle from private zone is slowly heated.

Statistical analysis of dust behavior-3
-Different position & initial velocity

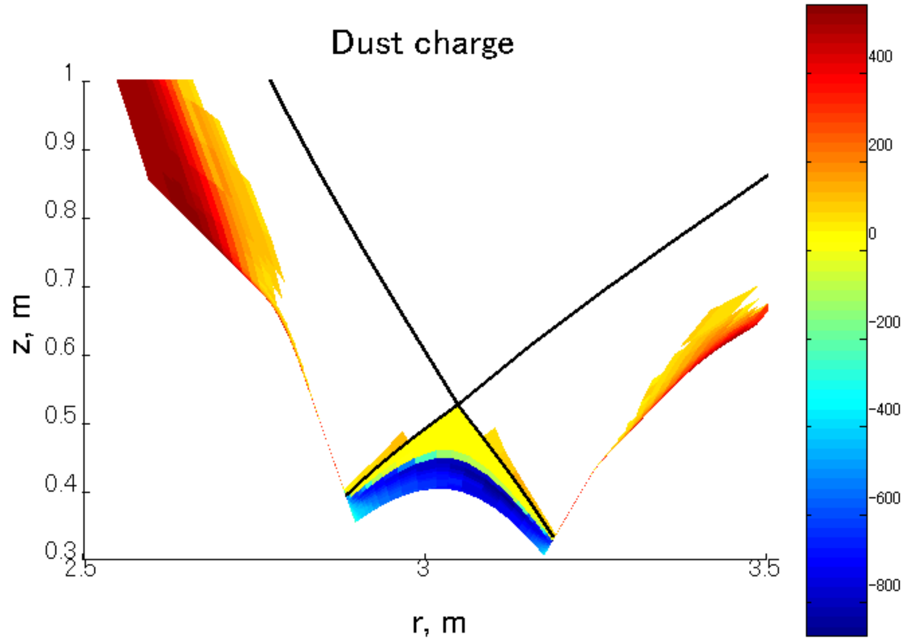

-Near the outer strike point and outer wall, a dust particle is accelerated in toroidal direction counter-clockwise.
This arises from ion drag force due to ion flow.
-Near the inner strike point, clockwise acceleration occurs on a dust particle.

Fundamental study on dust particle behavior Using polymer spallation particles.

-Polymer Ablation for Application to Arc Quenching

実験条件，実験装置及び対象バルク材料

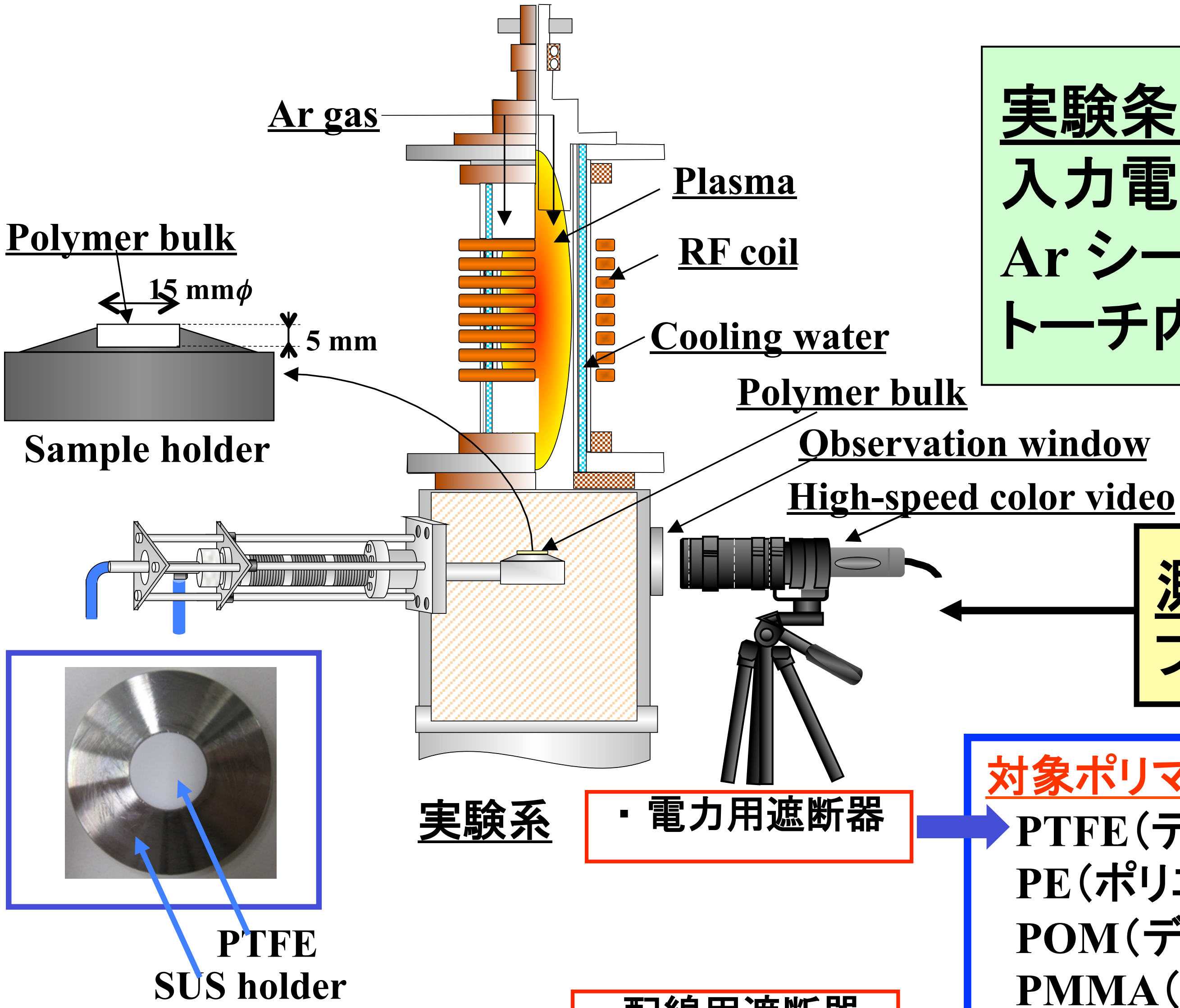

実験条件

入力電力	8.54 kW
Ar シースガス流量	30 slpm
トーチ内圧力	760 Torr

測定条件

フレームレート 1000 fps

実験系

- 電力用遮断器

- 配線用遮断器
- アークホーン

- 宇宙分野（熱遮蔽）

対象ポリマー材料

PTFE（テフロン）	$[-C_2F_4-]_n$
PE（ポリエチレン）	$[-C_2H_4-]_n$
POM（デルリン）	$[-CH_2O-]_n$
PMMA（アクリル）	$[-C_5H_8O_2-]_n$
PA66（ナイロン66）	$[-C_{12}H_{22}O_2N_2-]_n$
PA6（ナイロン6）	$[-C_6H_{11}ON-]_n$
PF（フェノール樹脂）	$[-C_7H_6-]_n$

高速度カラービデオカメラ撮影結果

(a) PTFE
$[-C_2F_4-]_n$

(b) PE
$[-C_2H_4-]_n$

(c) POM
$[-CH_2O-]_n$

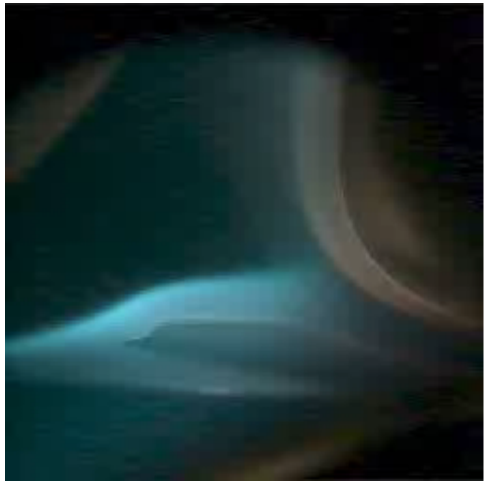

(d) PMMA
$[-C_5H_8O_2-]_n$

(e) PA66
$[-C_{12}H_{22}O_2N_2-]_n$

(f) PA6
$[-C_6H_{11}ON-]_n$

(g) PF
$[-C_7H_6-]_n$

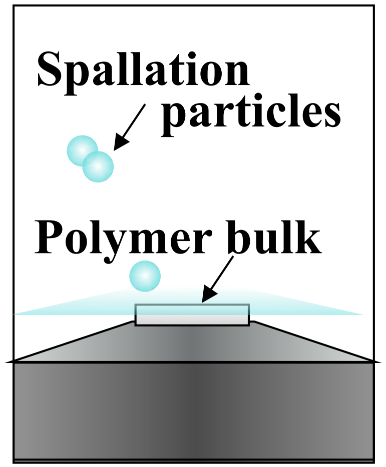

sample

＊露光時間50μs（POMとPFは250μs）　*再生速度は15 fps　フレームレート 1000 fps

高速度カラービデオカメラ撮影結果

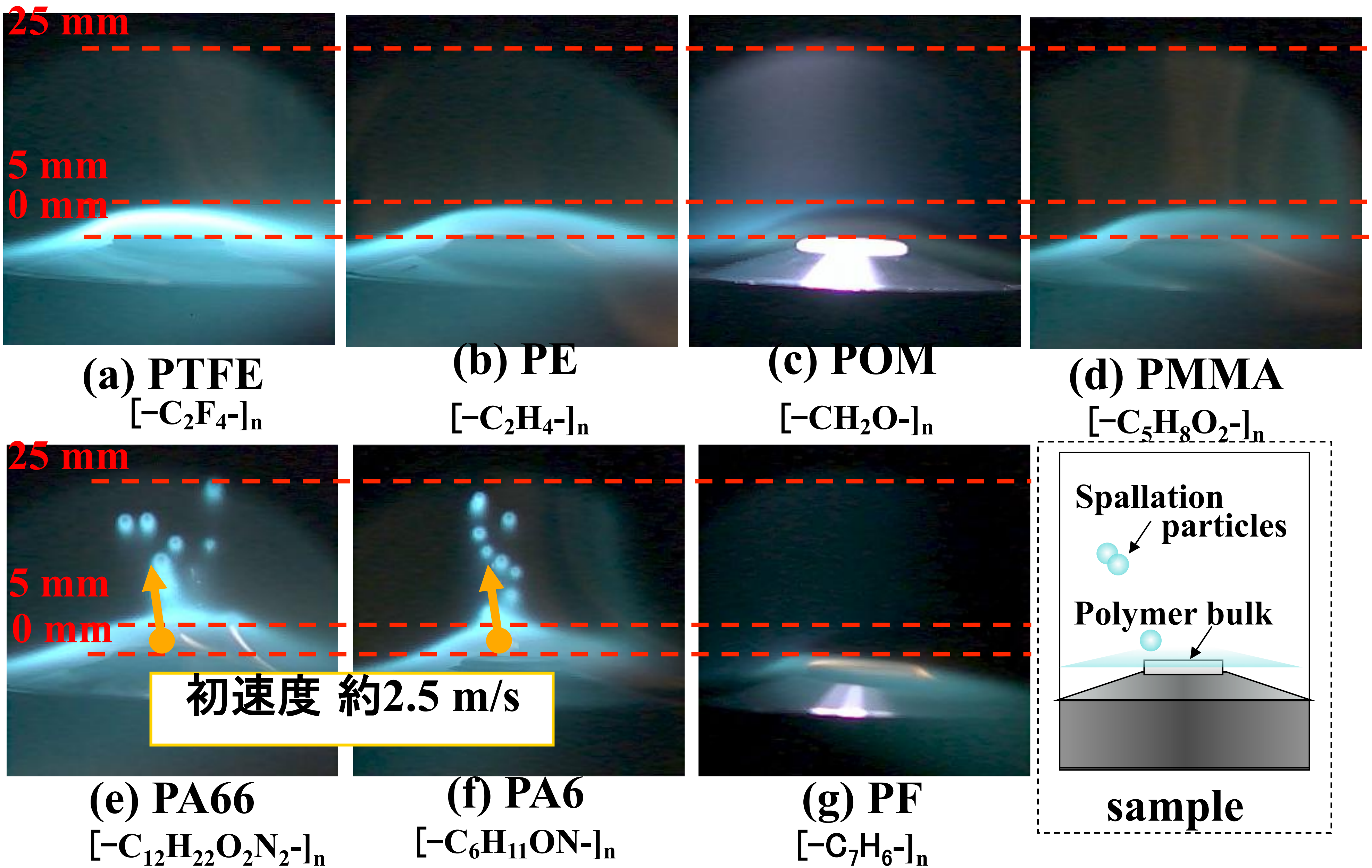

＊露光時間50μs（POMとPFは250μs）　*再生速度は15 fps　フレームレート 1000 fps

スポレーション粒子の飛翔の様相

⇒ 100枚(0.1
⇒ 各ピクセル

飛翔粒子が

飛翔粒子が

ポリマー表

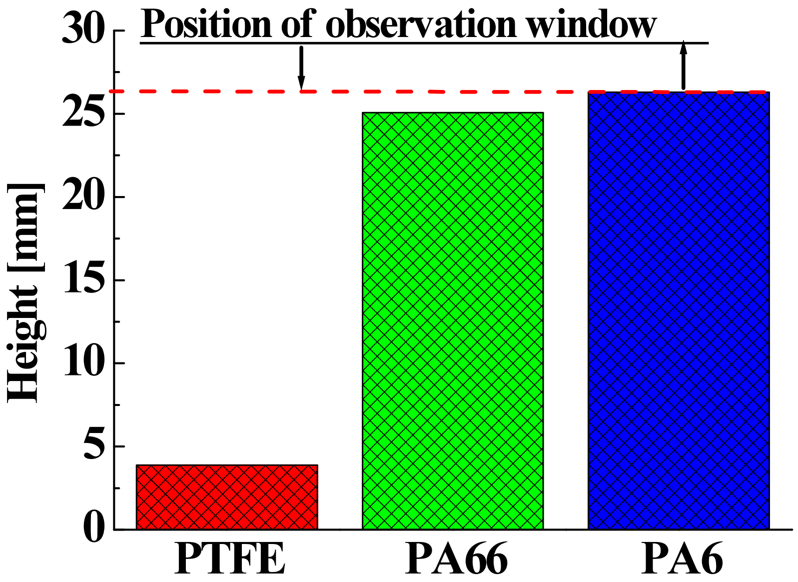

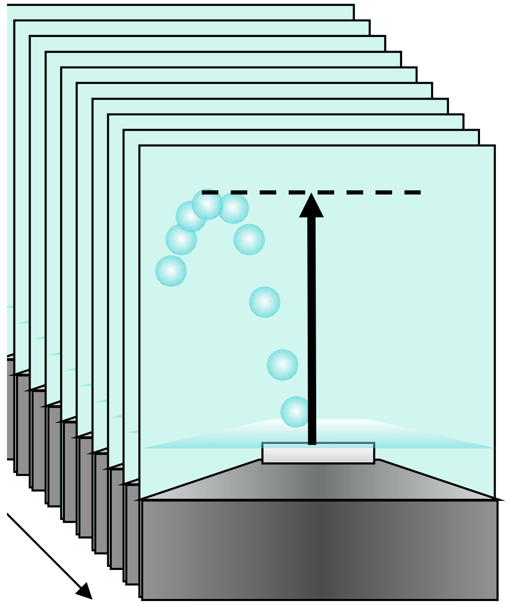

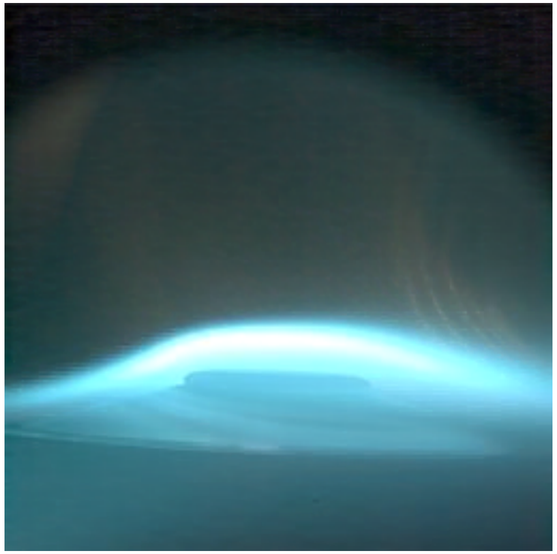

(a) PTFE
[$-C_2F_4-$]$_n$

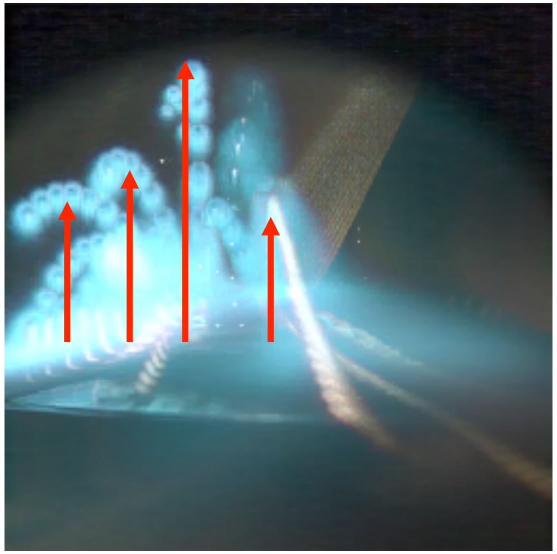

(b) PA66
[$-C_{12}H_{22}O_2N_2-$]$_n$

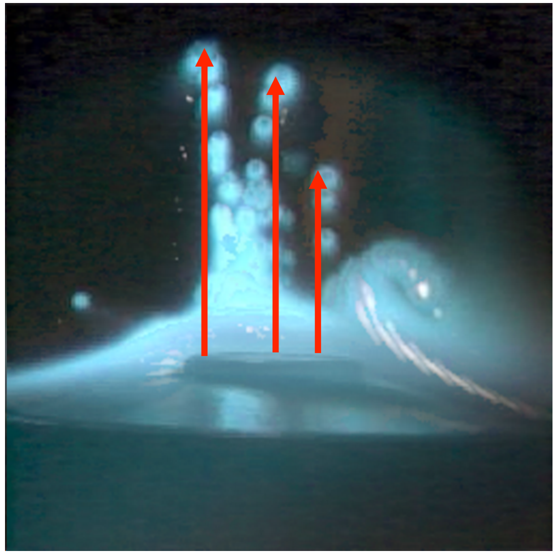

(c) PA6
[$-C_6H_{11}ON-$]$_n$

スポレーション粒子飛翔軌跡の数値解析

運動方程式

$$\frac{d\boldsymbol{v}_\mathrm{d}}{dt} = -\frac{3}{4}C_\mathrm{D}(\boldsymbol{v}_\mathrm{d}-\boldsymbol{u})\left|\boldsymbol{v}_\mathrm{d}-\boldsymbol{u}\right|\frac{\rho}{\rho_\mathrm{p}(2r_\mathrm{p})} + \boldsymbol{g}$$

粒子に加わる力 ⇒ ドラッグ力　重力

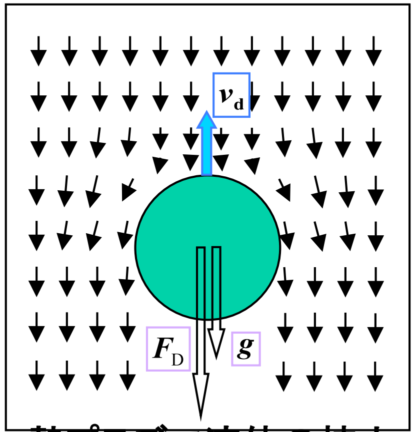

熱プラズマ流体の抗力

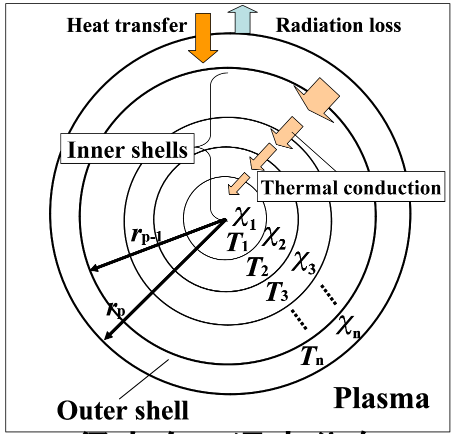

径方向の温度分布

エネルギー保存式

Innershells

$$\rho_\mathrm{p}C_\mathrm{pp}\frac{\partial T_\mathrm{p}(r,t)}{\partial t} = \frac{1}{r^2}\frac{\partial}{\partial r}\left(r^2\kappa_\mathrm{p}\frac{\partial T_\mathrm{p}(r,t)}{\partial r}\right) \qquad (T_\mathrm{p} < T_\mathrm{melt}, T_\mathrm{melt} < T_\mathrm{p} < T_\mathrm{boil})$$

$$\rho_\mathrm{p}H_\mathrm{m}\frac{\partial \chi_\mathrm{p}(r,t)}{\partial t} = \frac{1}{r^2}\frac{\partial}{\partial r}\left(r^2\kappa_\mathrm{p}\frac{\partial T_\mathrm{p}(r,t)}{\partial r}\right) \qquad (T_\mathrm{p} = T_\mathrm{melt})$$

Outershell

$$\frac{4\pi}{3}\rho_\mathrm{p}C_\mathrm{pp}(r_\mathrm{p}^3 - r_\mathrm{p-1}^3)\frac{\partial T_\mathrm{p}(r,t)}{\partial t} = Q \qquad (T_\mathrm{p} < T_\mathrm{melt}, T_\mathrm{melt} < T_\mathrm{p} < T_\mathrm{boil})$$

$$\frac{4\pi}{3}\rho_\mathrm{p}H_\mathrm{m}(r_\mathrm{p}^3 - r_\mathrm{p-1}^3)\frac{\partial \chi_\mathrm{p}(r,t)}{\partial t} = Q \qquad (T_\mathrm{p} = T_\mathrm{melt})$$

$$Q = 4\pi r_\mathrm{p}^2(h_\mathrm{c}(T - T_\mathrm{p}) - \sigma_\mathrm{s}\varepsilon(T_\mathrm{p}{}^4 - T_\mathrm{a}{}^4)) - 4\pi r_\mathrm{p-1}^2\kappa_\mathrm{p}\left.\frac{\partial T_\mathrm{p}(r,t)}{\partial r}\right|_{r=r_\mathrm{p-1}}$$

質量保存式

$$\frac{\partial r_\mathrm{p}}{\partial t} = -\frac{Q}{4\pi\rho_\mathrm{p}H_\mathrm{v}r_\mathrm{p}^2} \qquad (T_\mathrm{p} \geq T_\mathrm{boil})$$

⇒ **Next**
背景プラズマ場の計算手法

- r ：径方向位置
- $\boldsymbol{v}_\mathrm{d}$ ：粒子の速度
- $\boldsymbol{u}$ ：プラズマの速度
- r_p ：粒子の半径
- ρ ：プラズマの質量密度
- ρ_p ：粒子の質量密度
- C_D ：ドラッグ係数
- $\boldsymbol{g}$ ：重力加速度
- T_p ：粒子の温度
- χ_p ：粒子の液化率
- C_pp ：ポリマーの定圧比熱
- H_m ：ポリマーの融点の潜熱
- H_v ：ポリマーの沸点の潜熱
- κ_p ：ポリマーの熱伝導率
- h_c ：熱伝達係数

計算空間と各計算条件

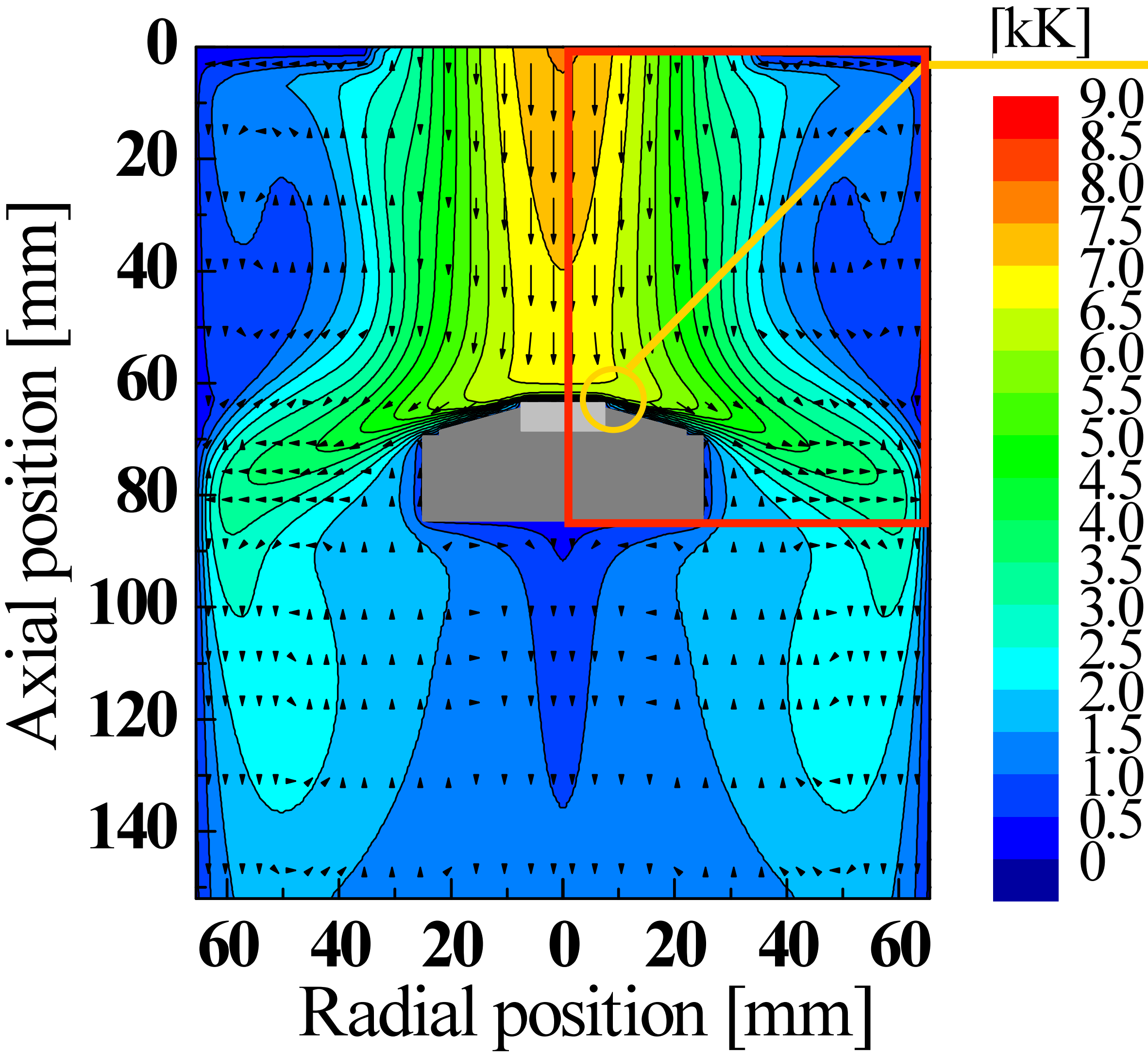

熱プラズマの温度場と流速ベクトル

ポリマーバルク材の端から放出

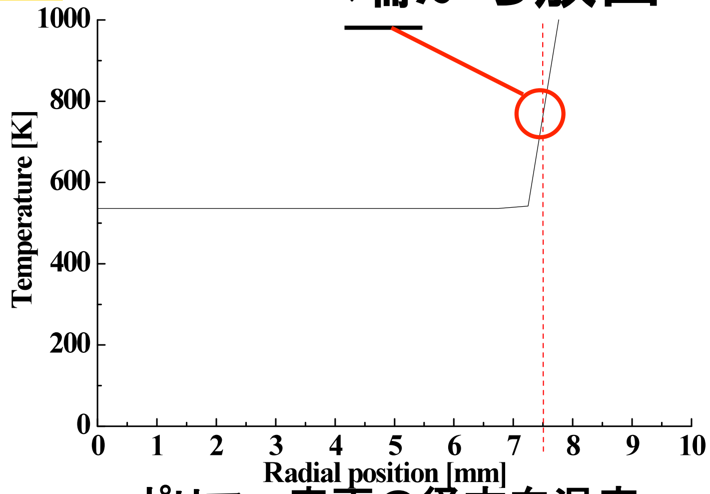

ポリマー表面の径方向温度

スポレーション粒子の初期条件

対象ポリマー材料	PA66
初期温度	500 K
初期直径	0.5 mm
初期速度	1.5 m/s

計算終了条件

初期直径の1/100以下
⇒ 蒸発して消滅した

スポレーション粒子の飛翔軌跡

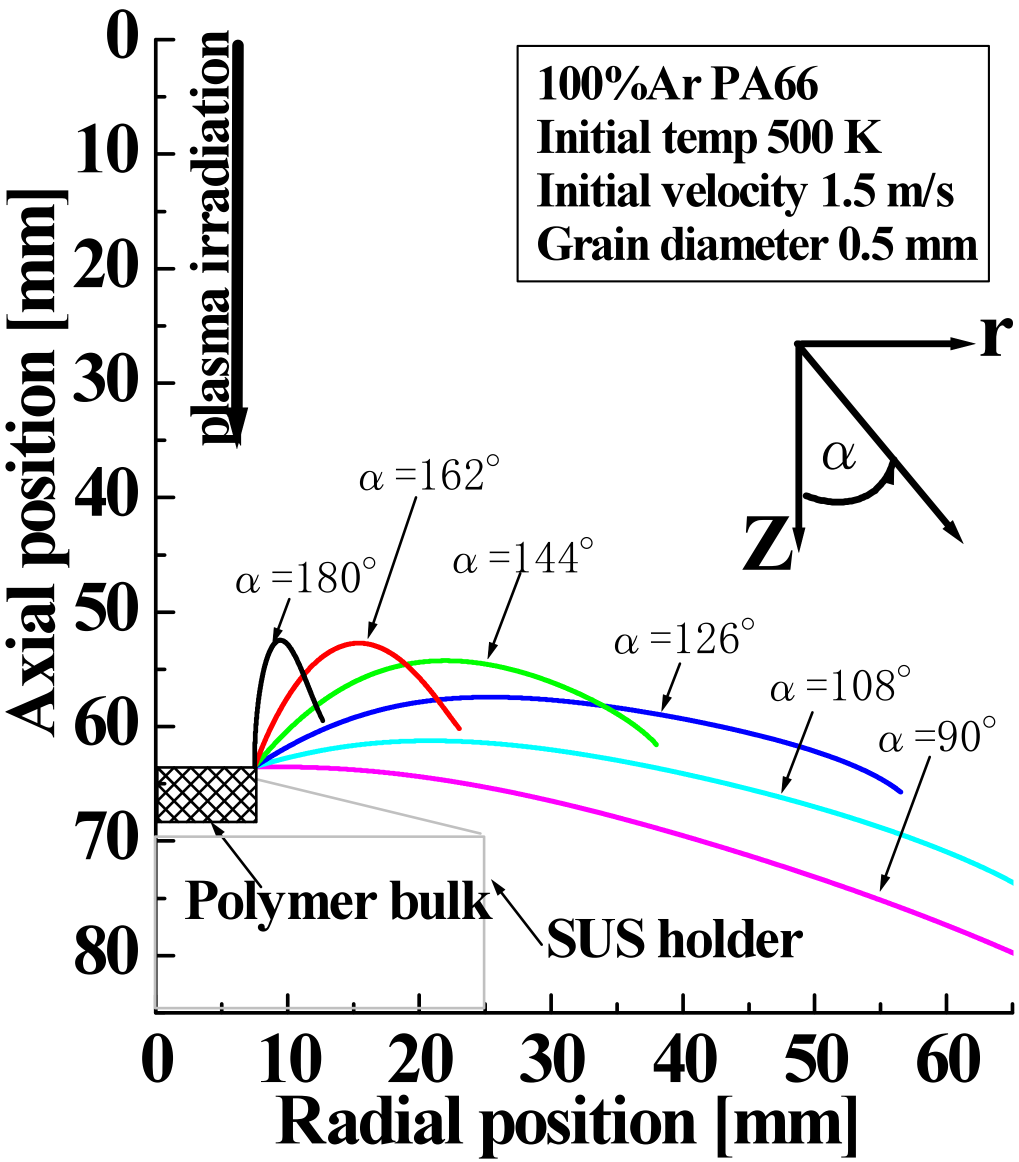

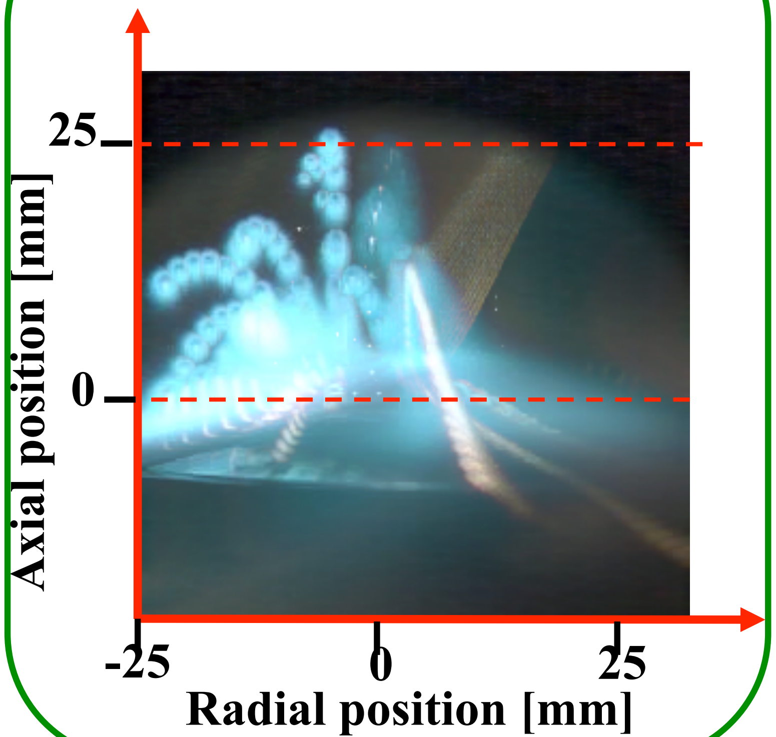

PA66の飛翔様相

軸方向に近い方向角
⇒ ほぼ同様な軌跡

飛翔軌跡の撮影結果と計算結果との比較

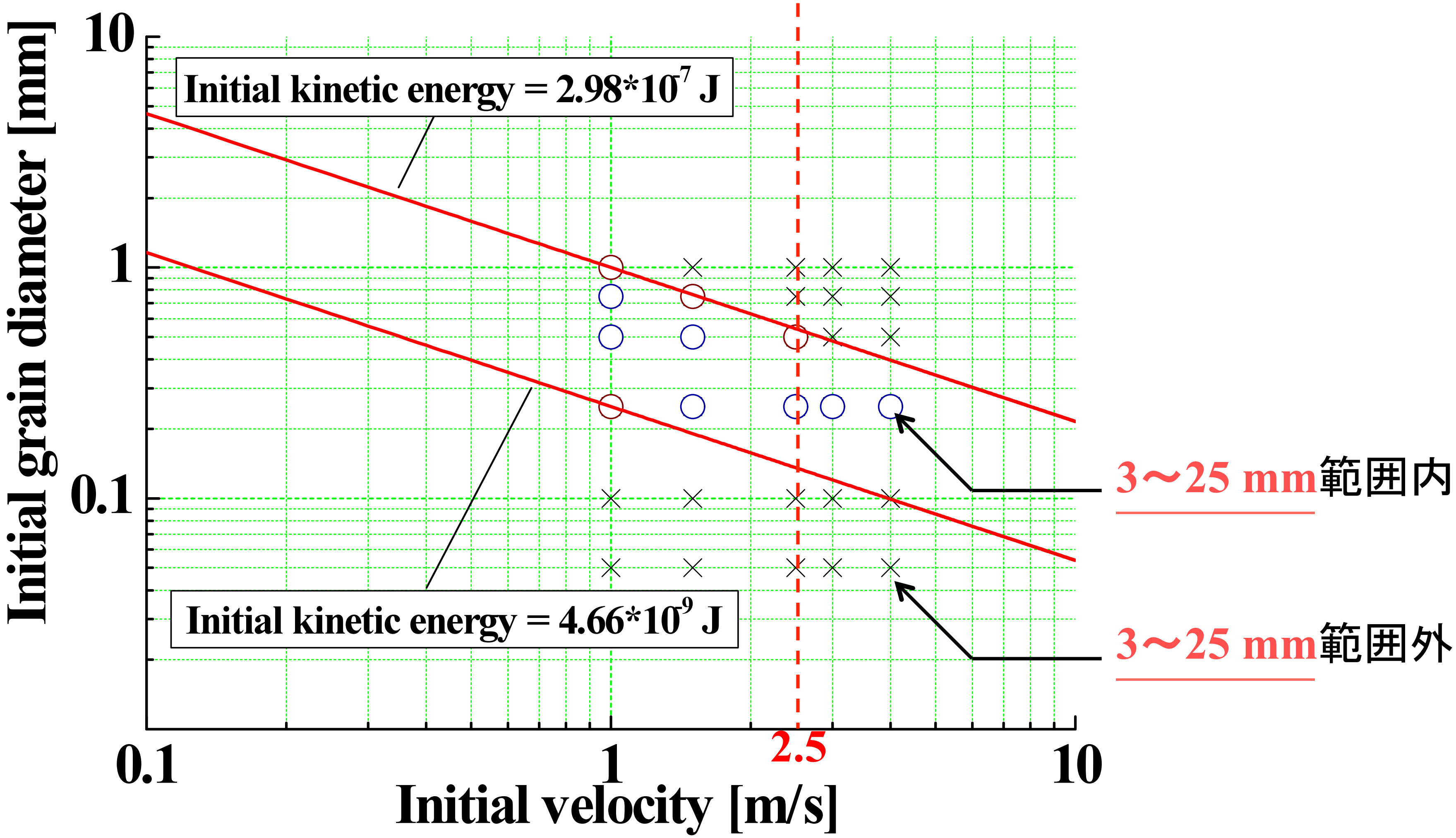

スポレーション粒子が飛翔時に持つ初期エネルギー ➡ **1～100 nJ程度**

高速度ビデオカメラ撮影 ⇒ 初期速さ 約2.5 m/s ➡ **直径約0.15 mm**

The present case

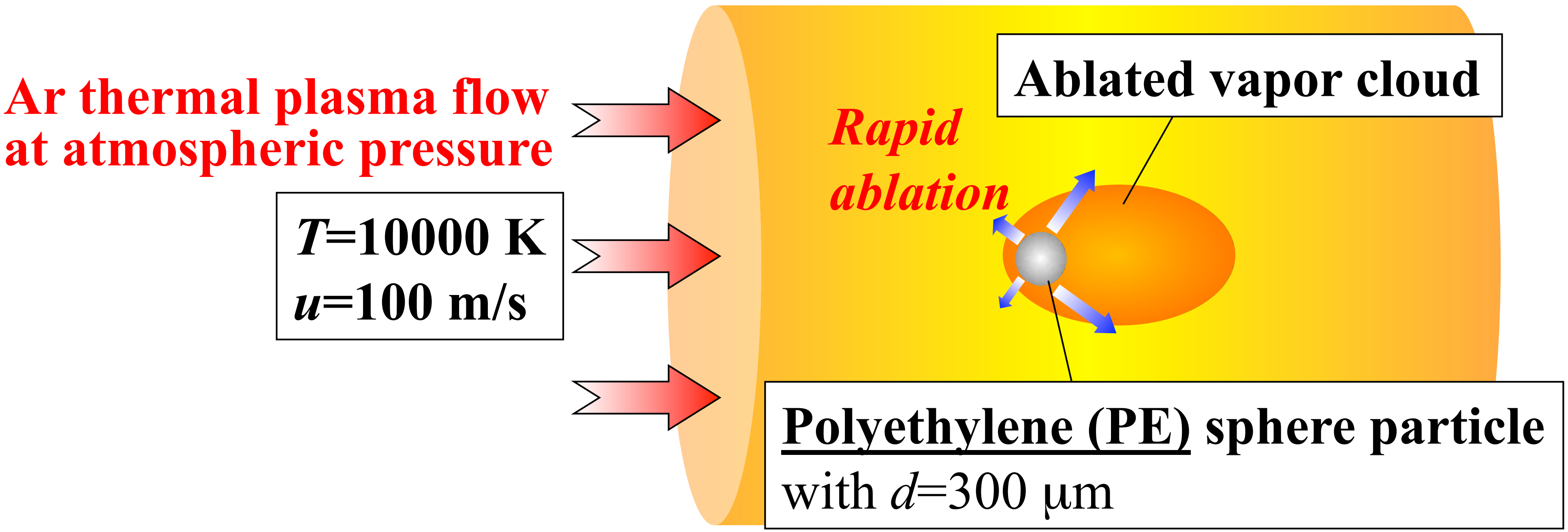

The physics to be considered:

-Heat transfer

-Rapid ablation → Rapid pressure rise → Strong gas flow

-Rapid ablation → Energy loss

-Change in properties of the surrounding plasma

-Transport of ablated vapor

-Shielding due to the ablated vapor from Ar plasmas

Governing Equations

-Mass equatio

$$\frac{D\rho}{Dt} = -\rho(\nabla$$

-Momentum e

$$\frac{D\boldsymbol{u}}{Dt} = -\frac{1}{\rho}\nabla$$

These equations are solved by the CIP-CUP method developed by Prof. Yabe.
The **CIP-CUP method** is an **unified algorithm to solve <u>incompressible and compressible</u> flow, and thus it can simulate <u>multiphase flow</u>**.

-Energy equation:

$$\frac{DT}{Dt} = -\frac{p_{\mathrm{th}}}{\rho C_{\mathrm{v}}}(\nabla \bullet \boldsymbol{u}) + \overbrace{\frac{1}{\rho C_{\mathrm{v}}}\left[\nabla \bullet (\lambda \nabla T) - P_{\mathrm{rad}} - S_{\mathrm{abl}} - \varepsilon_{\mathrm{emit}}\sigma_{\mathrm{sb}}(T^4 - T_{\mathrm{a}}^4)\delta\Omega\right]}^{Q_{\mathrm{heat}}}$$

-Mass fraction of ablated vapor:

$$\frac{DY_{\mathrm{pol}}}{Dt} = \frac{1}{\rho_{\mathrm{g}}}\left[\nabla \bullet (\rho_{\mathrm{g}} D_{\mathrm{pol}} \nabla Y_{\mathrm{pol}}) + S_{\mathrm{Cg}}\right]$$

f: the volume of fraction

$$f = \frac{V_{\mathrm{solid}}}{V_{\mathrm{CV}}}$$

-VOF function:

$$\frac{Df}{Dt} = -S_f$$

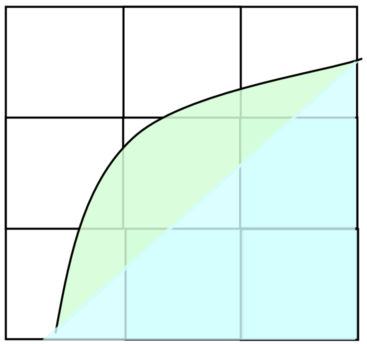

$$\begin{cases} f=1\text{: Solid} \\ 0<f<1\text{: containing solid surface} \\ f=0\text{: Gas or plasma} \end{cases}$$

-Equation of state (EOS):

$$p = p(\rho, T)$$

Thermodynamic and transport properties of Ar and ablated vapor

Equilibrium composition of Ar, and ablated vapor

Thermodynamic properties

The first order approximation of Chapman-Enskog method

Transport properties

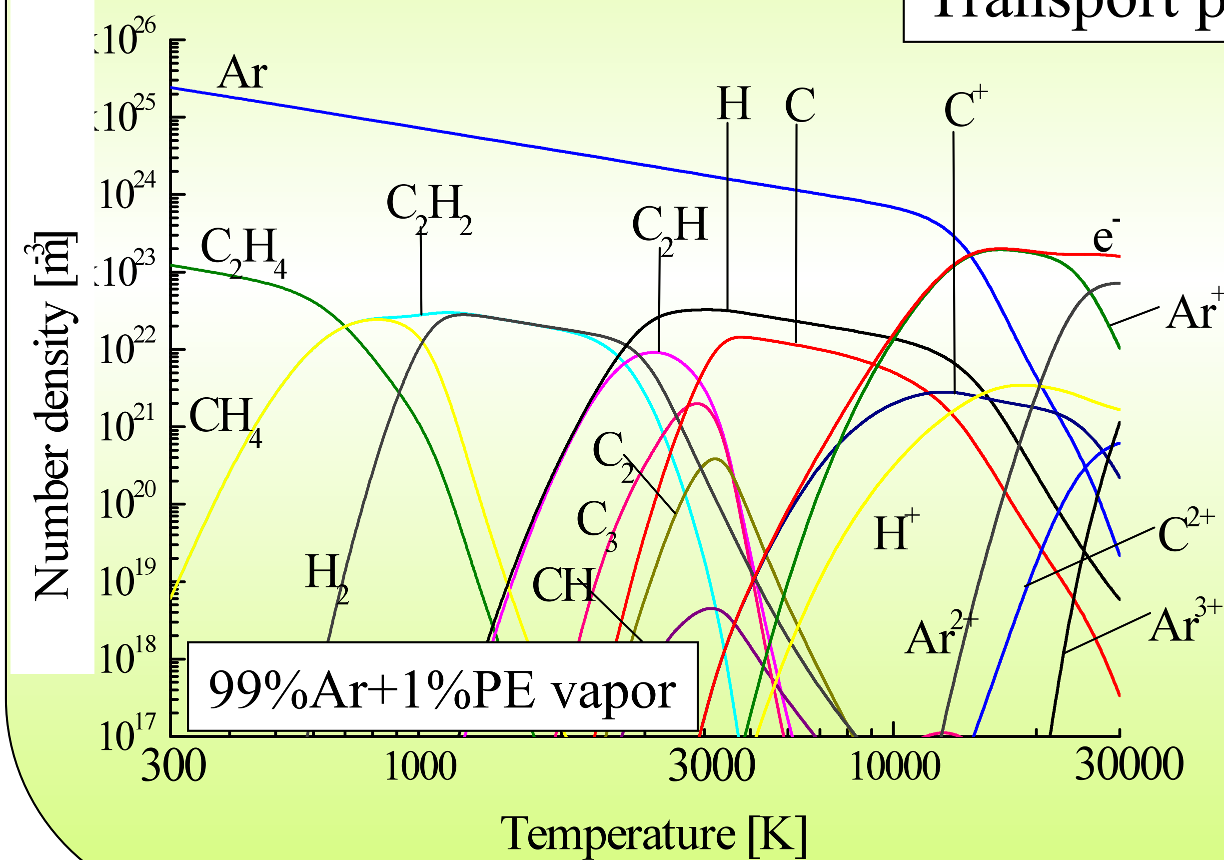

Thermal conductivity

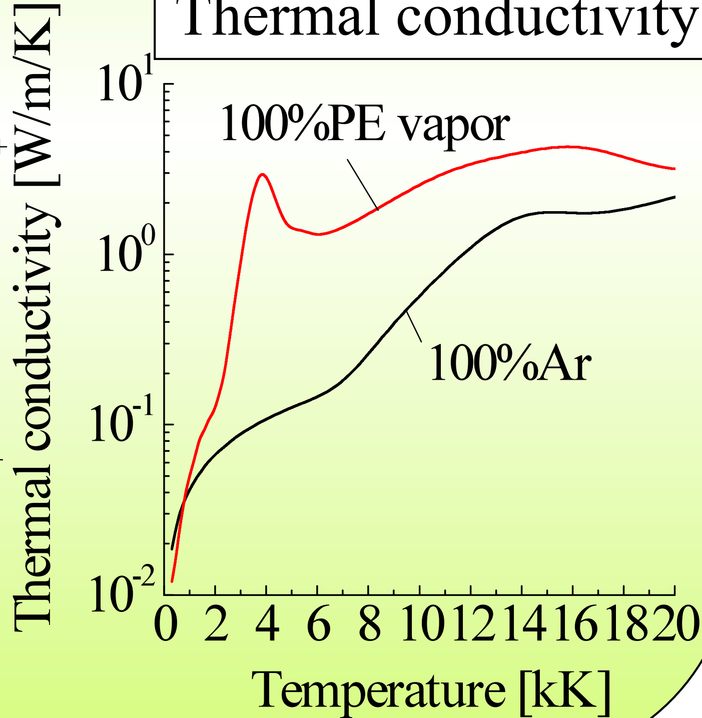

Calculation space

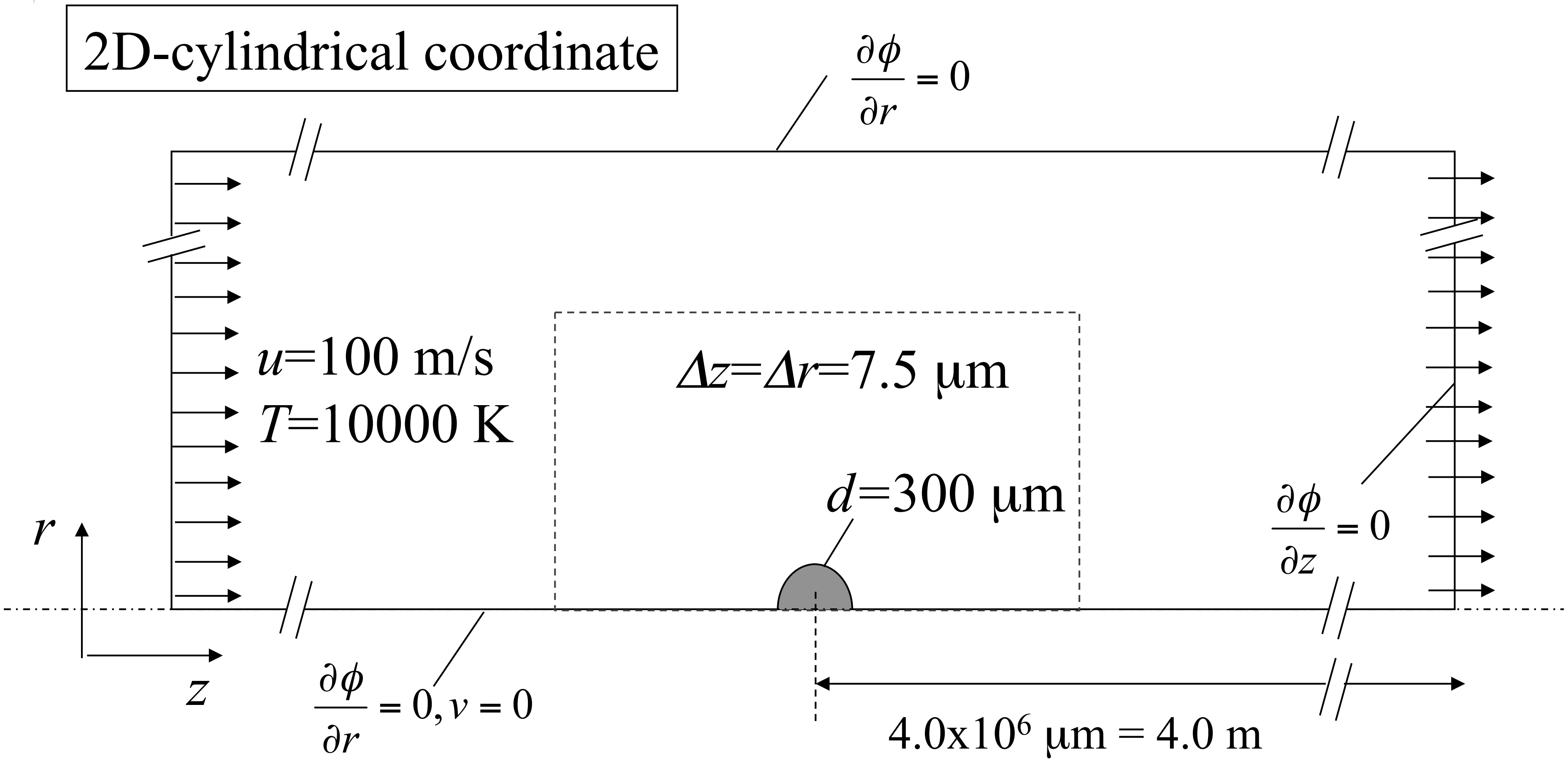

-Kundsen number: Ku~0.03

-Reynolds number: Re~0.65

Gas flow velocity and temperature fields

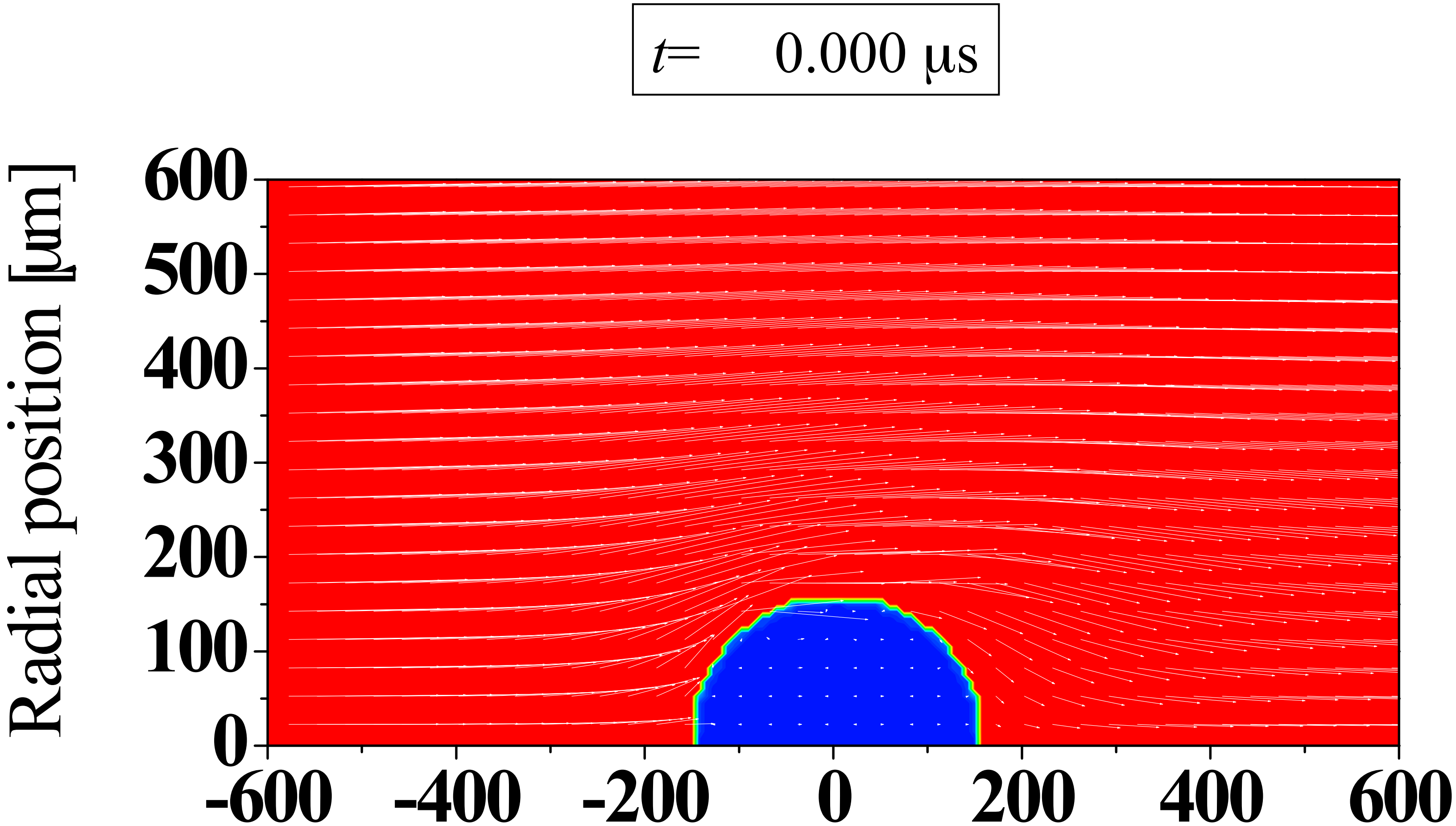

Initial temperature: T=10000 K for Ar plasma, T=300 K for PE particle
Initial gas flow field was calculated without ablation

Gas flow velocity and temperature fields

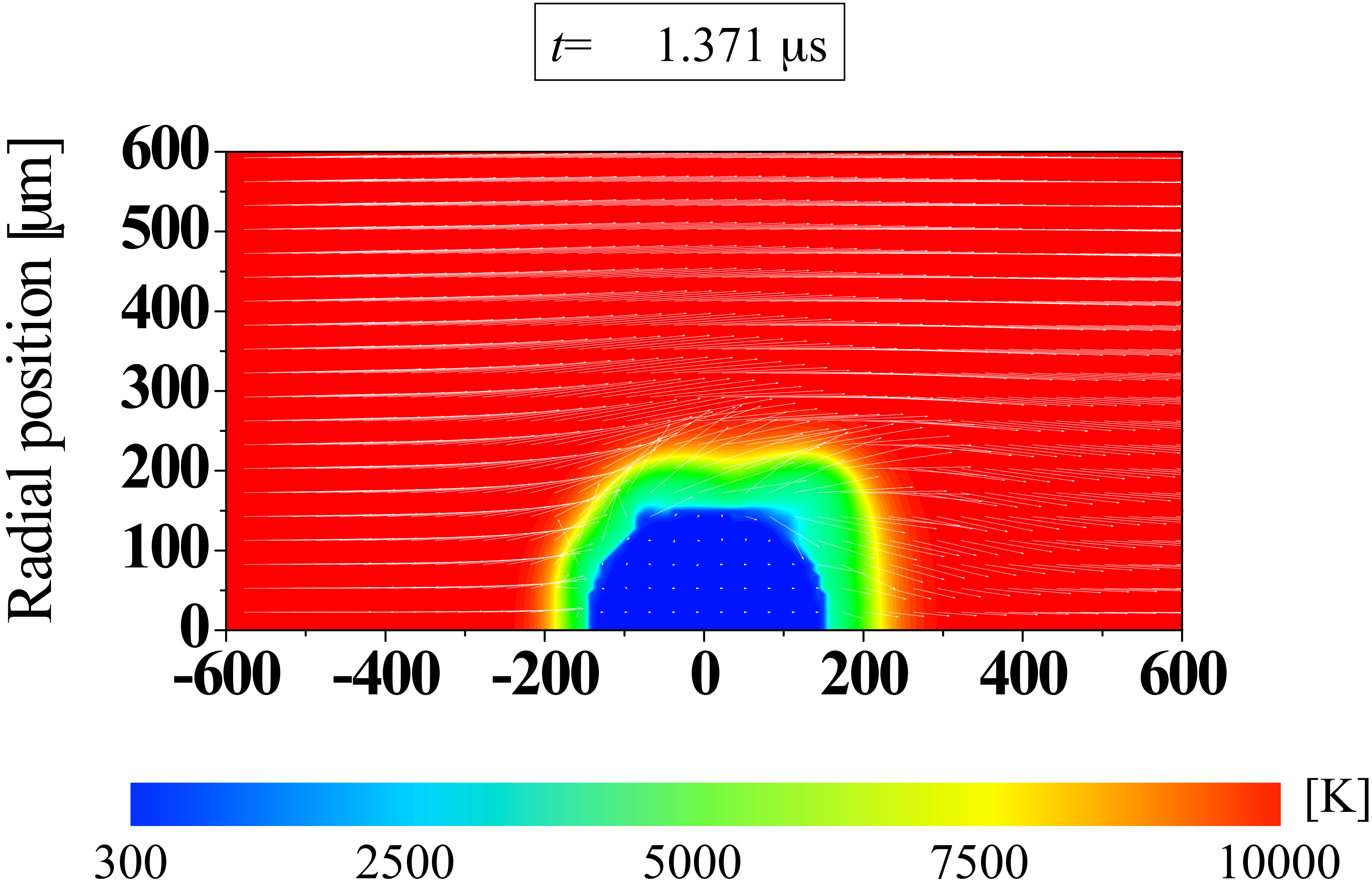

Gas flow velocity and temperature fields

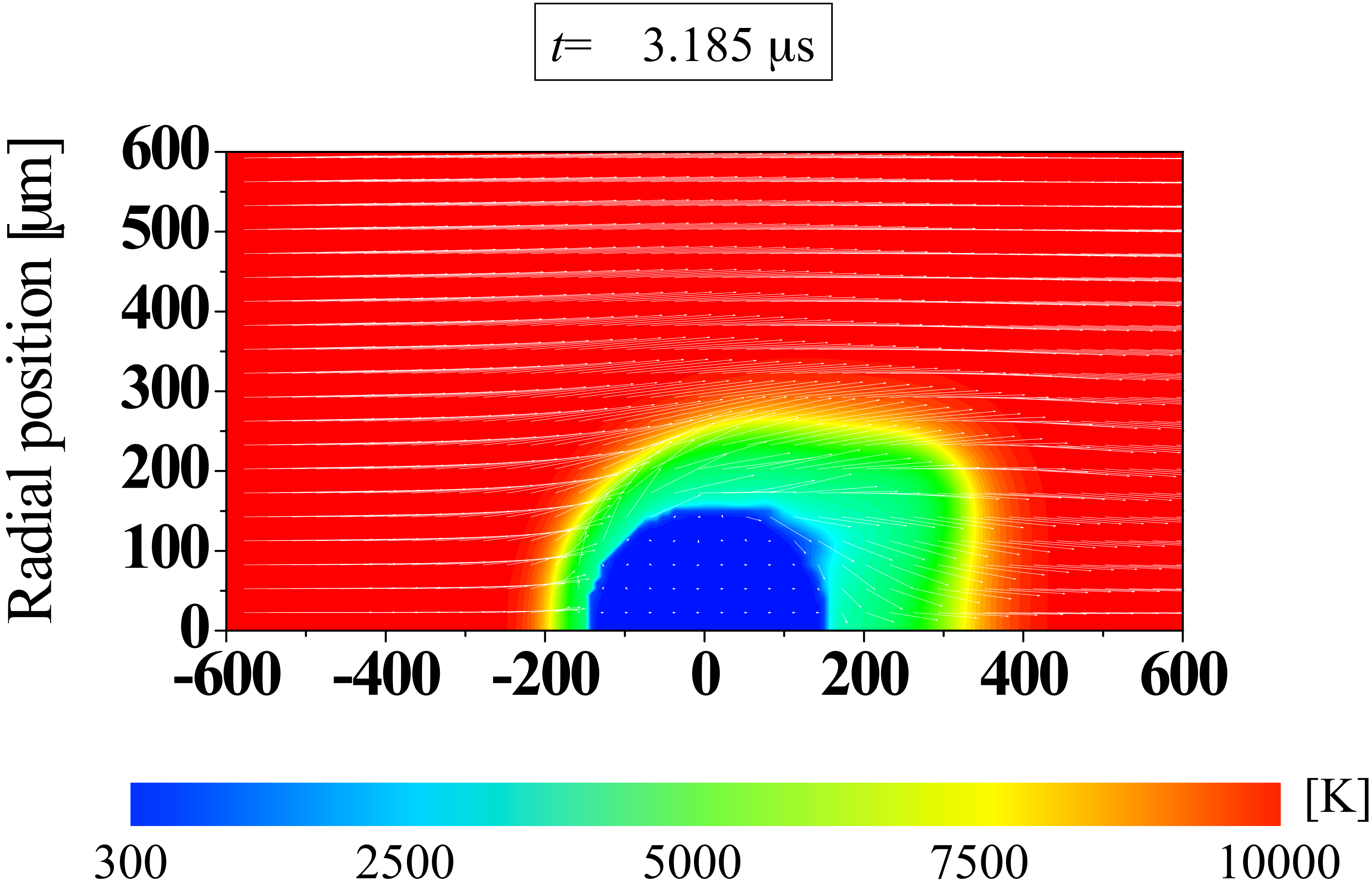

Gas flow velocity and temperature fields

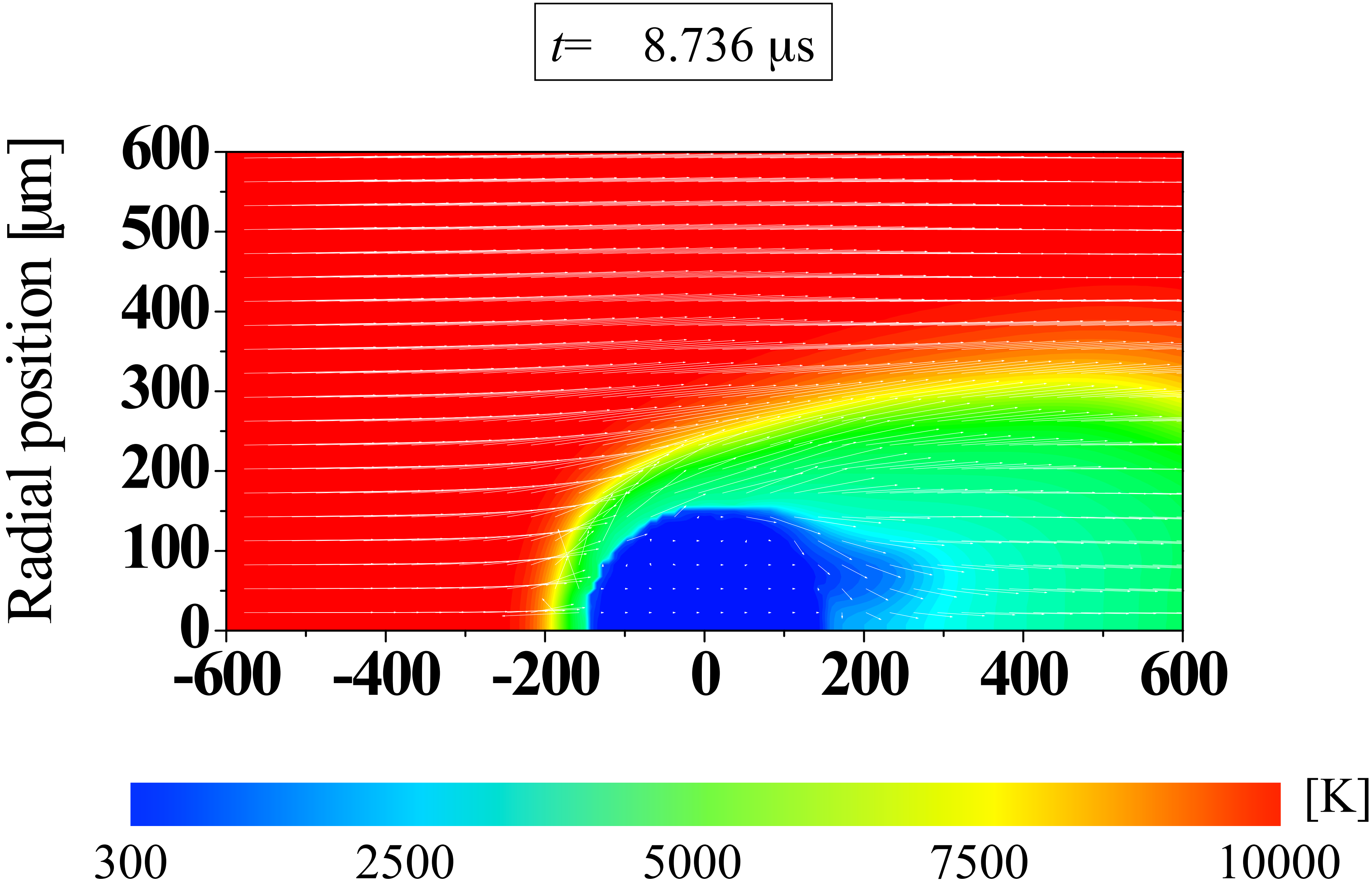

Gas flow velocity and temperature fields

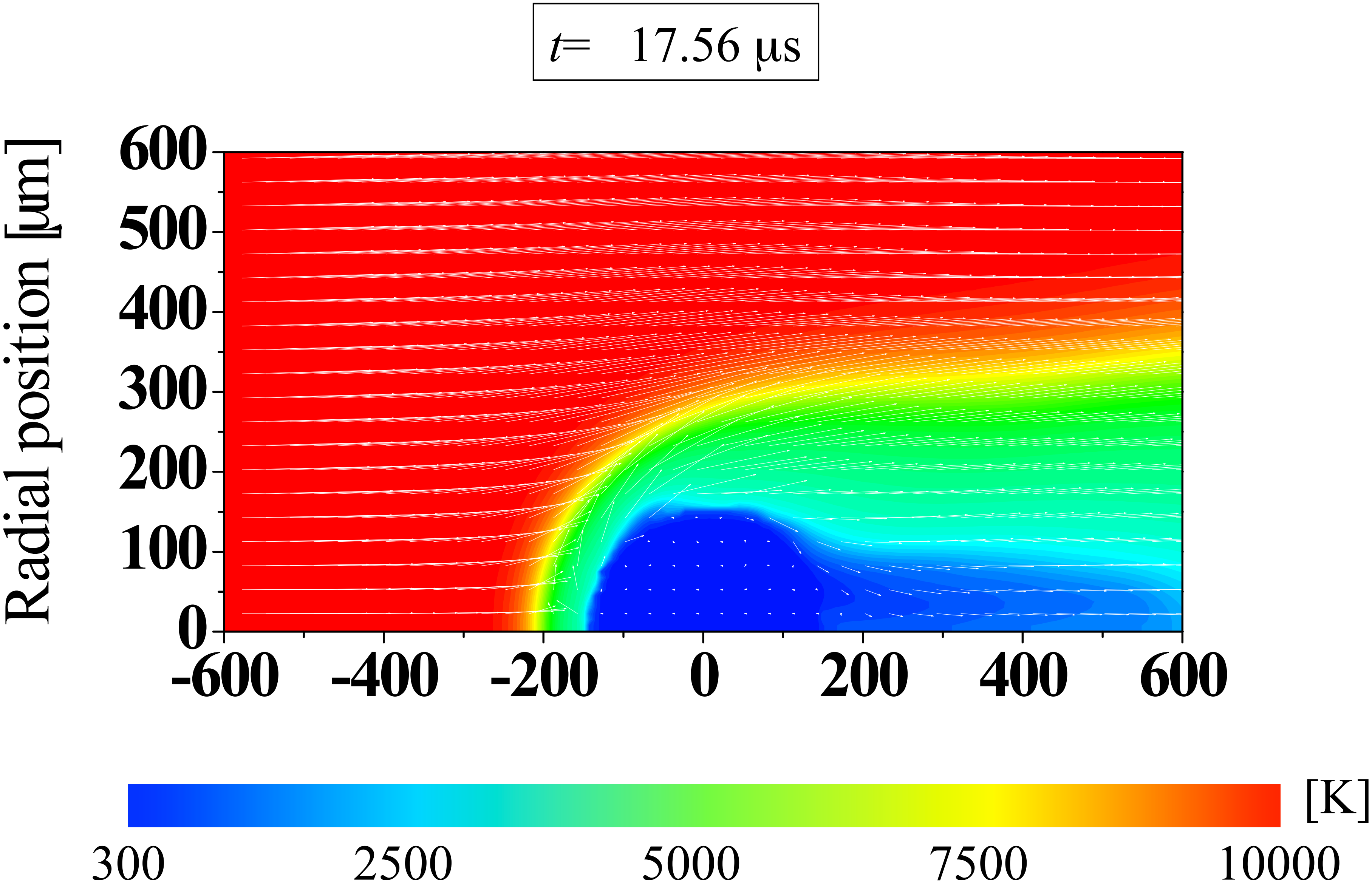

Gas flow velocity and temperature fields

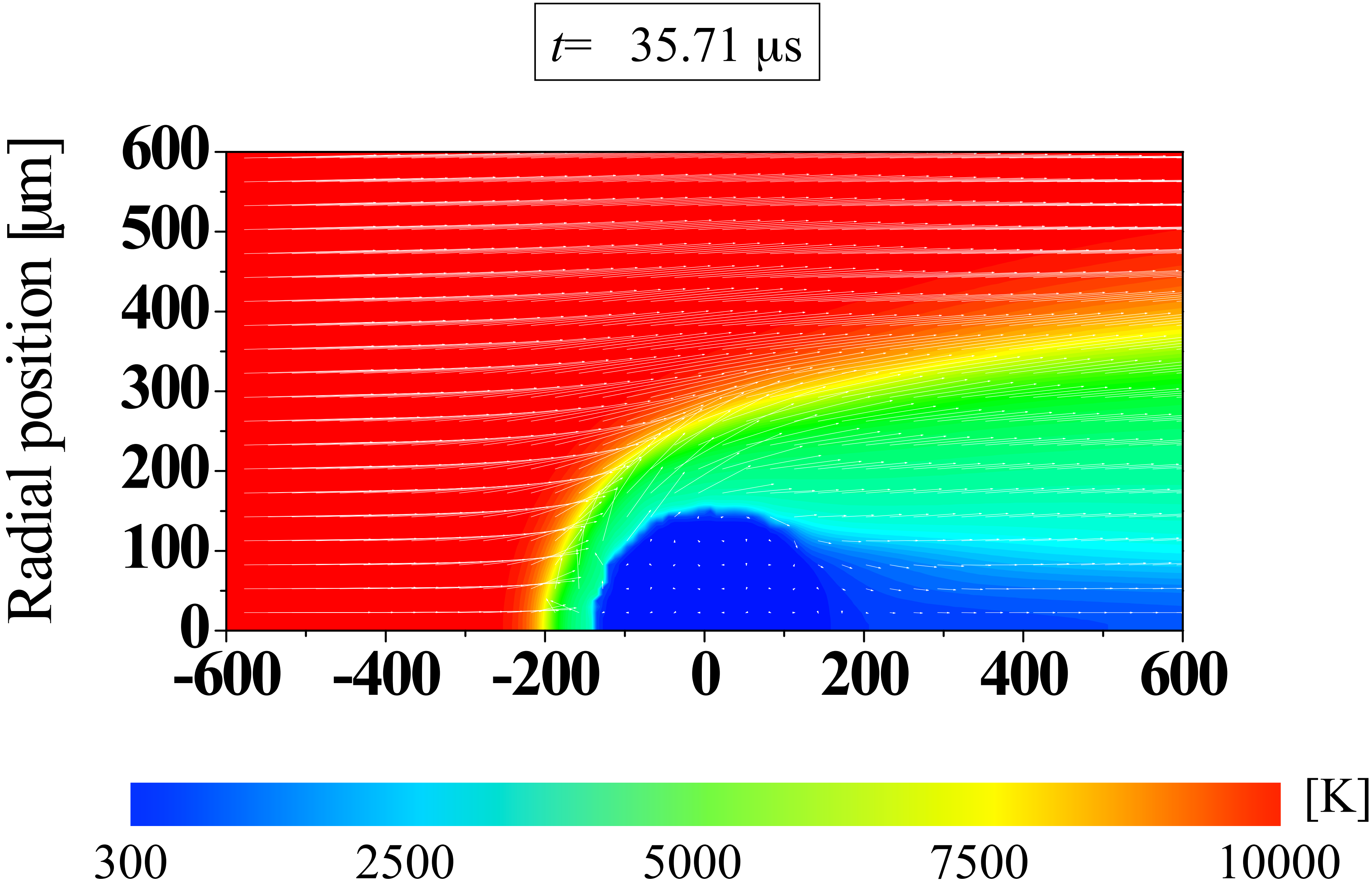

Gas flow velocity and temperature fields

t = 91.25 μs

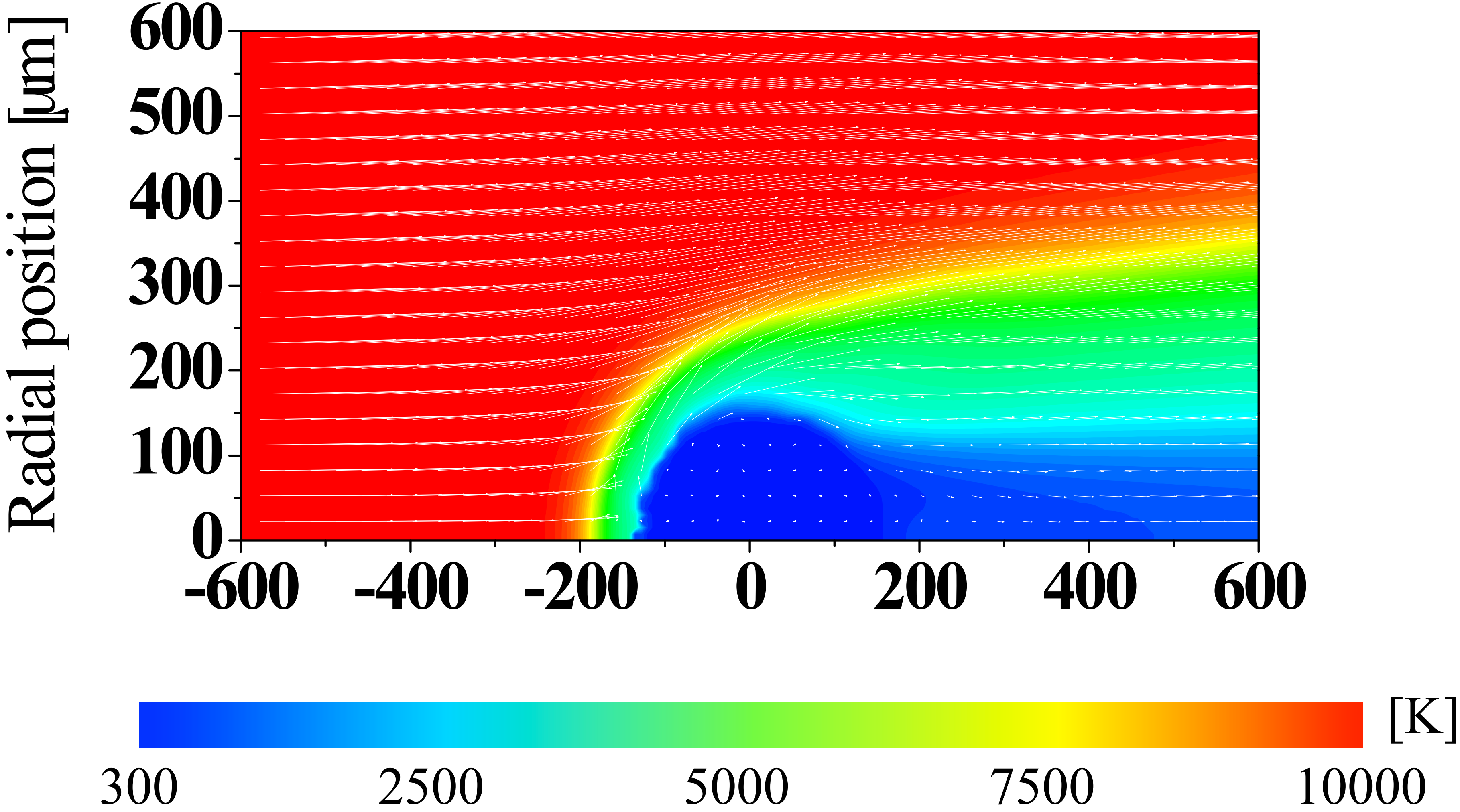

Gas flow velocity and temperature fields

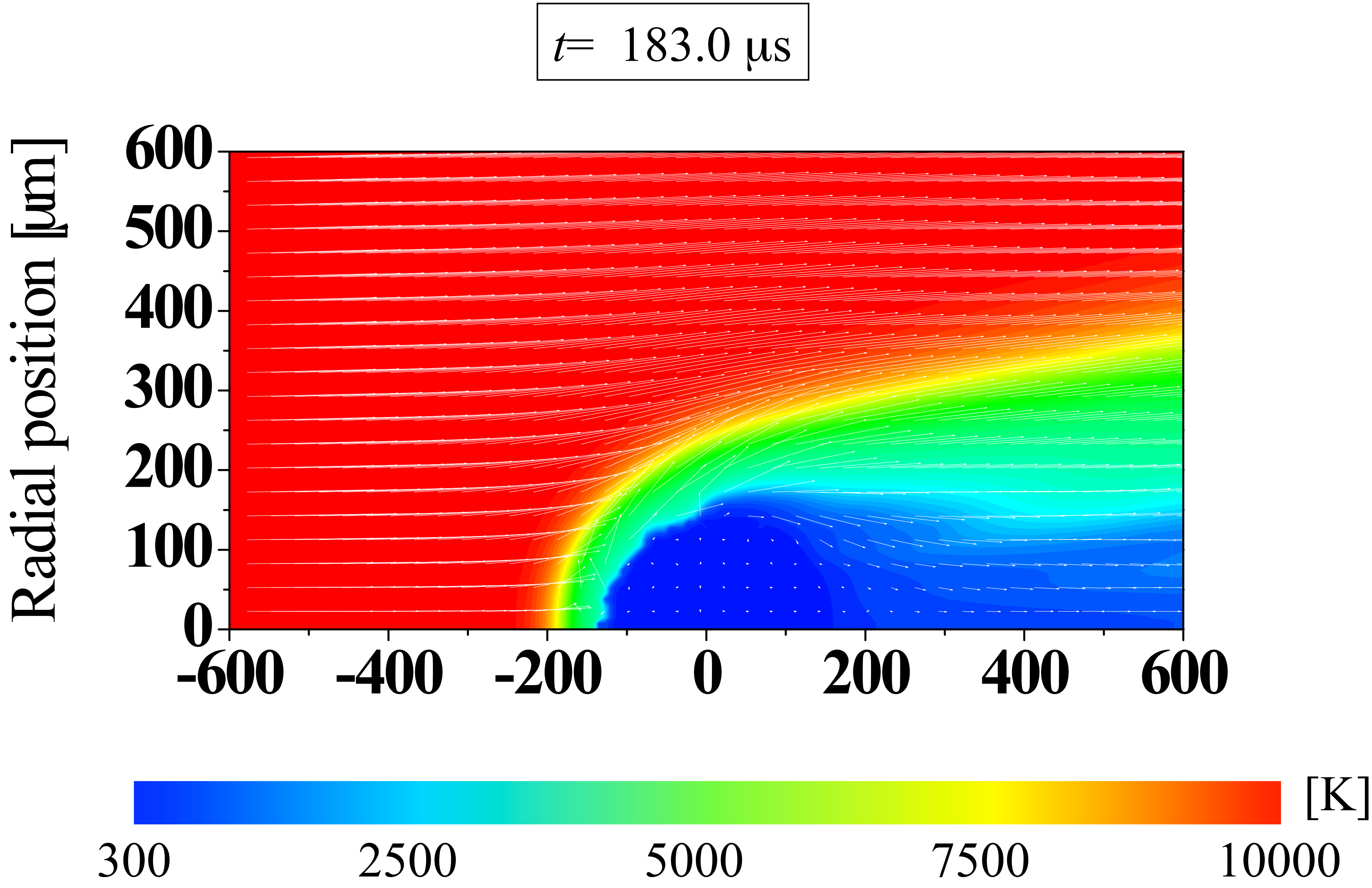

Gas flow velocity and temperature fields

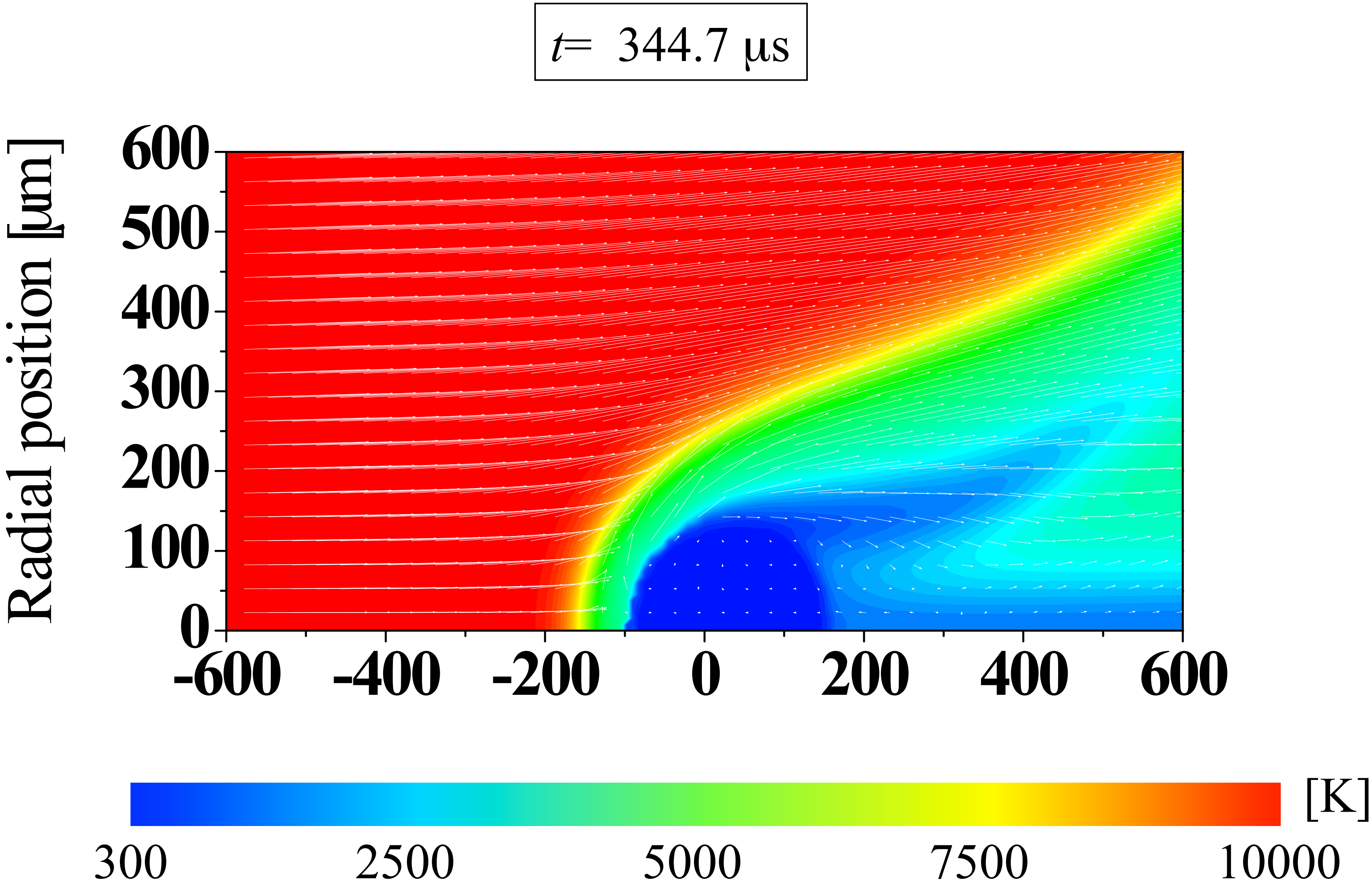

Gas flow velocity and temperature fields

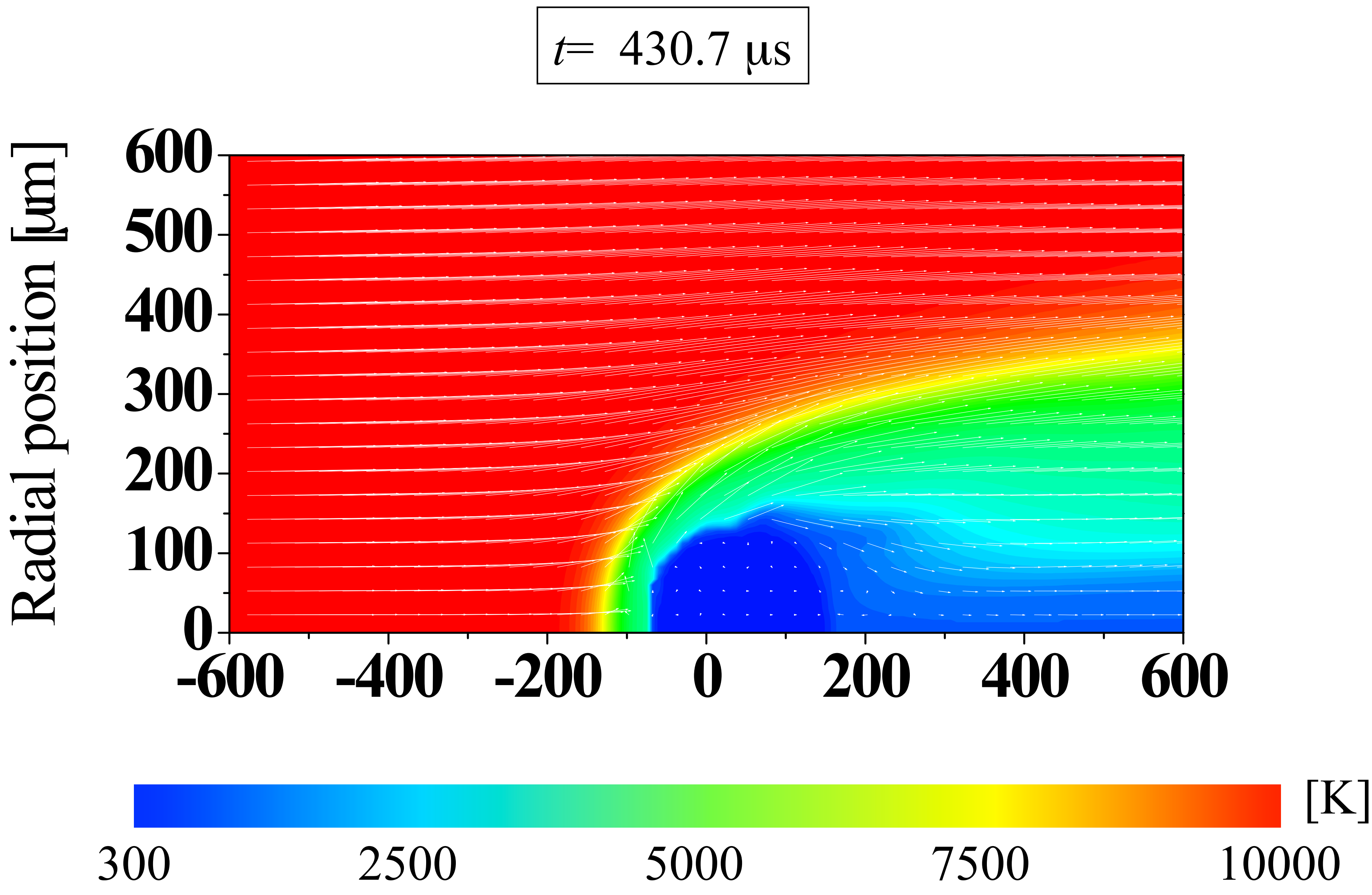

Gas flow velocity and temperature fields

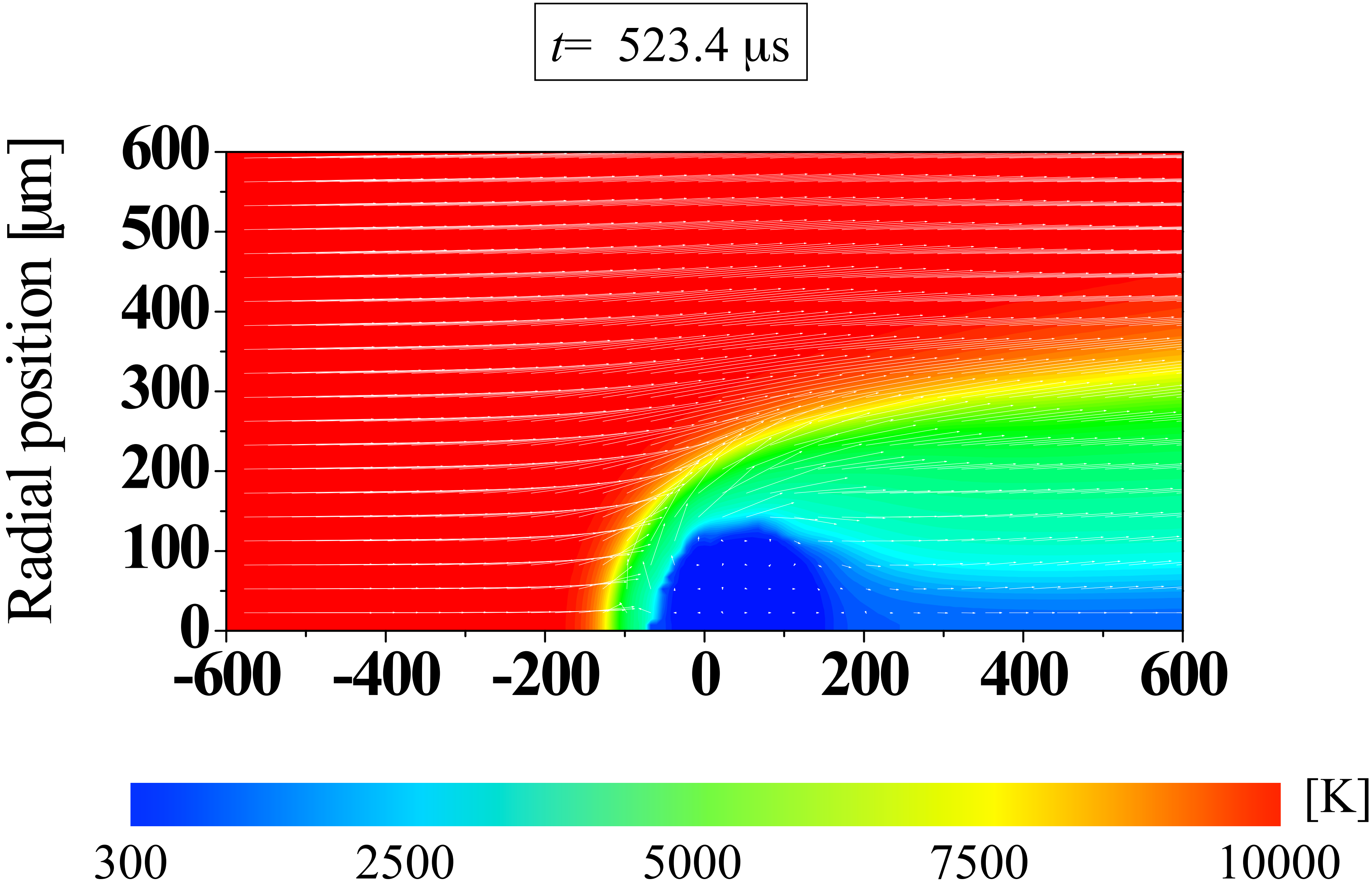

Gas flow velocity and temperature fields

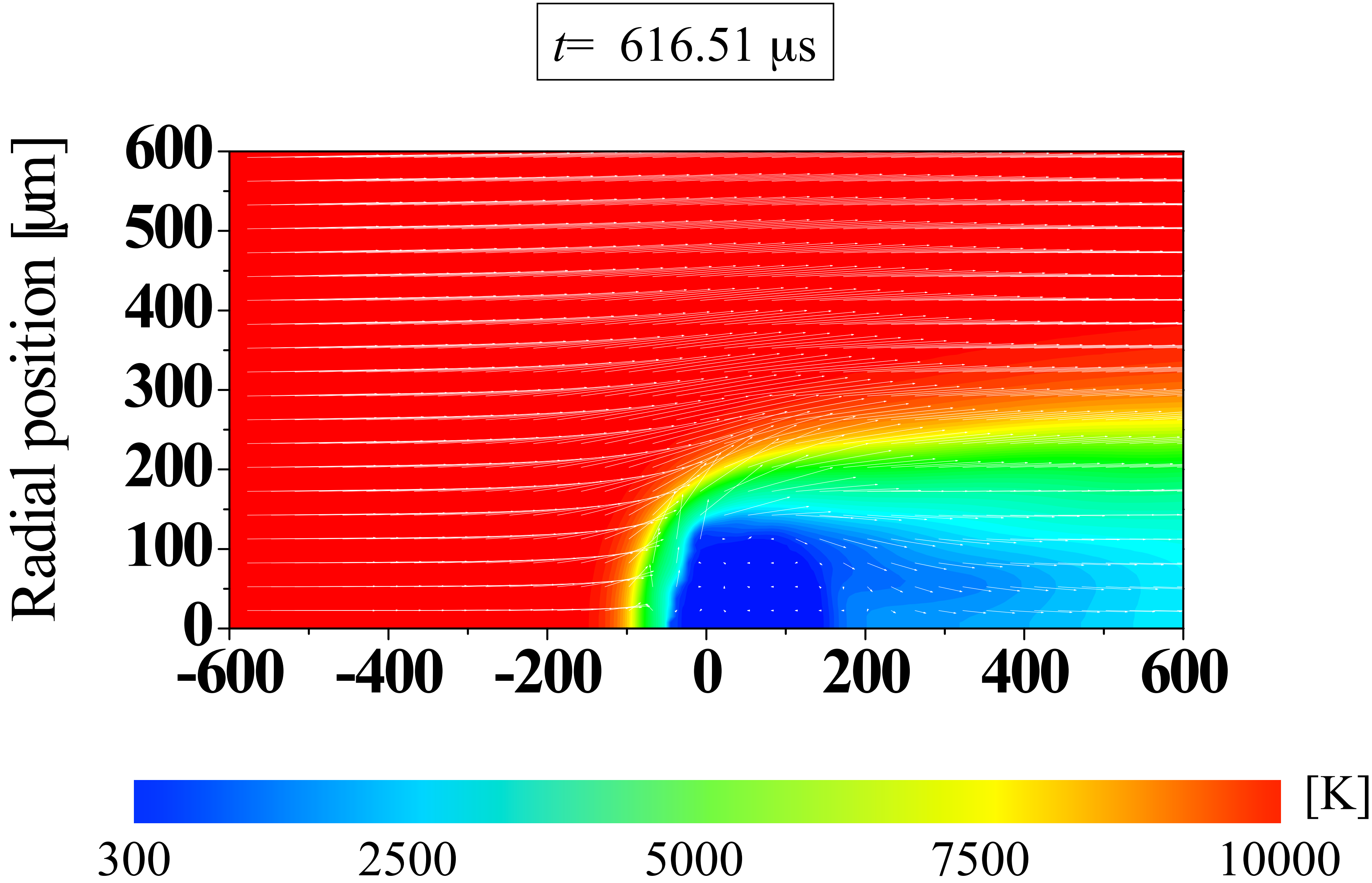

Gas flow velocity and temperature fields

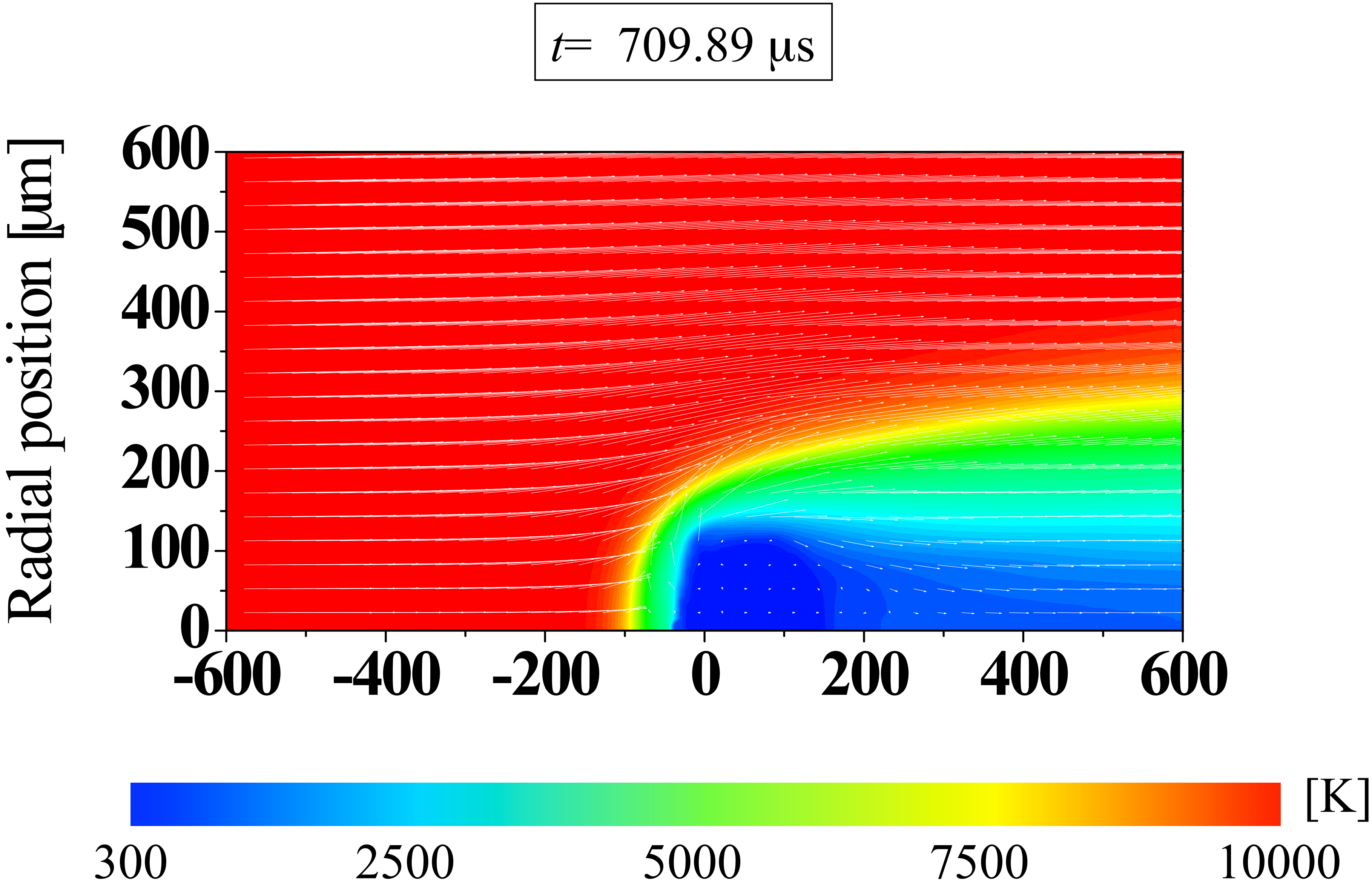

Gas flow velocity and temperature fields

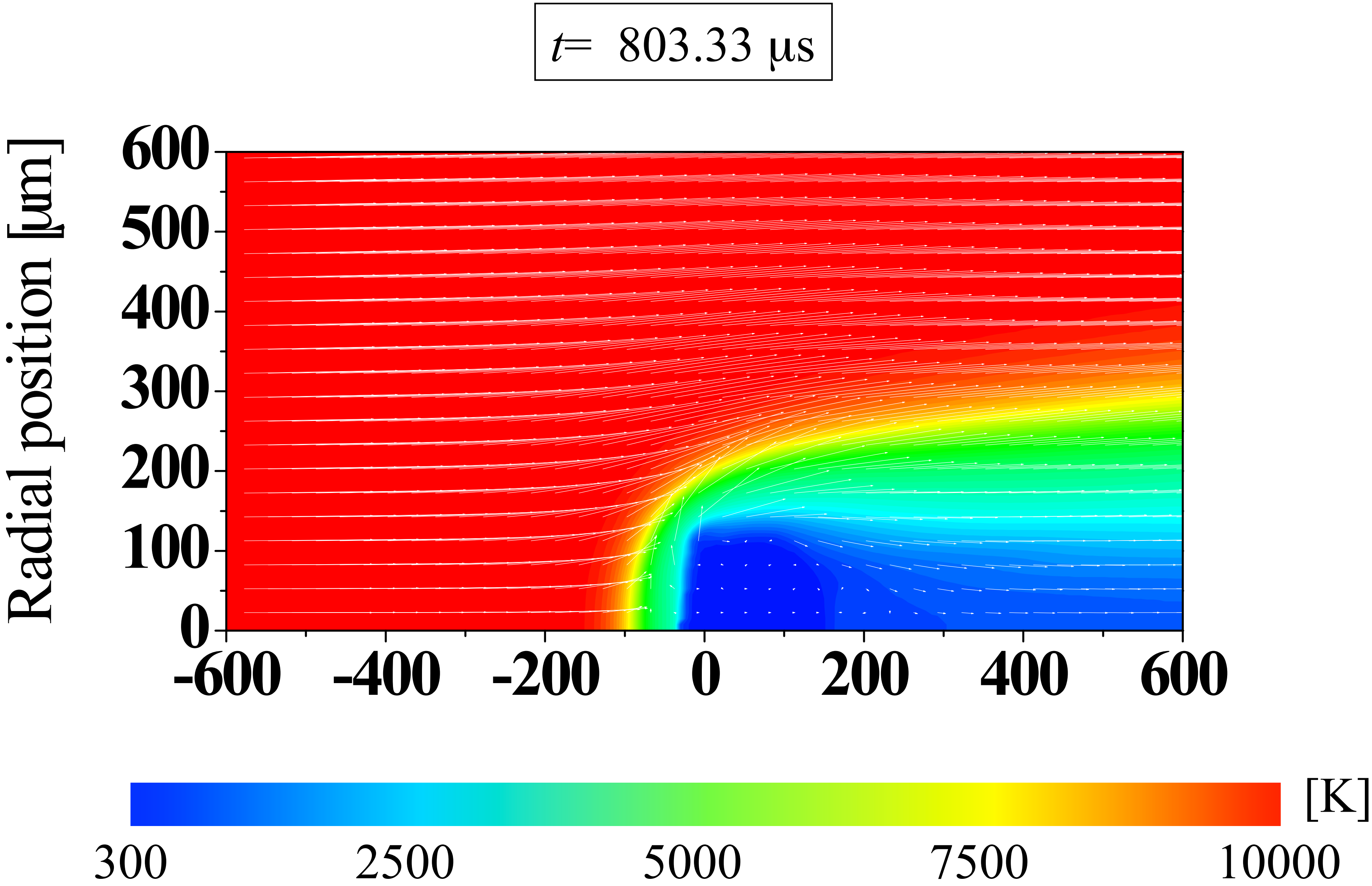

Time evolution in gas flow and temperature fields

-Rapid ablation occurs especially at upstream surface of the solid particle, which produces gas flow.

-Temperature around the particle is decreased because of thermal conduction and convection by low temperature ablated vapor.

-The ablated vapor shields the solid particle from direct interaction with the Ar plasma.

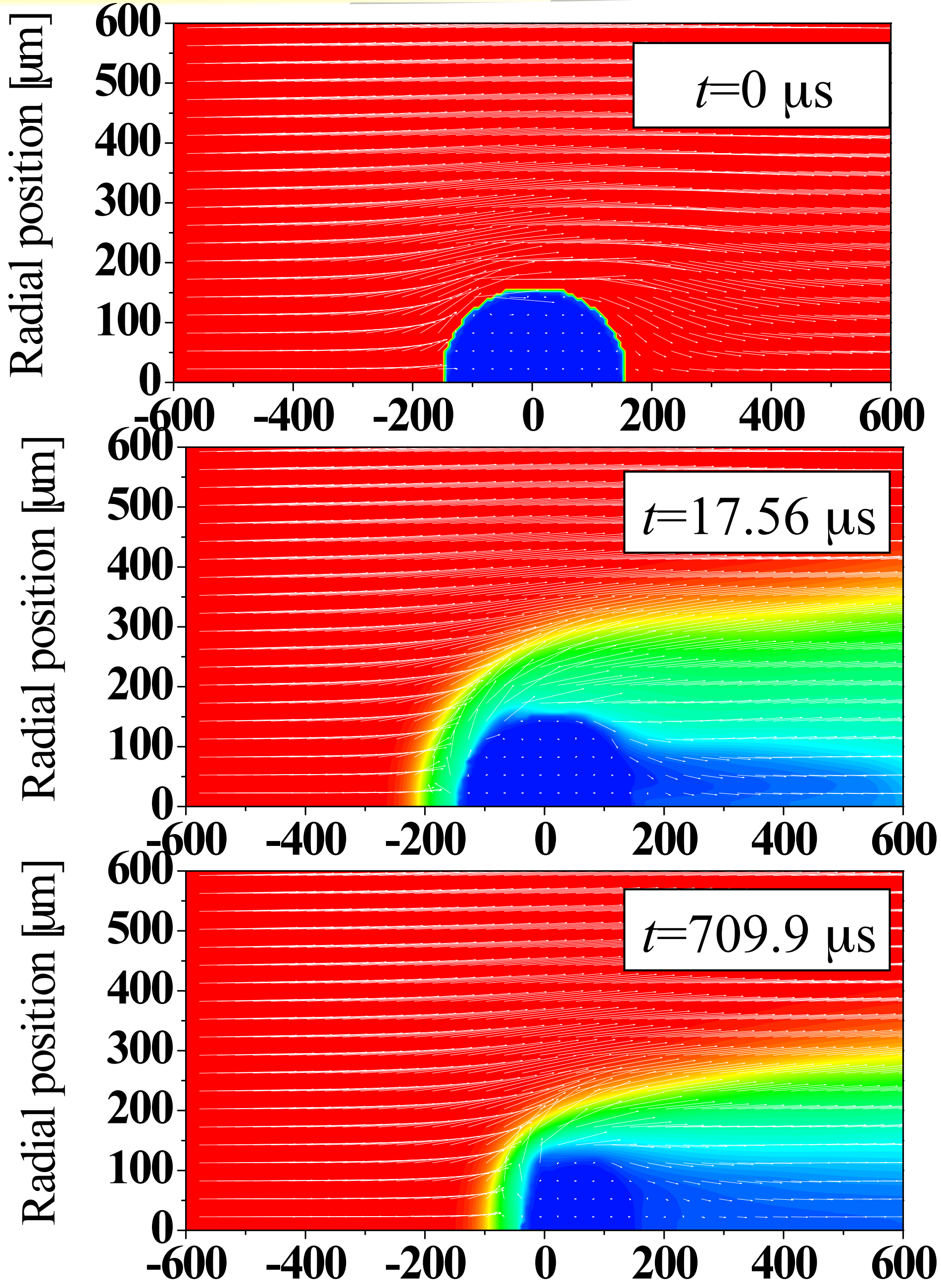

Mass fraction of ablated vapor and VOF function

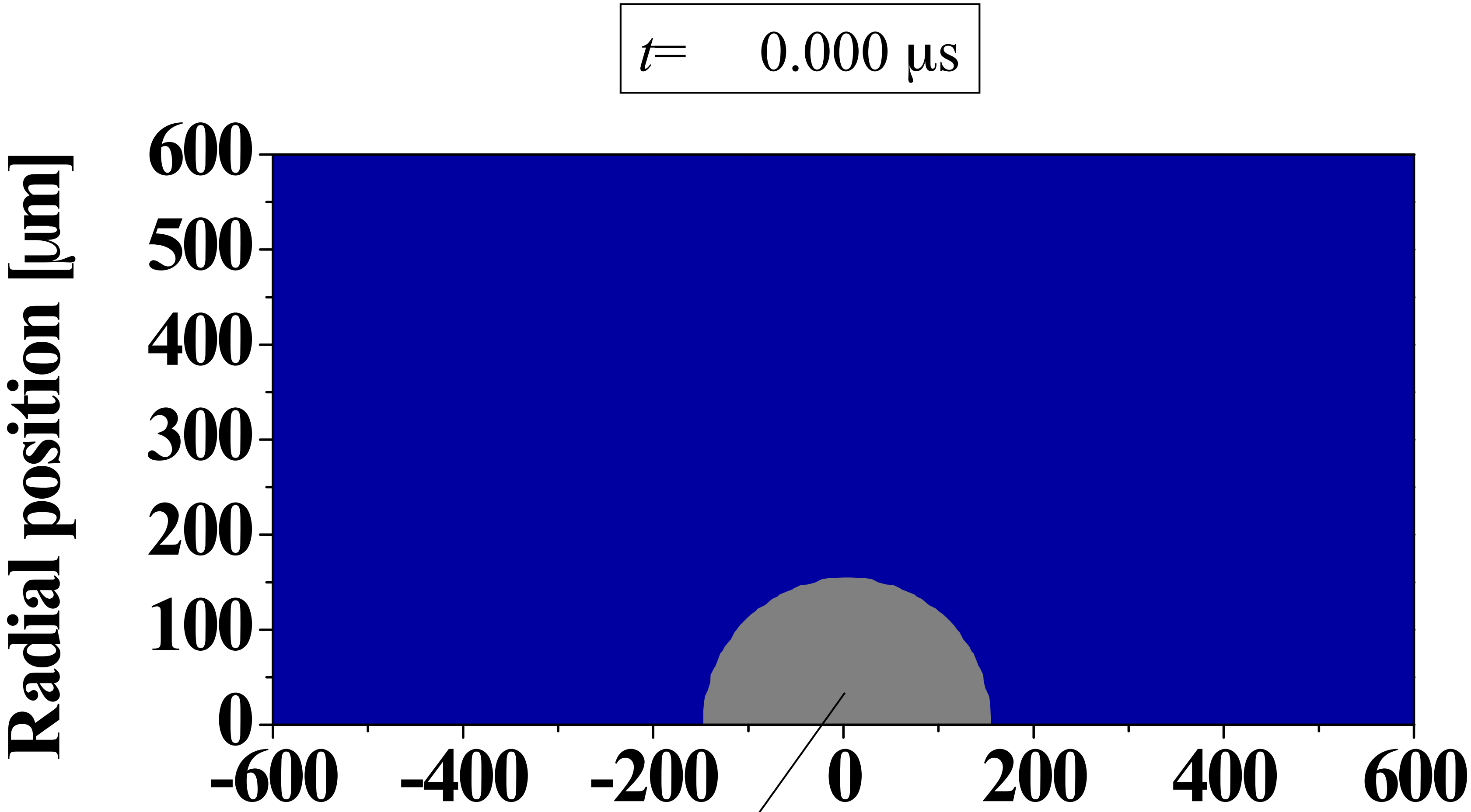

The VOF function. If f >0.5, the color is gray

Mass fraction of ablated vapor

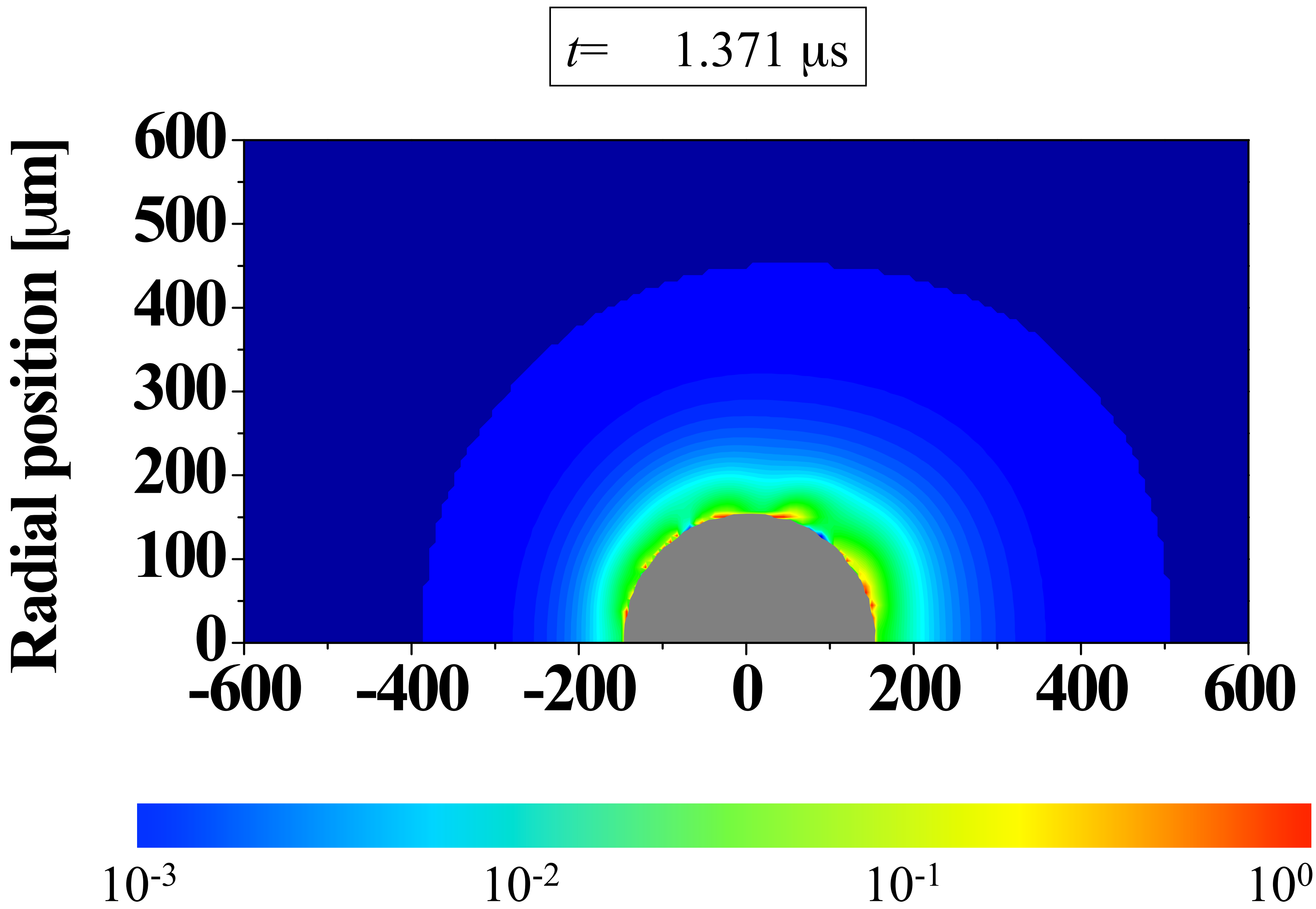

Mass fraction of ablated vapor

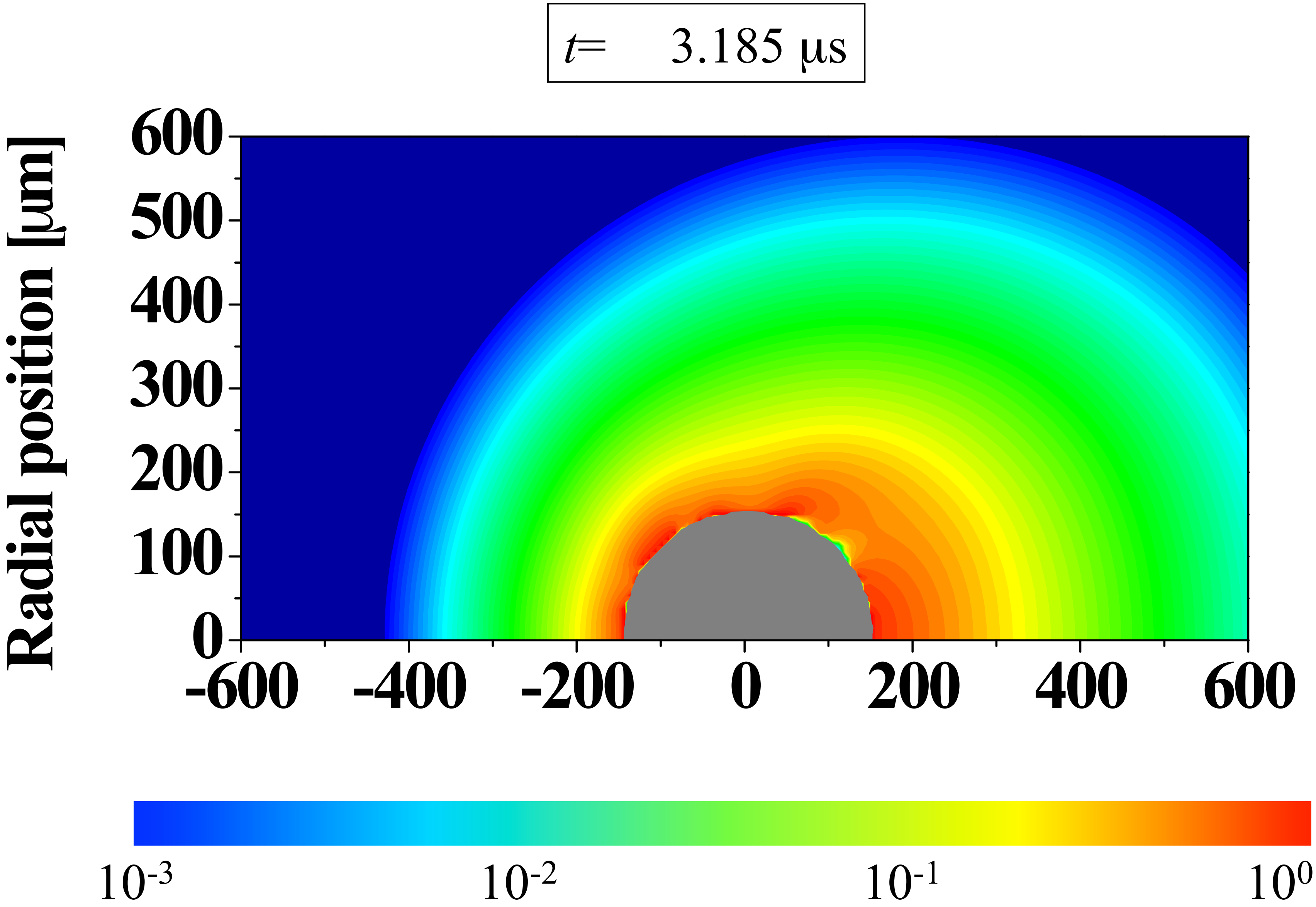

Mass fraction of ablated vapor

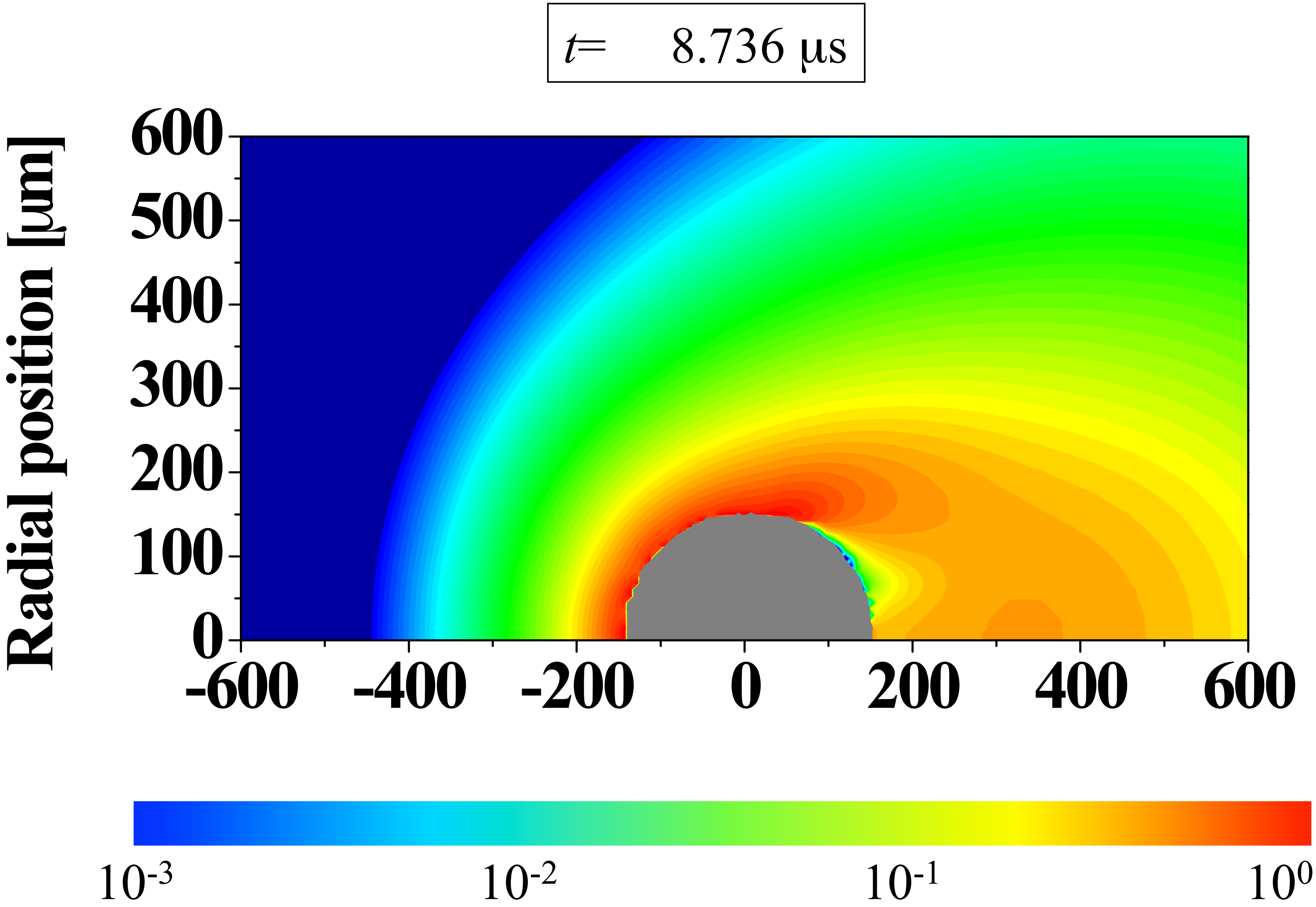

Mass fraction of ablated vapor

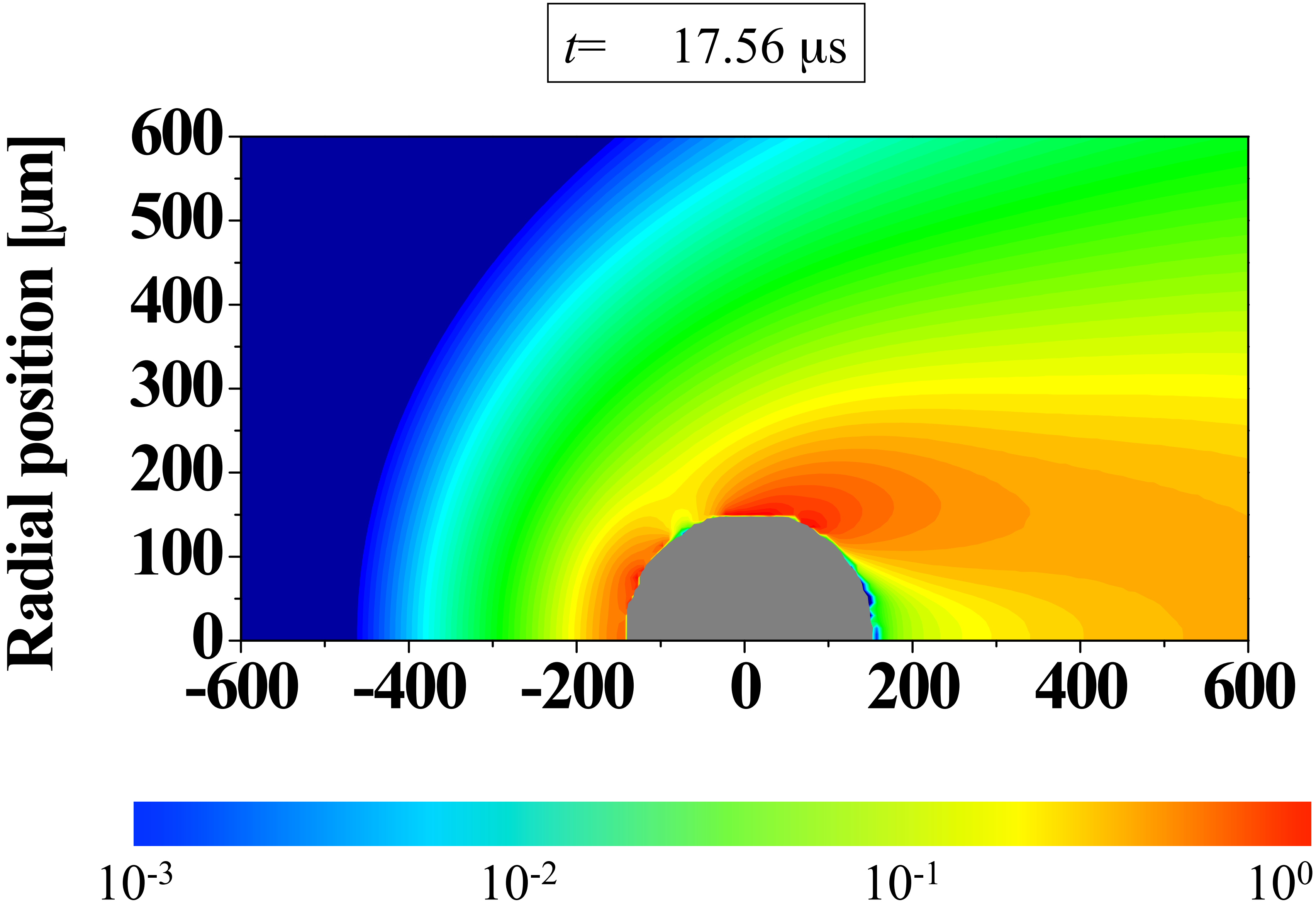

Mass fraction of ablated vapor

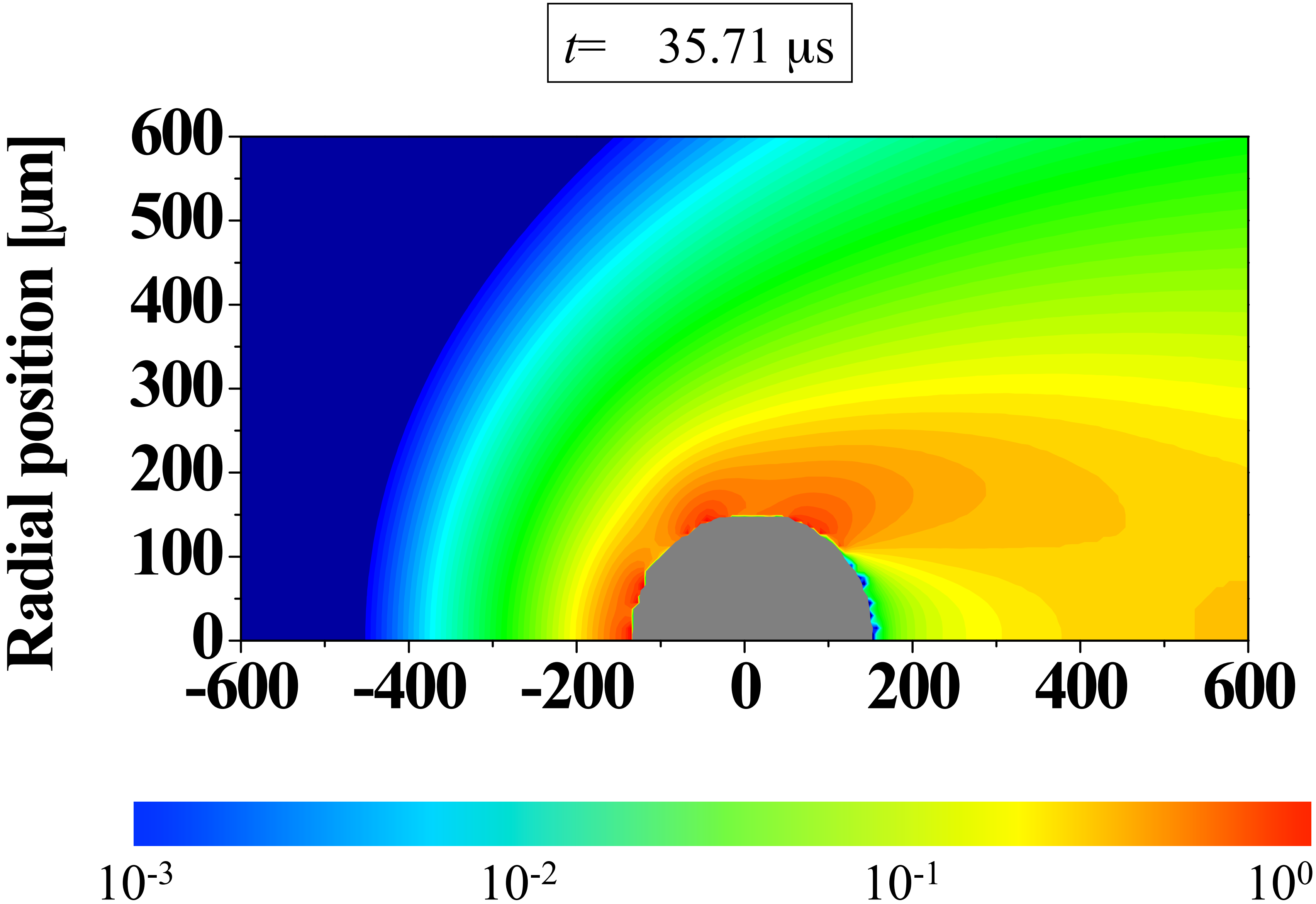

Mass fraction of ablated vapor

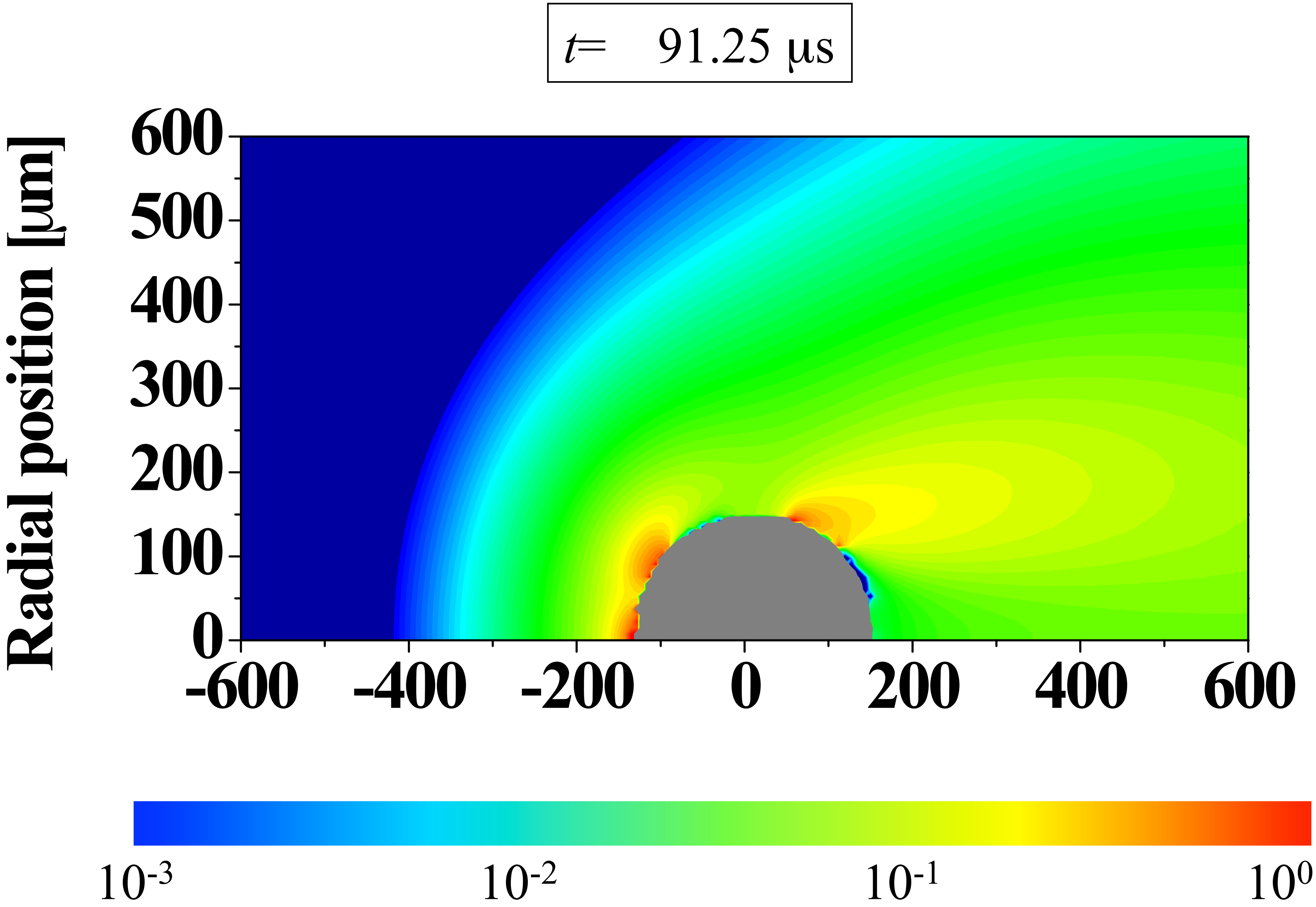

Mass fraction of ablated vapor

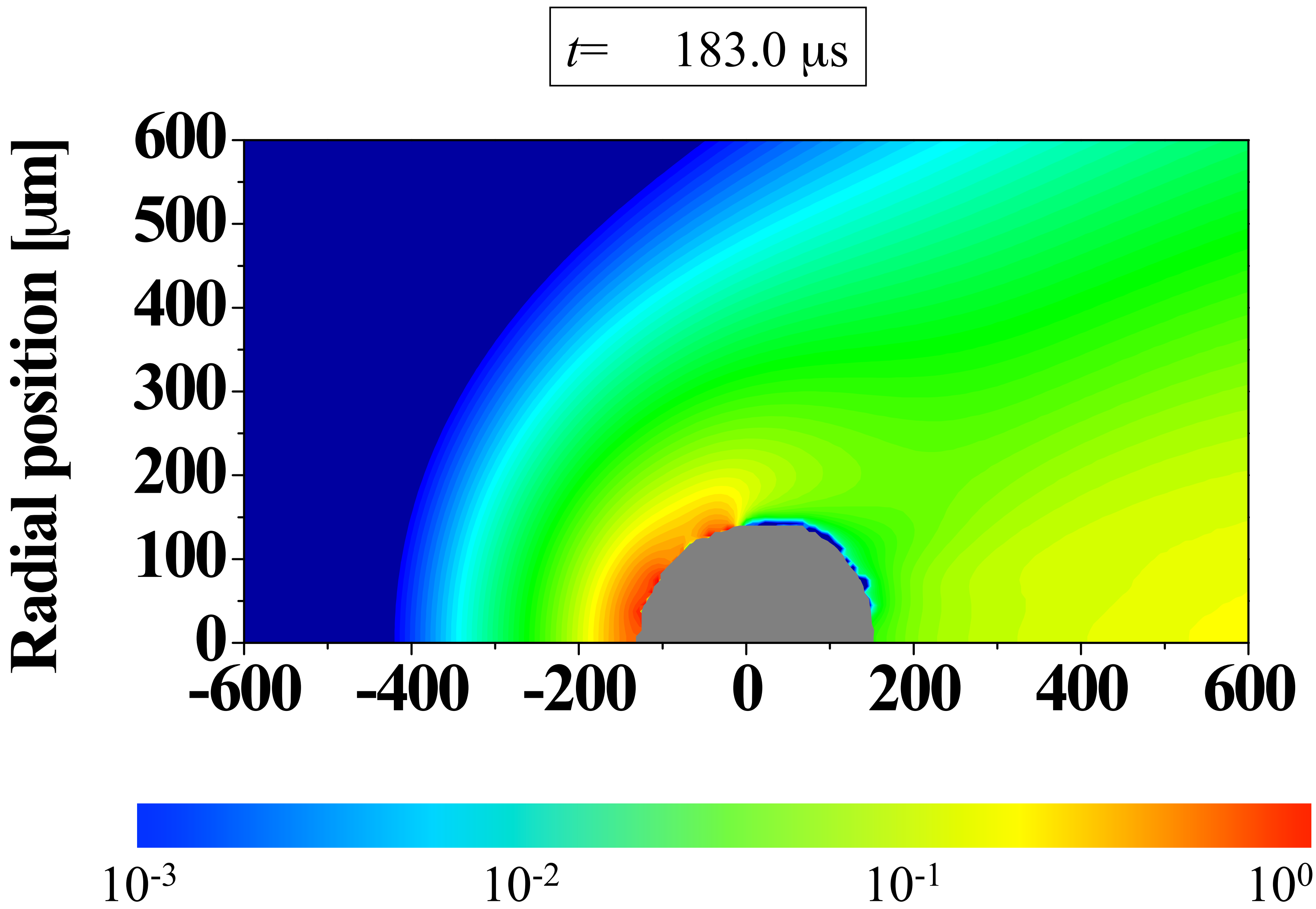

Mass fraction of ablated vapor

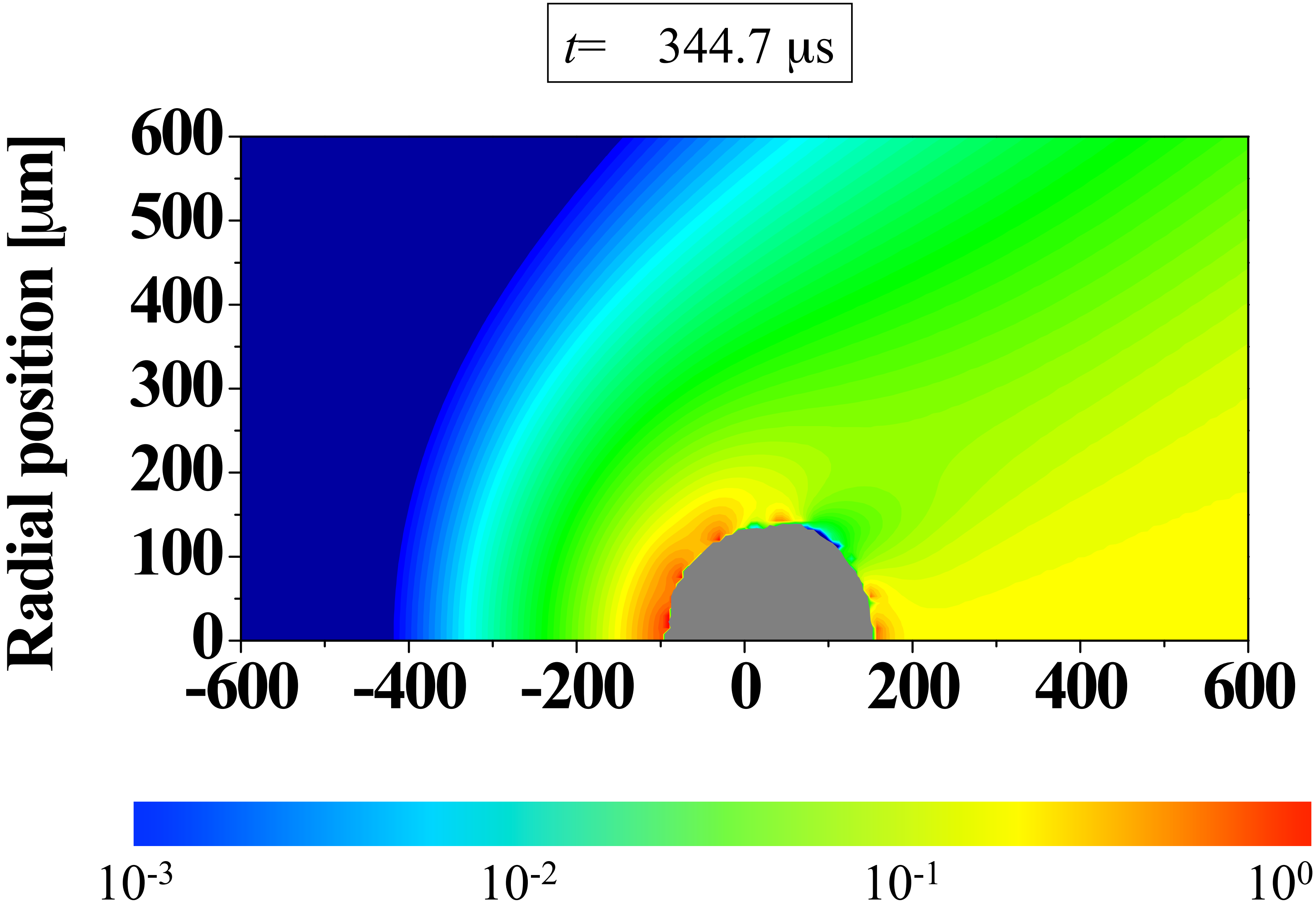

Mass fraction of ablated vapor

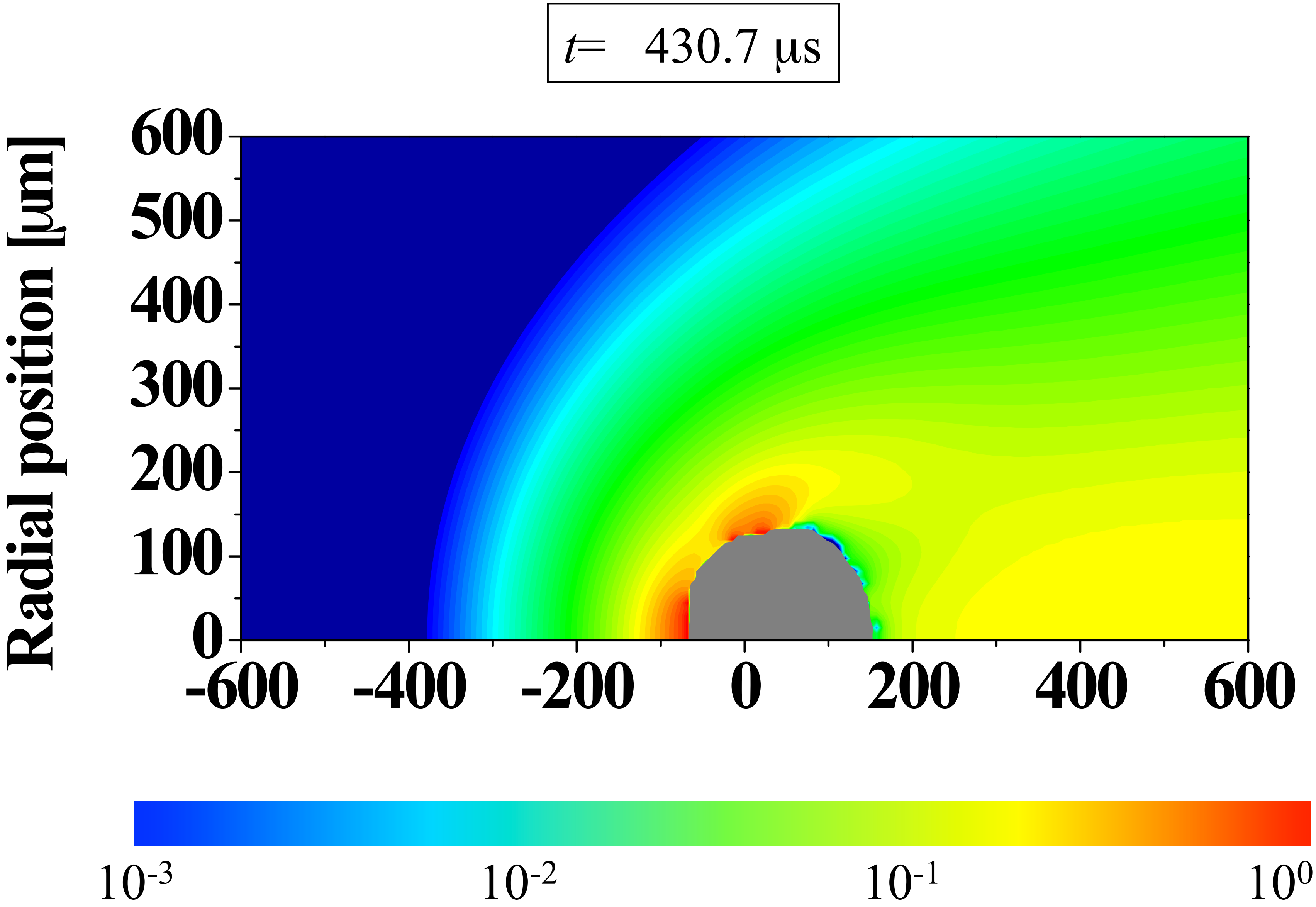

Mass fraction of ablated vapor

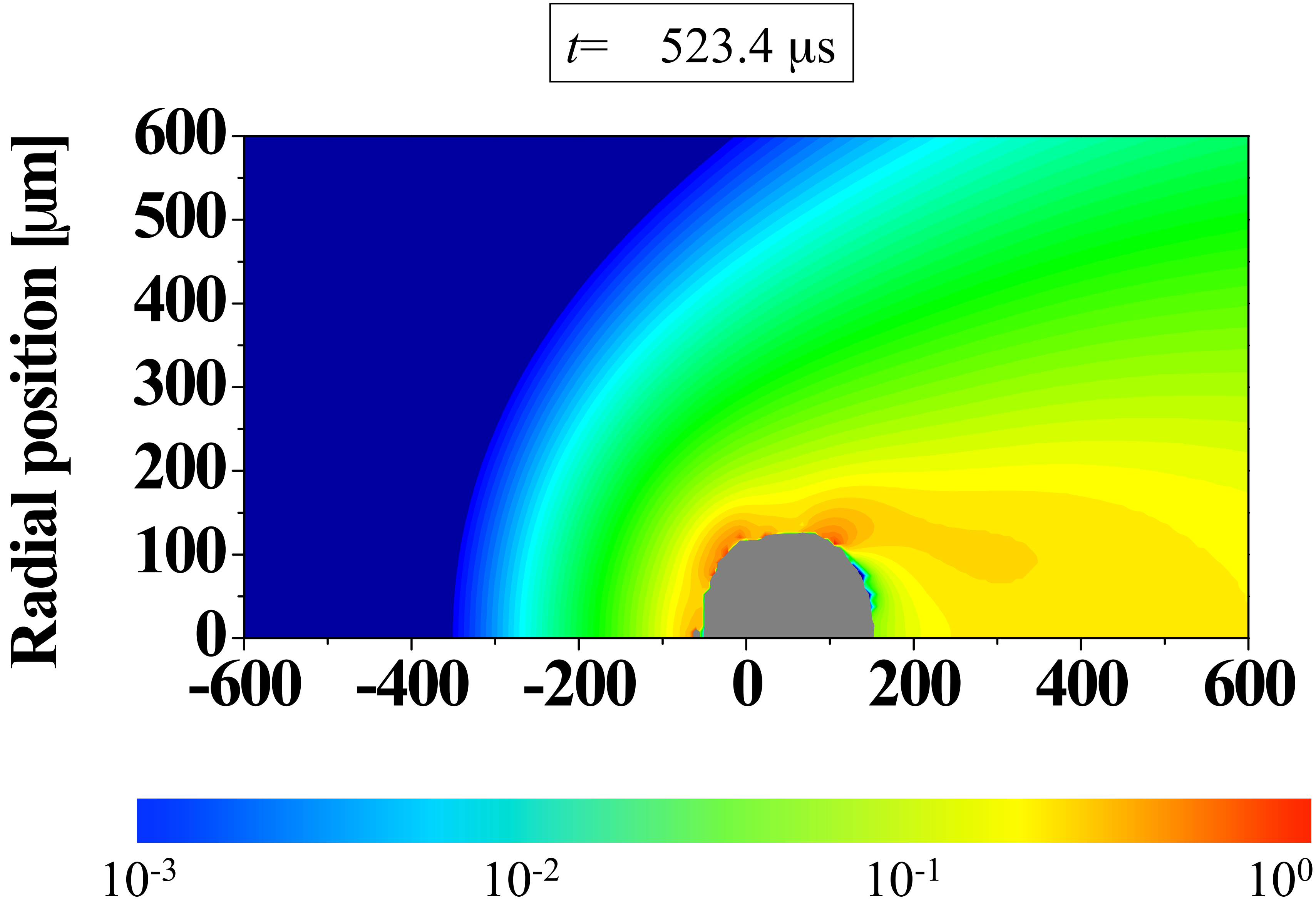

Mass fraction of ablated vapor

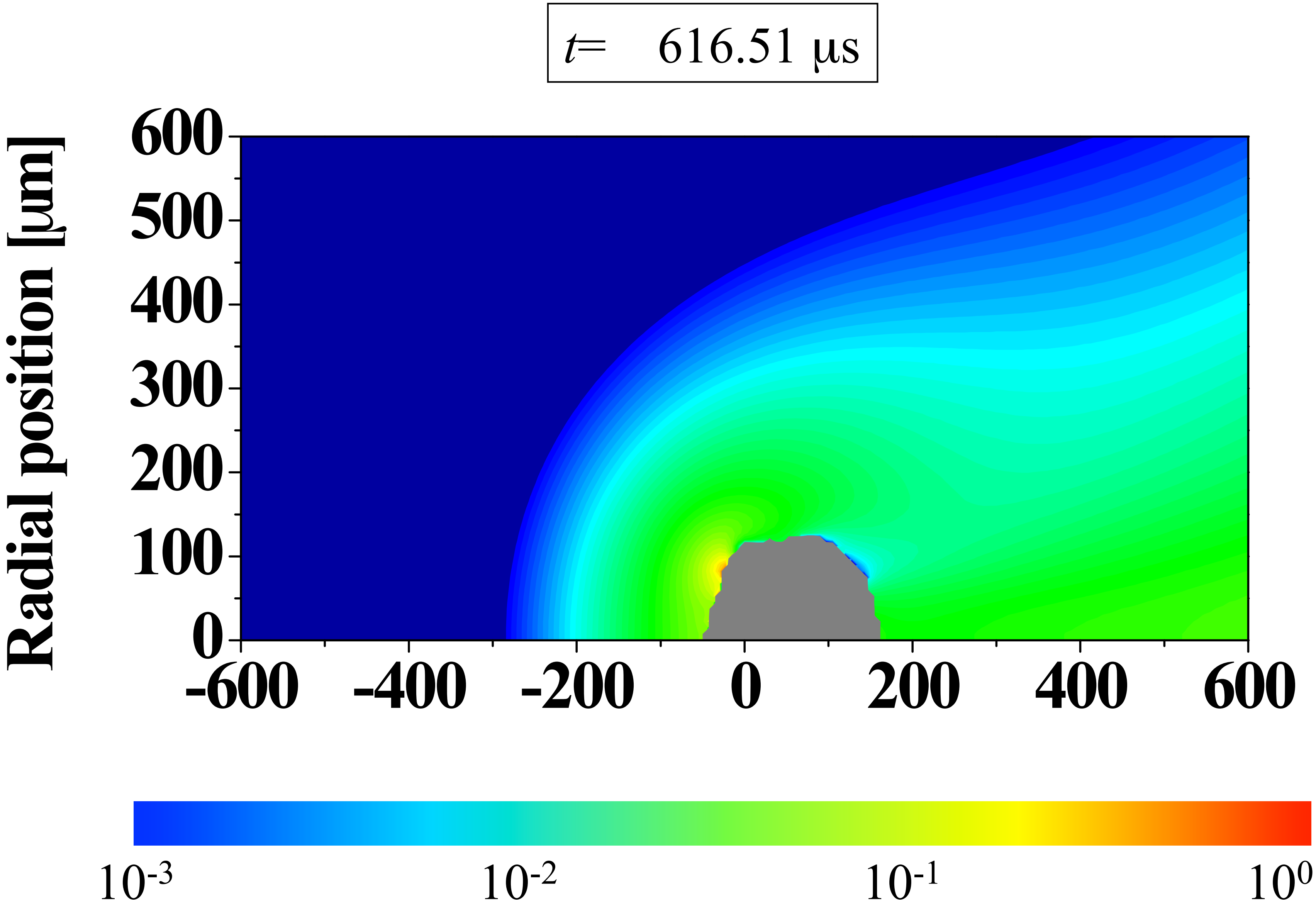

Mass fraction of ablated vapor

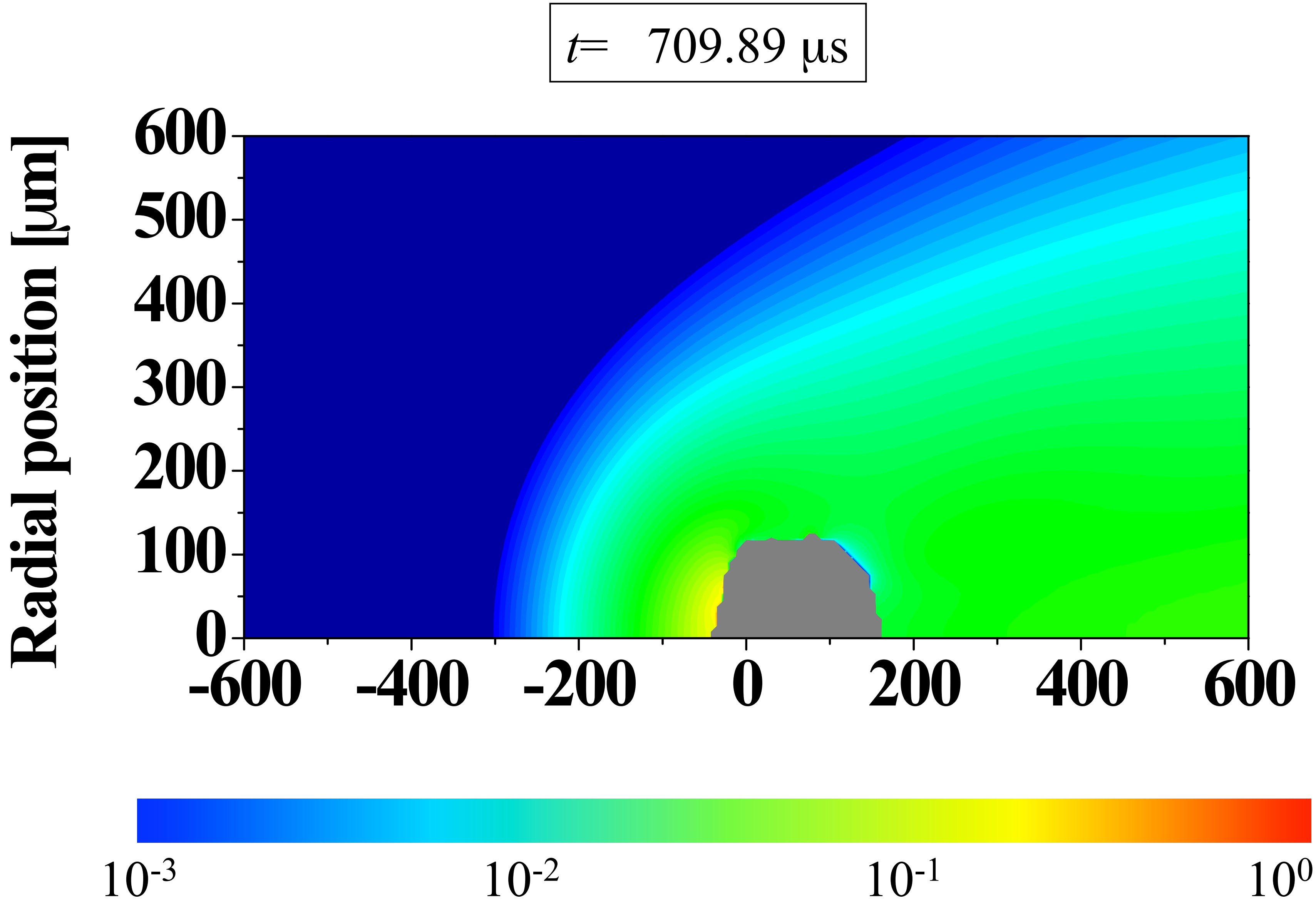

Mass fraction of ablated vapor

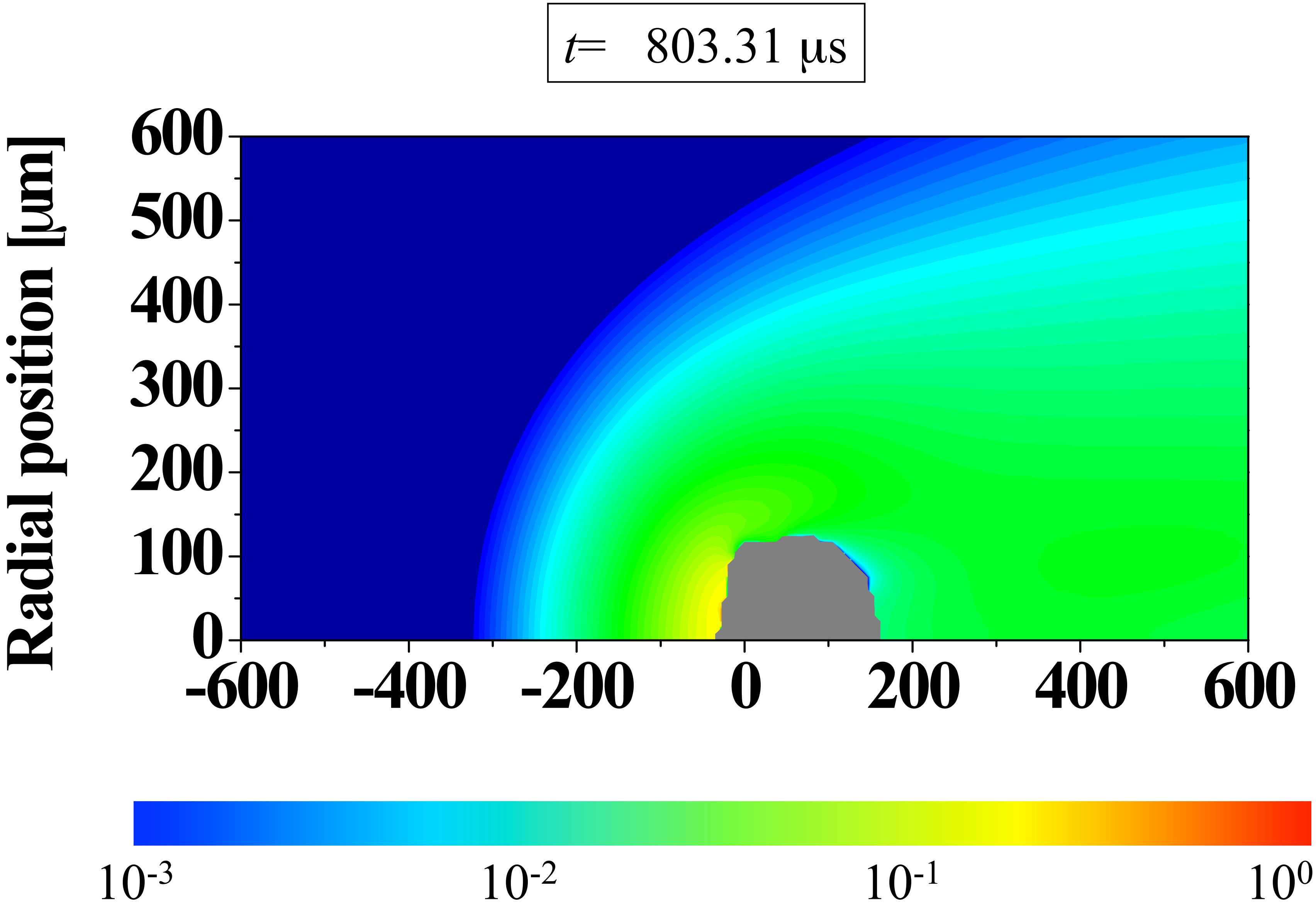

Transport of ablated vapor and shape change of the particle

-Ablated vapor is transported by diffusion, and by also convection due to the external Ar gas flow and the gas flow produced by the ablation.

-Rapid ablation especially around upstream of the particle decreases the upstream radius of the particle.

-Lifetime of dust particle was estimated to be 6 times longer than the conventional method without considering temperature decrease around the particle.

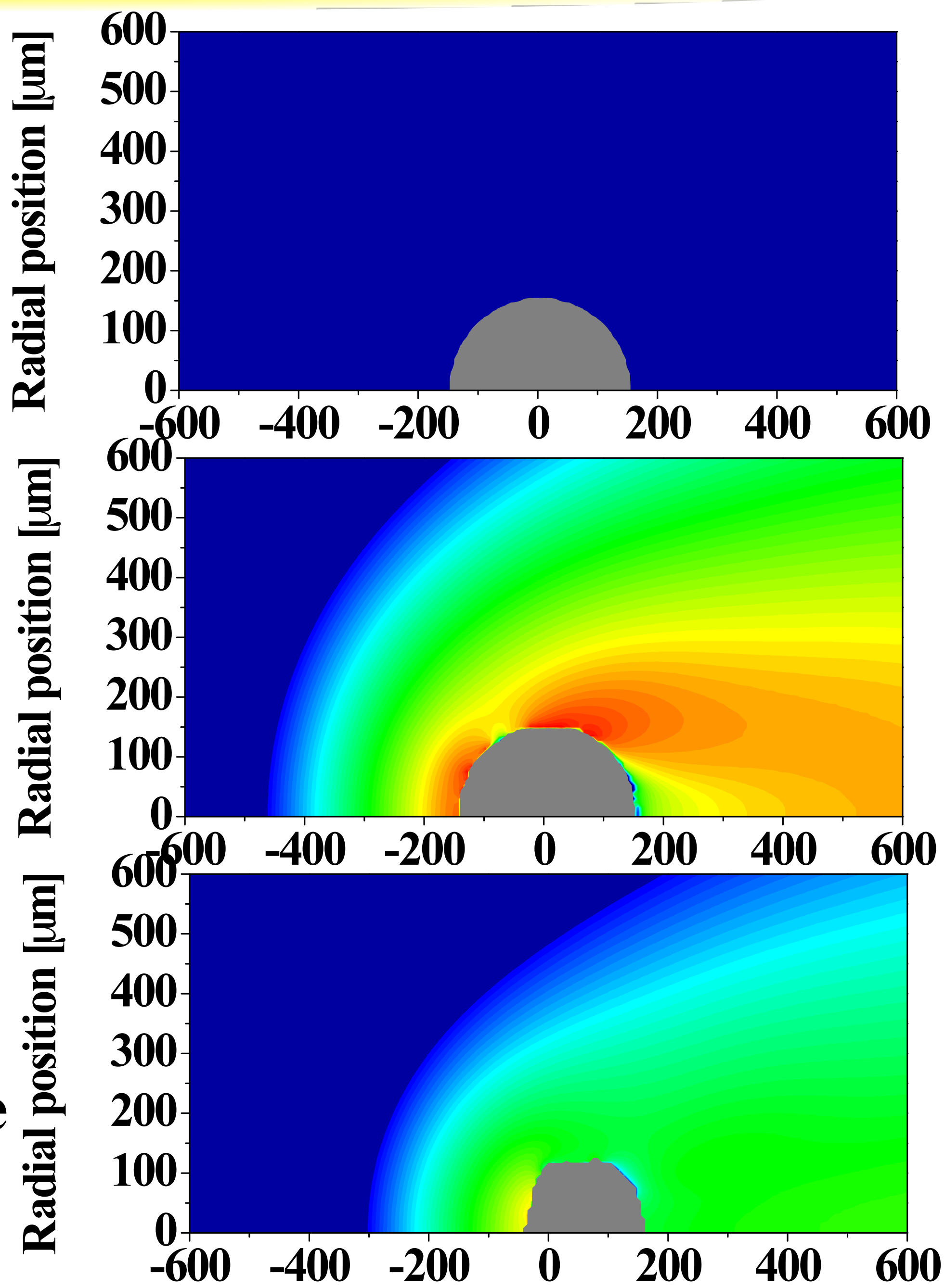

Conclusions

-The DUSTT code was adopted to a dust particle in plasma of JT-60U configuration.
-Behaviors of carbon dust particles with radii of 1-100 μm from different walls were calculated by solving mass, motion and energy equations.

-Behavior of dust particle is dominated by ion drag force.
-Dust radius is reduced mainly by thermal sublimation.

Future work
-Comparison with experimental data
-Statistical analysis of dust particles with other radii